

# Cranial morphology and masticatory biomechanics in the Canidae.

Thesis submitted in accordance with the requirements of the  
University of Liverpool for the degree of Doctor in Philosophy by

Fay Penrose

December 2018



## Abstract

Cranial form is closely allied to diet and feeding behaviour in the Canidae, with the force and velocity of jaw closing depending on both the bony morphology of the skull and mandible, and the mass and architecture of the jaw adductor muscles. Previously, little has been reported on the details of the form and function of the jaw adductor muscles, with earlier studies basing functional biomechanical hypotheses on data derived from dry skull specimens. For this study, empirically derived muscle data was recorded from 12 species of wild canid to examine how the jaw adductor muscles are scaled across the range of body sizes, phylogenies and trophic groups. I also considered how the muscles are accommodated on the skull, and how this is influenced by differences of endocranial size. Findings reveal that all jaw adductor muscles scale isometrically against body mass, regardless of phylogeny or trophic group, but that endocranial volume scales with negative allometry against body mass. Gross dissection techniques were used to explore the architecture of the muscles, and findings were used to inform the building of finite element models that predict bite force and strain energy density values. The inclusion of muscle architectural detail is shown to influence masticatory muscle force production capability calculations, indicating that muscles with longer fascicles were disadvantaged compared to muscles with shorter fascicles. Dietary groups were differentiated by temporalis fascicle angles, which, when allied with the differentiation of rostral length, may further contribute to specialisations of fast jaw closing or forceful jaw closing species. The most biomechanically demanding masticatory function is canine biting, and the highest strain energy values were reported in these loading conditions, particularly in the zygomatic arches and caudal rostrum. Specific head shapes may be constrained by size, with scaled strain energy density models predicting that some bony morphologies may only be viable in species with small body masses. Lastly, *ex vivo* laboratory experiments and *in silico* models were used to explore the role of a previously underreported structure, the postorbital ligament, during biting. This study found that the postorbital ligament plays a minimal role in attenuating stress during mastication and that it need not be included in any future FEA bite force studies in canids. This work provides both original data and methodological recommendations for future projects. It is hoped that these findings can help to inform future studies on masticatory function in extant and extinct wild canid species and domesticated canid breeds.

## Acknowledgements

Firstly, I would like to thank my primary supervisor, Dr Nathan Jeffery, for his continued and long-standing support and enthusiasm. In particular Nathan has helped regarding experimental design and implementation and has had the patience to teach me new techniques and has offered many suggestions for manuscript improvement. His generous advice and support over the years has been invaluable and is much appreciated.

I would also like to thank Professor Graham Kemp for his continued encouragement and his help in concept development and critical revision of the thesis in general, and of Chapters Three and Four in particular.

Dr Philip Cox was always very supportive of this work and was especially kind in reviewing and offering suggestions for the improvements to Chapter Five. I hope we can work together in future projects.

I would like to thank Professor Susan Dawson and all of the senior management team of the Institute of Veterinary Science for supporting this work, both financially and academically. I would also like to thank all of my friends and colleagues in the Institute of Veterinary Science, in particular Kieron Salmon, Alison Reid, Rosie MacDiarmid, Emma Ormandy, Karen Noble, Zeeshan Durrani and John McGarry, for their ongoing help and advice.

Lastly, I would like to thank my family and friends, in particular my husband, Matt, and my own canids, Bobbie and Roman for their love, encouragement and making me laugh.

## Table of Contents

Abstract.....	2
Acknowledgements .....	3
Table of Contents .....	4
List of Figures .....	8
List of tables.....	11
List of abbreviations .....	12
Chapter One. Introduction, taxonomy, phylogeny, anatomy and hunting strategies. ....	14
1.1 Introduction.....	15
1.2 Taxonomy and phylogeny of canids.....	18
1.2.1 Taxonomic and phylogenetic techniques and their limitations .....	18
1.2.2 Evolutionary history .....	22
1.2.3 The rise of the Caninae .....	27
1.2.4 Extant canid taxonomy.....	30
1.2.5 Phylogenetic trees .....	31
1.3 Canid anatomy.....	34
1.3.1 Post cranial form and function. ....	34
1.3.1.1 Spine.....	35
1.3.1.2 Neck.....	36
1.3.1.3 Limbs .....	37
1.3.1.4 The gastrointestinal tract .....	44
1.3.2. Anatomy of the head. ....	46
1.3.2.1. The skeleton of the head.....	46
1.3.2.2 Dentition.....	57
1.3.2.3 Movement of canid jaws. ....	63
1.4 Canid Diet and hunting strategies .....	72
1.4.1 Diet.....	72
1.4.2 Hunting strategies.....	75
1.4.3.1 Hunting large prey .....	75
1.4.3.2 Hunting small prey .....	77
1.5 Summary .....	78
Chapter Two. Sampling, Imaging and Dissection .....	80
2.1 Introduction.....	81
2.2 Sampling.....	81
2.2.1 Review of species and numbers used in previous studies. ....	81
2.2.3 Description of sample .....	85

2.3.4 Ethical approval. ....	91
2.3 Imaging.....	92
2.3.1 Computed Tomography (CT) .....	92
2.3.2 Magnetic resonance imaging.....	94
2.3.3 Method.....	95
2.3.4 Muscle imaging and validation .....	97
2.3.5 Combined computer tomography and magnetic resonance scans. ....	98
2.4 Dissection and the gross anatomy of the jaw adductor muscles. ....	103
2.4.1 Review.....	103
2.4.2 Method.....	104
2.4.3 Dissection notes on the masseter muscle.....	108
2.4.4 Dissection notes on the temporalis muscle .....	115
2.4.5 Dissection notes on the pterygoid muscles.....	121
2.5 Discussion.....	126
Chapter Three. Scaling and accommodation of the jaw adductor muscles in the Canidae....	129
3.1 Introduction.....	130
3.2 Aims of the study.....	132
3.3 Materials and Methods.....	134
3.3.1 Specimens, imaging and skull reconstruction. ....	134
3.3.2 Form, Shape and Morphometric Analysis .....	138
3.3.2.1 Landmarking. ....	139
3.3.2.2 Modularity.....	141
3.3.2.3 Geometric morphometric analysis.....	146
3.3.3 Muscle origin surface areas, endocranial volumes and surface areas.....	150
3.3.4 Phylogenetic Analyses.....	154
3.3.5 Statistics .....	156
3.4 Results. ....	157
3.4.1 Muscle morphology .....	157
3.4.2 Surface area, endocranial volume and endocranial volume surface area.....	159
3.4.3 Metric analysis.....	160
3.4.4 Form analyses of the bony morphology.....	164
3.4.5 Form analyses of the muscle morphology .....	170
3.5 Discussion.....	172
3.6 Summary .....	175
Chapter Four. Functional morphology of the jaw adductor muscles in the Canidae.....	177
4.1 Introduction.....	178

4.2 Materials and methods .....	184
4.2.1 Specimens, imaging and landmarking.....	184
4.2.2. Gape angle at wide gape .....	187
4.2.3 Reconstruction of muscle function .....	187
4.2.3.1 Review .....	187
4.2.3.2 Method for calculating RPCSA and force of muscle.....	193
4.2.4 Computer Modelling. ....	195
4.2.4.1. Review .....	195
4.2.4.2 Finite element analysis method.....	201
4.2.5. Mechanical efficiency.....	213
4.2.6. Mechanical advantage .....	214
4.2.7 Temporalis muscle angles relative to the occlusal plane .....	215
4.2.8 Statistical analysis .....	216
4.3 Results. ....	217
4.3.1 Muscle density.....	217
4.3.2 Dissection, muscle mass, fascicle length and muscle force. ....	217
4.3.3 Bite forces.....	223
4.3.4 Scaling .....	224
4.3.5 Mechanical efficiency.....	225
4.3.6. Finite element strain energy density models. ....	225
4.3.7. Mechanical advantage .....	234
4.3.8. Temporalis muscle angles relative to the occlusal plane .....	235
4.4. Discussion.....	238
4.5 Conclusion .....	245
Chapter Five. The biomechanical role of the orbital ligament in load transmission during canine biting in the Canidae.....	246
5.1 Introduction.....	247
5.2 Materials and Method. ....	252
5.2.1 Specimens.....	252
5.2.2 Experimental condition.....	253
5.2.3 Finite Element models .....	254
5.2.4 Laboratory experiments.....	256
5. 3 Results .....	262
5.4 Discussion.....	268
5.5 Conclusions.....	271
Chapter Six. Discussion. ....	272

6.1 Introduction.....	273
6.2 Aims of the study.....	273
6.3 Generating and managing force.....	274
6.4 Adapting to allometry.....	276
6.5 Is head shape a consequence of diet or is diet a consequence of head shape?.....	278
6.6 Head shape in the domestic canid breeds.....	280
6.7 Summary.....	282
Bibliography.....	284
Appendices.....	357
Appendix 1. Species details.....	358
<i>Alopex lagopus</i> , Arctic fox.....	358
<i>Canis lupus</i> , Grey wolf.....	359
<i>Canis mesomelas</i> , Black backed jackal.....	360
<i>Chrysocyon brachyurus</i> , Maned wolf.....	361
<i>Cuon alpinus</i> , Dhole.....	362
<i>Lycaon pictus</i> , African hunting dog.....	363
<i>Nyctereutes procyonoides</i> , Raccoon dog.....	364
<i>Otocyon megalotis</i> , Bat eared fox.....	365
<i>Speothos venaticus</i> , Bush dog.....	366
<i>Vulpes corsac</i> , Corsac fox.....	367
<i>Vulpes vulpes</i> , Red fox.....	368
<i>Vulpes zerda</i> , Fennec fox.....	369
Appendix 2. Dhole body mass in captivity details.....	370
Appendix 3. Soft tissue landmarks.....	371
Appendix 4. Pruned tree after Nyakatura (2012).....	372

## List of Figures

### Chapter One

Figure 1.1 Diversity of Canidae species through time.....	27
Figure 1.2 Phylogenetic tree of the extant Caninae from Lindblad-Toh <i>et al.</i> (2005).....	32
Figure 1.3 Phylogenetic tree of the extant Caninae after Nyakatura <i>et al.</i> (2012).....	33
Figure 1.4 Bones of the skull.....	49
Figure 1.5 Generic canid dentition.....	61

### Chapter Two

Figure 2.1 MR axial slices of <i>Canis lupus familiaris</i> .....	99
Figure 2.2 Imaging validation study of <i>Vulpes vulpes</i> . .....	100
Figure 2.3 RMA regression of mass from MR vs Mass derived from dissection.....	101
Figure 2.4 <i>Canis lupus</i> , co-registered MR and reconstructed skulls from CT scans .....	102
Figure 2.5 <i>Lycaon pictus</i> , intact head. ....	106
Figure 2.6 <i>Lycaon pictus</i> , fur and skin removed .....	106
Figure 2.7 <i>Lycaon pictus</i> . The digastricus muscle .....	107
Figure 2.8 <i>Canis mesomelas</i> . The superficial layer of temporal fascia.....	107
Figure 2.9 <i>Lycaon pictus</i> . Superficial masseter, caudoventral aspect. ....	109
Figure 2.10 <i>Lycaon pictus</i> . Superficial masseter lateral aspect. ....	109
Figure 2.11 <i>Nyctereutes procyonoides</i> . The origin of superficial masseter.....	110
Figure 2.12 <i>Canis lupus</i> . Division of the superficial masseter.....	110
Figure 2.13 <i>Canis lupus</i> . The superficial masseter leaflets.....	111
Figure 2.14 <i>Lycaon pictus</i> and <i>Vulpes corsac</i> , the deep masseter.....	112
Figure 2.15. The preangular process .....	113
Figure 2.16 The zygomaticomandibularis muscle.....	114
Figure 2.17 The extent of temporalis.....	116
Figure 2.18 The deep temporal fascia in <i>Vulpes zerda</i> .....	117
Figure 2.19 The deep temporal fascia in <i>Canis mesomelas</i> .....	117
Figure 2.20 The extent of the temporalis muscle in <i>Lycaon pictus</i> .....	118
Figure 2.21 The extent of the suprazygomatic division of the temporalis .....	118
Figure 2.22 Insertion of the suprazygomatic division of temporalis.....	119
Figure 2.23 The suprazygomatic division of temporalis <i>Nyctereutes procyonoides</i> .....	119
Figure 2.24 <i>Lycaon pictus</i> . Superficial temporalis.....	120
Figure 2.25 <i>Alopex lagopus</i> . Superficial temporalis, reflected. ....	120
Figure 2.26 <i>Vulpes vulpes</i> . The deep temporalis. ....	121
Figure 2.27 The pterygoids, ventral aspect, <i>Canis lupus</i> .....	123



Figure 2.28. <i>Vulpes vulpes</i> . The pterygoids, lateral aspect, <i>Vulpes vulpes</i> .....	123
Figure 2.29 <i>Ex situ</i> pterygoid muscles, <i>Vulpes vulpes</i> . .....	124
Figure 2.30 <i>Vulpes vulpes</i> , the origin of the pterygoid muscles. ....	124

### Chapter Three

Figure 3.1 Dissection images .....	137
Figure 3.2 <i>Canis lupus familiaris</i> , bony landmarks.....	143
Figure 3.3 Coronal slices and isosurface used to identify landmarks .....	144
Figure 3.4 MorphoJ mapping of CT derived bony landmarks.....	147
Figure 3.5 Eigenvalue scale of the proportion of variance within the dataset.....	150
Figure 3.6 CT reconstructions of the jaw adductor muscle attachment sites .....	152
Figure 3.7 <i>Vulpes corsac</i> endocranial cavity and endocast of <i>Chrysocyon brachyurus</i> .....	153
Figure 3.8 Phylogenetic tree structures after Garland (2005).....	155
Figure 3.9 RMA regression, log body mass vs log total jaw adductor muscle mass .....	162
Figure 3.10 RMA regression, log body mass vs log endocranial volume.....	164
Figure 3.11. Scree plots of the PC eigenvalues. ....	168
Figure 3.12 Whole skull principal component scores PC1 vs PC2.....	169
Figure 3.13 Cranial principal component scores PC1 vs PC2. ....	169
Figure 3.14 Scatterplot of PCA analyses from geometric morphometric analysis.....	170
Figure 3.15 Dorsoventral view wireframes taken PC1 of the cranial component analysis .....	171
Figure 3.16 Dorsoventral view of cranial wireframes .....	171

### Chapter Four

Figure 4.1 <i>Vulpes vulpes</i> MR, dissection and FE model showing the mandible at wide gape....	187
Figure 4.2. Angle of pennation and fascicle length measurement. ....	194
Figure 4.3. Components of a tetrahedral element .....	199
Figure 4.4 Finite element analysis workflow .....	201
Figure 4.5 Manual segmentation into separate materials. ....	205
Figure 4.6 <i>Vulpes vulpes</i> diagram with areas of muscle attachment and sampling points.....	213
Figure 4.7 The preangular process and the angular process.....	219
Figure 4.8 Percentage contributions of muscles toward muscle mass and muscle force.....	222
Figure 4.9 Temporalis force as predicted by RPCSA and dry skull methods. ....	223
Figure 4.10 SED nodal values from seven midline sampling sites .....	229
Figure 4.11 SED values in all species at canine closed bite, dorsal aspect. ....	231
Figure 4.12 SED colour maps of <i>Canis lupus</i> , in all four loading conditions. ....	233
Figure 4.13 Lines of action for the temporalis muscle. ....	237

## Chapter Five

Figure 5.1. FE model of <i>Vulpes vulpes</i> , with orbital ligaments intact .....	256
Figure 5.2. Prepared <i>Vulpes vulpes</i> with strain gauge attachment site .....	257
Figure 5.3. Strain gauge and Wheatstone bridge electronic circuit.....	257
Figure 5.4. Frontal region of <i>Vulpes vulpes</i> skull with strain gauge attached. ....	259
Figure 5.5. Loading of <i>Vulpes vulpes</i> head to simulate masseteric biting. ....	261
Figure 5.6. Output from strain gauge grid.....	262
Figure 5.7. FE models of <i>Vulpes vulpes</i> skull loaded with left masseter force. ....	266
Figure 5.8. Drawings of strain gauge magnitudes and vectors.....	267

## Appendix

Appendix Figure 1.1 <i>Alopex lagopus</i> .....	358
Appendix Figure 1.2 <i>Canis lupus</i> .....	359
Appendix Figure 1.3 <i>Canis mesomelas</i> .....	360
Appendix Figure 1.4 <i>Chrysocyon brachyurus</i> .....	361
Appendix Figure 1.5 <i>Cuon alpinus</i> .....	362
Appendix Figure 1.6 <i>Lycaon pictus</i> .....	363
Appendix Figure 1.7 <i>Nyctereutes procyonoides</i> .....	364
Appendix Figure 1.8 <i>Otocyon megalotis</i> .....	365
Appendix Figure 1.9 <i>Speothos venaticus</i> .....	366
Appendix Figure 1.10 <i>Vulpes corsac</i> , A.....	367
Appendix Figure 1.11 <i>Vulpes vulpes</i> .....	368
Appendix Figure 1.12 <i>Vulpes zerda</i> .....	369
Appendix Figure 1.13 <i>Cuon alpinus</i> , animal weight report .....	370
Appendix Figure 1.14 Pruned Nyakatura phylogenetic tree.....	372

## List of tables.

### Chapter One

Table 1.1 Summary of Canidae evolution.....	26
---	----

### Chapter Two

Table 2.1. Comparison of sample size with previous studies. ....	83
Table 2.2. Details of specimens used in this thesis.....	87
Table 2.3 Image slice thickness and pixel spacing for all scanned specimens.....	96
Table 2.4. MR and dissection muscle volumes validation study.....	101
Table 2.5 Mean muscle contribution to total jaw adductor mass. ....	125
Table 2.6 Comparative mammalian jaw adductor muscles.....	128

### Chapter Three

Table 3.1. Details of specimens used in this chapter. ....	136
Table 3.2 List of skull component landmarks and their landmark types.....	145
Table 3.3 Surface area, endocranial volume, and endocranial volume surface area. ....	160
Table 3.4. Reduced Major Axes regressions of variables scaled against body mass. ....	163
Table 3.5 Summary statistics for form analyses. ....	167
Table 3.6 Statistical tests for the differences between the dietary groups .....	170

### Chapter Four

Table 4.1 Details of specimens used in this chapter.....	186
Table 4.2 Material properties used in finite element models.....	208
Table 4.3 Muscle masses, predicted volumes and volumes from two species. ....	217
Table 4.4 RMA regression analyses of jaw adductor muscle variables. ....	220
Table 4.5 Predicted bite force and mechanical efficiency in all conditions.....	224
Table 4.6 Raw and scaled SED values from sample site 2. ....	228
Table 4.7 Mechanical advantage in all loading conditions.....	235
Table 4.8 Temporalis lines of action .....	236

### Chapter Five

Table 5.1. FE model and <i>ex vivo</i> experimental pre-cut and post-cut values. ....	265
---	-----

### Appendix

Table Appendix 4. Soft tissue landmarks used in GMM.....	371
--	-----

### List of abbreviations

<b>ANOVA</b>	Analysis of variance
<b>C</b>	Canine tooth
<b>cm</b>	Centimetre
<b>cm<sup>3</sup></b>	Cubic centimetre
<b>CT</b>	Computed Tomography
<b>EV</b>	Endocranial volume
<b>EVSA</b>	Endocranial volume surface area
<b>F</b>	Force
<b>FE</b>	Finite Element
<b>FEA</b>	Finite Element Analysis
<b>g</b>	Gram
<b>GMM</b>	Geometric Morphometrics
<b>GPa</b>	Gigapascals
<b>I</b>	Incisor tooth
<b>J</b>	Joule
<b>kg</b>	Kilograms
<b>kV</b>	Kilovolt
<b>LM</b>	Lower molar tooth
<b>LPM</b>	Lower premolar tooth
<b>M</b>	Molar tooth
<b>MA</b>	Mechanical advantage
<b>Ma</b>	Mega annum
<b>mA</b>	Milliampere
<b>MDA</b>	Multibody dynamic analysis
<b>ME</b>	Mechanical efficiency
<b>MicroCT</b>	Microscopic computed tomography
<b>mJ</b>	Millijoule
<b>mm</b>	Millimetre
<b>MPa</b>	Megapascal
<b>MRI</b>	Magnetic resonance imaging
<b>MYA</b>	Million years ago
<b>N</b>	Newtons
<b>NO</b>	Nitrous oxide

<b>NS</b>	Not significant
<b>Pa</b>	Pascals
<b>PC</b>	Principal component
<b>PCA</b>	Principal component analysis
<b>PCSA</b>	Physiological cross sectional area
<b>PD</b>	Proton density
<b>PIC</b>	Phylogenetic independent contrasts
<b>PM</b>	Premolar tooth
<b>POL</b>	Postorbital ligament
<b>R<sup>2</sup></b>	Coefficient of determination
<b>RMA</b>	Reduced Major Axis
<b>RPCSA</b>	Reduced physiological cross sectional area
<b>SA</b>	Surface area
<b>SD</b>	Standard Deviation
<b>SE</b>	Strain energy
<b>SED</b>	Strain energy density
<b>SNR</b>	Signal to noise ratio
<b>TMJ</b>	Temporomandibular joint
<b>UM</b>	Upper molar tooth
<b>UPM</b>	Upper premolar tooth
<b>V</b>	Volume
<b>μCT</b>	MicroCT
<b>με</b>	Microstrain
<b>%</b>	Percentage
<b>†</b>	Extinct species
<b>3D</b>	Three dimensional

**Chapter One. Introduction, taxonomy, phylogeny, anatomy and hunting strategies.**

## **1.1 Introduction**

How species adapt to new opportunities or threats is the overarching theme in evolutionary biology. Throughout this thesis 'carnivoran' is used to refer to any of the order of Carnivora. Carnivoran adaptations have been widely studied because their evolutionary history is well documented within the fossil record. In addition, ecological studies of the many extant carnivoran species allow for behavioral correlates to be made with morphological traits. Comparative biological studies explore the differences and similarities between individuals, species or genera to identify adaptive traits. Many previous studies have looked at morphological differences between different families within the carnivoran order, often with a focus on masticatory function, which is a key feature of carnivorans (Greaves, 1983; Biknevicius and Ruff, 1992; Goswami, 2006b; Van Valkenburgh, 2007; Figueirido *et al.*, 2011; Goswami *et al.*, 2011). These broad approach studies allow for identification of traits that distinguish groups at a high taxonomic level. Other work has focused specifically on masticatory function within the Canidae, although these have been primarily based on osteological material (Van Valkenburgh, 1991; Kieser and Groeneveld, 1992; Van Valkenburgh *et al.*, 2004; Finarelli, 2007; Slater *et al.*, 2009; Damasceno *et al.*, 2013; Drake *et al.*, 2015; Figueirido *et al.*, 2015; Meloro *et al.*, 2015; Slater, 2015).

The Caninae are the only extant subfamily of the Canidae family and arose around 40Ma (megaannum ago) in the North American landmass (Wang and Tedford, 2010). It was only with the demise of the other Canidae subfamilies, firstly Hesperocyoninae in the Miocene and subsequently the Borophaginae in the late Pleistocene, that the Caninae underwent a rapid and extensive expansion (Wang and Tedford, 2010). They flourished throughout the Pleistocene epoch and diversified into not only new ecological niches, but also began to spread into new geographical locations (Berta, 1987; Wozencraft, 1993; Van Valkenburgh, 1999; Sillero-Zubiri *et al.*, 2004; Perini *et al.*, 2010; Prevosti, 2010; Tchaicka *et al.*, 2016). Caninae are now found in all environments from equatorial forests, to arid desert and the

high artic, and their widespread success is reflected by their morphological diversity. Body masses range from less than one kilogram to in excess of eighty (Wozencraft, 1993, 2005; Macdonald and Sillero-Zubiri, 2004; Nowak, 2005; MacDonald, 2009; Wang and Tedford, 2010). Even a cursory look at the skulls of different canid species reveals that, although they are all identifiable as canids, they are also easily distinguishable from one another. Skull shapes range from the delicate gracile heads of the small foxes to the broad skulls and short muzzles of the dholes and wolves. Their diet is equally varied with some species specialised in hunting large mammals, whilst others eat mainly insects and fruit. The evolution of a wide variety of extant morphologies and diets over a relatively short period of evolutionary time makes the Caninae an ideal group to study, as it raises intriguing questions about the plasticity of the canid blueprint, and the constraints and drivers for the development of adaptive traits.

This study compares 12 species in the canid subfamily of Caninae, using soft tissue and skeletal material to investigate the form and function of the masticatory apparatus. This represents one third of extant canid species. The aim is to quantify some of the differences in canid head shape, and to explore the impact of skull morphology on masticatory function.

Specifically:

- To describe for the first time, the mass and internal architecture of the jaw adductor muscles of twelve species of wild canid
- To explore muscle size and scaling and to quantify head shape with regard to the accommodation of the jaw muscles
- To determine how skull and muscle morphology impacts on bite force
- To determine how masticatory function impacts on skull strain energy density
- To explore the viability of different head shapes after rescaling
- To assess the biomechanical role of the orbital ligament during mastication.



Chapter One gives a brief summary of the evolutionary history of the Canidae, and discusses the circumstances and adaptations of the Caninae that allowed them to flourish and succeed as the only extant member of the family. The phylogeny of the extant canids is outlined and brief descriptions of generic mammalian and more specific canid anatomical features are given. I also very briefly compare the salient anatomical features of the extant canids to those of either their close competitors, i.e. other carnivorans, or their prey, as they must be functionally matched to both groups, at least to some degree. Diet and hunting strategies are also discussed here. Chapter Two discusses the methodologies common to the following chapters, and describes for the first time, the detailed anatomy of the jaw adductor muscles in 12 species of wild canid. Chapter Three explores and quantifies head shape with regard to the accommodation of the jaw adductor muscles using geometric morphometric analyses (GMM). Factors that could explain differences or similarities in head shape include allometry, dietary specialisation or phylogenetic constraints, and these are explored using bivariate analyses and regression analyses and independent phylogenetic contrast analyses. Chapter Four compares the generation of muscle force, simulated bite force and the biomechanical performance of the skull. Muscle force is determined using the reduced physiological cross-sectional area (RPCSA) method. Adaptations in skull shape to improve muscle and bite performance are identified and discussed. This is the first time such a complete dataset of any mammalian subfamily has been explored using finite element analyses (FEA). Comparison of the RPCSA findings with the dry skull method are made so as to compare methodologies. Chapter Five discusses the role of the orbital ligament with regard to biting. As a soft tissue structure this feature is usually overlooked in bite force studies but has been posited to play a role in dissipating stress or strain across the skull during masseteric contraction. I investigate this with a series of laboratory experiments using cadaveric material which were compared to computer generated models to record the change in strain

across the loaded skull when the orbital ligaments were severed. This part of the study also includes sensitivity and validation studies to ensure that *in silico* models were reliably modelled and thus, are adequate for testing the key hypothesis. Chapter Six summarises and discusses the implications of the findings.

## **1.2 Taxonomy and phylogeny of canids.**

Establishing the evolutionary history and relatedness of species allows for contextualisation and categorisation. The evolutionary history of canids is complex, with hundreds of species in three major subfamilies, spanning 40 million years and geographically dispersed across the globe. Dietary specialisation within extinct canids can be inferred to some extent from body mass and anatomical traits, and by comparison with extant correlates (Slater *et al*, 2009; Van Valkenburgh and Slater, 2009; Damasceno *et al*, 2013). The iterative pattern of repeated phenotypes throughout canid evolution demonstrates not only the variety of environmental niches where available to them at particular times, but also the plasticity or constraints of their morphologies.

### **1.2.1 Taxonomic and phylogenetic techniques and their limitations**

Taxonomy and the phylogenetic relationships amongst extinct and extant canids have been the focus of many studies, and yet some details at species or genus levels are still much debated and not fully resolved (Figueirido *et al.*, 2015; Rueness *et al.*, 2015; Slater, 2015). There has been a great deal of re-ordering of the canid family tree as new evidence is uncovered and analysed using increasingly sophisticated diagnostic techniques. The three main sources of evidence for categorising species are chronostratigraphy, morphology and molecular analysis. Palaeontological studies consider both chronostratigraphic and morphological evidence. Chronostratigraphy is particularly important for contextualising when species moved into new regions and how they adapted to novel environmental

conditions. Morphology compares form, and in most cases, focuses on bony or fossilised remains, but may also include soft tissue structures such as muscles and viscera, and integumentary structures such as skin, hair and claws. Fossil evidence is inevitably incomplete and biased toward skeletal material preserved in particular taphonomic conditions. That which has been found often consists of damaged, fragmentary or partial remains. Apart from obvious diagnostic features, such as teeth and mandibles, some small internal structures of the skull are used to aid in determining taxonomic grouping. Of particular interest in carnivorans is the bony morphology of the middle ear. This region exhibits some anatomical features that distinguish families within in the order Carnivora (Hunt, 1974; Radinsky, 1981). Canids have an enlarged entotympanic bulla that is divided by a partial septum along the entotympanic and ectotympanic suture (Hunt, 1974; Wang and Tedford, 2010). Other features seen within the middle ear in canids are the loss of the stapedal artery, and its corresponding bony groove, and the medial position of the partially enclosed internal carotid artery (Wang and Tedford, 2010), as evidenced by its corresponding bony groove. Felid species have a large bony septum subdividing the middle ear and an enclosed internal carotid artery, whereas ursid species have only moderately inflated bullae with no septum, and a wholly enclosed internal carotid artery (Wang & Tedford, 2010). These morphologically observable features have played a major role in identifying and categorising fossil evidence. Molecular evidence compares DNA (deoxyribose nucleic acid) sequences between species with the assumption that closely related species exhibit a high degree of homology between sequences. Molecular clocks, that is using the known mutation rate of DNA sequences to estimate clade divergence times, are used in many analyses to determine common ancestors and describe phylogenetic relationships (Delisle and Strobeck, 2005; Lindblad-Toh *et al.*, 2005; Horsburgh, 2008; Tedford *et al.*, 2009; Prevosti, 2010; Lee *et al.*, 2015; Tchaicka *et al.*, 2016). Each of the evidential sources utilised for categorizing species into taxonomic groups, are in their own way, imperfect, and due to limited

availability of material, any analyses can only be carried out on partial datasets. Chronostratigraphy is confined to sampling only geographically accessible areas and is biased towards areas where there is greatest tradition of paleontological sampling, notably Eurasia and North America. Newly discovered or analysed samples can lead to new interpretations of existing data. Examples of recently discovered species include *Cynarctus wangi* (Jasinski and Wallace, 2015), *Lycaon sekowei* (Hartstone-Rose et al., 2010) and *Nurocyon chonokhariensis* (Sotnikova, 2006), all of which need to be placed within the context of evolutionary history. Previously known species may be discovered in novel contexts, either geographically or within the fossil timeline. For instance, the recent discovery of *Sinicuon dubius* in the Himalayas, implies that this species is much older than previously thought, and hence may be ancestral to the extant *Cuon alpinus* and *Lycaon pictus* species (Wang et al., 2015). Similarly, until a sampling gap of fossil *Vulpes vulpes* in the middle of the Eurasian landmass was filled, little was known of this species dispersal pattern across the Holarctic region (Kutschera et al., 2013). It is also possible that geological phenomena may disturb the spatial relationships of strata and confound expected timescales. In addition, the processes involved in the preservation of fossils, taphonomy, are subject to local geological and meteorological conditions. Certain landscapes such as floodplains, rivers and lakes are better at producing and preserving fossil remains, whereas high and low altitude environments are only poorly represented in the fossil record (Wang and Tedford, 2010; Fernández-Jalvo and Andrews, 2016). This results in only a narrow set of conditions where fossil evidence may be successfully created, protected and later, uncovered. Such evidence should be viewed with this in mind, as seemingly very speciose clades in the fossil record may reflect a preservation or accessibility artefact. In addition to naturally occurring taphonomic bias, sampling bias and erroneous interpretation of data may also lead to inaccurate conclusions.

Many morphological studies rely on comparison with, and inference from, other fossil samples, and new discoveries may result in reclassification of existing material. In addition, morphological comparisons are not only limited to available material, but also to the choice of the investigator as to what to features to compare. Until recent advances in imaging, many deep or fragile structures would have been hard to access. Even when using techniques such as micro computed tomography ( $\mu$ CT) or magnetic resonance (MR), small or delicate structures may have been lost in poorly preserved samples. Soft and integumental tissues are also difficult to preserve, and studies using this type of material are far fewer than those investigating bony morphologies. Even when non-osteological materials are evident in the fossil record they can usually provide only morphological, rather than molecular data. Molecular phylogenetic techniques depend upon access to DNA. However, evolutionary trends such as differential extinction and rate heterogeneity, cannot be inferred from studying only modern DNA, and so inferred phylogenies using only this evidence are also potentially flawed (Finarelli and Goswami, 2013). To overcome this, techniques using ancient DNA (aDNA) have been used in several studies determining relationships within the canid clade, many of them focusing on domestication (Horsburgh, 2008; Byrd *et al.*, 2013; Druzhkova *et al.*, 2013; Lee *et al.*, 2015; Brzeski *et al.*, 2016). However, as these techniques are only viable in specimens dating from the late Pleistocene onwards, they are not applicable to specimens from the early evolution of the canids. Sampling of aDNA material is subject to very limited datasets and also, as aDNA is generally degraded to some extent, to missing data within the sample. Even when using extant species DNA samples, phylogenetic relationships are difficult to fully resolve. Choices of how to partition gene sequences into sites where similar evolutionary characterizes are grouped, is subject to interpretation. Different types of algorithmic analyses of the data (for example: maximum likelihood, maximum parsimony, Bayesian) often give varying results (Yang and Rannala, 2012). Some researchers have used combined techniques, using two or more of

the above methods, to attempt to resolve the phylogeny of the canids (Wayne et al., 1997; Zrzavý and Řičánková, 2004). Here I endeavor to give a broad overview of the evolution and phylogenetic relationships of the canids, taking into account the often-conflicting evidence available in the current literature.

### **1.2.2 Evolutionary history**

Canidae are the oldest of the extant families within the Order Carnivora (Macdonald and Sillero-Zubiri, 2004), and were first seen as a distinct group in the middle to late Eocene. During the late Eocene and early Oligocene canids underwent three periods of diversification resulting in three subfamilies (Wang and Tedford, 2010): Hesperocyoninae, appeared 40Ma and became extinct 15Ma, Borophaginae, appeared 35Ma and became extinct 2Ma and Caninae appeared 35Ma and are currently represented by 34 - 36 extant species (Janis, 1993; Valkenburgh, 1999; Wang *et al.*, 1999; Andersson and Werdelin, 2003; Wang *et al.*, 2004; Tedford *et al.*, 2009; Wang and Macdonald, 2009; Wang and Tedford, 2010).

The timeline of canid evolution is summarised in Table 1.1 and Figure 1.1. There have been at least 244 (McKenna and Bell, 1997; Wang and Tedford, 2010) identified species of canid across their 40 million year history, although this number is set to increase as new discoveries are made. The first two subfamilies to arise, Hesperocyoninae and Borophaginae, were confined throughout their lineage to North America. The third family to arise, Caninae, remained small in both body size and number of species throughout much of its history, but flourished after the Borophaginae became extinct in the Pleistocene (Wang and Tedford 2010) (Figure 1.1). Caninae are now found worldwide in all continents except Antarctica. The introduction of *Canis lupus dingo*, a subspecies of grey wolf, to the Australian landmass, is assumed to have been facilitated by humans around 1000-5000 years ago, and is not a true indigenous species (Fillios and Taçon, 2016). The sequential iterations of canids were closely related to the successes of their competitors and prey. Prey species, in turn, are

ultimately if not directly, dependent on plant material which itself responds to, and contributes toward, global climatic changes. Global cooling and drying throughout the Eocene, Oligocene and Miocene epochs lead to a decline in broad leaf forests, and an increase in bushlands and grasslands. Although not happening geographically simultaneously, this broad shift in habitat occurred in all continents (Janis *et al.*, 2004). Many of the small herbivorous mammals that had browsed on forest plants, evolved into larger grazing species, capable of processing tougher and drier vegetation (Janis, 1993; Lovegrove and Mowoe, 2013). The diet of grazing mammalian herbivores consists mainly of grass, and these species exhibit morphological adaptations to cope with a coarse diet that is low in nutrients. Some of these adaptations relate directly to the processing of food such as the development of hypsodont dentition, and the enlargement of the gastrointestinal tracts into fermentation chambers to allow nutrient extraction from cellulose (Janis, 1993; Lovegrove and Mowoe, 2013). In addition, their limbs became elongated and simplified to achieve an unguligrade form (Figueirido *et al.*, 2015). The shift from browsing to grazing forced an increase in body mass. Fermentation requires bulk processing of vegetation and animals below ~10kg cannot ferment enough material at a fast enough rate to meet their basal metabolic requirements. The mean body mass of the unguligrade predecessors was ~2kg in the early Paleocene. The early unguligrade species had an increased mean body mass of ~50kg by the middle Miocene, which increased to ~ 200kg by the late Miocene (Lovegrove and Mowoe, 2013). Consequently, predators capable of tackling them coevolved in terms of size and behavior (Figueirido *et al.*, 2015). Canid predators of large herbivorous mammals not only had to be capable of tackling substantial prey, they also had to compete with other carnivorous species. In North America, the decline of other meat-eating guilds such as the creodonts and nimravids (false sabre toothed cats) in the late Oligocene and early Miocene, coincided with the expansion and diversification the Hesperocyonid canids. As Hesperocyonid body size increased, their morphology indicates a move toward specialized

hypercarnivory, with larger teeth and shorter muzzles (Van Valkenburgh, 1999). These early canids were then largely superseded by species from other families, Amphicyonids, Hemicyonines, Mustelids and Ursids, many of whom had more pronounced cursorial adaptations (Van Valkenburgh, 1999). The mid-late Miocene saw the rise of the Borophaginae canids, alongside felids, in North America (Hunt and Tedford, 1993; Hunt, 1996). The Borophaginae canids were very diverse and occupied the greatest number of ecological niches of any canid subfamily. The larger hypercarnivorous Borophagines appeared to outcompete the Amphicyonids and Hemicyonines (Van Valkenburgh, 1999). Hypercarnivorous canids appeared at times when other North American hypercarnivorous species, including creodonts (extinct carnivorous mammals), Nimravids, Mustelids and Amphicyonids (extinct bear dogs), were less diverse and offered less competition for food (Van Valkenburgh, 2007). The Borophagines were the dominant group of carnivores in North America for several million years throughout the Miocene period (Wang and Tedford, 2010). Even after the reappearance of felids in North American fossil record at around 18Ma, Borophaginae canids continued to prosper, possibly because each group developed broadly different hunting strategies, and as such were not direct competitors. Felids tend to be lone stealth hunters and prefer to remain under the cover of densely wooded forest (Wang and Tedford, 2010; Walmsley, 2012). The Borophaginae canids became differentiated from felids by developing rudimentary cursorial adaptations, such as the lengthening of the limbs (Van Valkenburgh, 1987). They also sacrificed the sharp retractile claws of the felids in favour of short tough claws to aid grip on terrain at speed, and so became more dependent on their dentition for dealing with prey (Wang, 1993; Van Valkenburgh *et al.*, 2003; Andersson, 2005). A major extinction event in the late Miocene at around 5-8Ma removed up to 80% of North American genera (Janis, 1993; Van Valkenburgh, 1999). This period saw the decline of the Borophaginae canids. Low diversity, high specialisation and giant size are often signs of terminal lineages in carnivores (Wang and Tedford, 2010). This pattern was seen as the



Borophaginae first increased in body size and hypercarnivory, and then began to die out and were superseded by the less specialized Caninae.

**Table 1.1 Summary of Canidae evolution**

Epoch	Ma	Event
Palaeocene (66-57Ma)	65	Dinosaurs become extinct, mammals start to diversify to fill the newly vacated niches, carnivorans first appear (in the Viverradae family) <sup>2,5,8</sup> .
Eocene (56 -34Ma)	56	The ancestral group of the canids, the Miacidae, arise from the Viverravids. These early canids are the size of weasels to small foxes <sup>2</sup> . They continue to slowly diversify throughout the Eocene <sup>8</sup> .
	40	The first identifiable canid, Prohesperocyon, appears in North America. This displays the diagnostic anatomy of canids - inflated auditory bullae, carnassial teeth and lack of upper third molar tooth. This is shortly followed by the emergence of Hesperocyon <sup>2,5,6</sup> .
	37	Climatic cooling resulted in less tropical forests, and more open grasslands <sup>1</sup> . Canids start to move away from plantigrade stance to a more digitigrade one. Adaptations to enable running allows them to co-evolve with the increasingly cursorial herbivores and may be key to their future success <sup>4</sup> .
	36	
	35	
Oligocene (33- 24Ma)	30	Three subfamilies evolve from Hesperocyon; Hesperocyoninae, Borophaginae, and Caninae <sup>2,4,7,9</sup> . Caninae were confined to a few small fox-like species of <i>Leptocyon</i> <sup>8</sup> .
Miocene (23- 6Ma)	18	Hesperocyoninae begin to die out and the Borophaginae increase in number and diversity. At this time point many hyper and hypocarnivorous species existed, and canids filled more environmental niches than at any other timepoint in their history <sup>8</sup> . Borophaginae start to become larger and more hypercarnivorous <sup>2,3,4,9</sup> .
	15	Caninae species start to diversify. This is attributed to a change in climate favouring grassland, which in turn favoured cursorial herbivores, in turn favouring the cursorial canids above other predators <sup>1</sup> . The Caninae already exhibited some cursorial adaptations that were lacking in the Borophaginae (slender distal limbs with a reduced first phalanx), which put them at a greater advantage <sup>4</sup> during pursuits. Borophaginae start to decline. Vulpini tribe within Caninae appear <sup>5,8</sup> .
	6	Caninae begin to prosper due to the dying off of the smaller Borophagines. For the first-time canids break out of north America via the Bering strait and start to colonise Europe and then, Africa <sup>8</sup> .
Pliocene (5- 3Ma)	5	Canids arrive in Asia <sup>5,8</sup> .
	3	The isthmus of Panama land bridge between north and south America appears and canids start to migrate to south America <sup>2,5,8</sup> .
Pleistocene	2	The last of the Borophagines become extinct leaving Caninae as the only surviving subfamily of canids. The combination of anatomical adaptations for cursorial hunting, an abundance of prey and land bridges opening access to most of the land masses of the world created the greatest period of canid expansion <sup>2,3,4,5,7,8</sup> .
Holocene	1	36 extant species of canid

1. Janis, 1993
2. Valkenburgh, 1999
3. Wang *et al*, 1999
4. Andersson and Werdelin, 2003
5. Wang *et al.*, 2004
6. MacDonald, 2009
7. Tedford *et al.*, 2009
8. Wang and Tedford, 2010

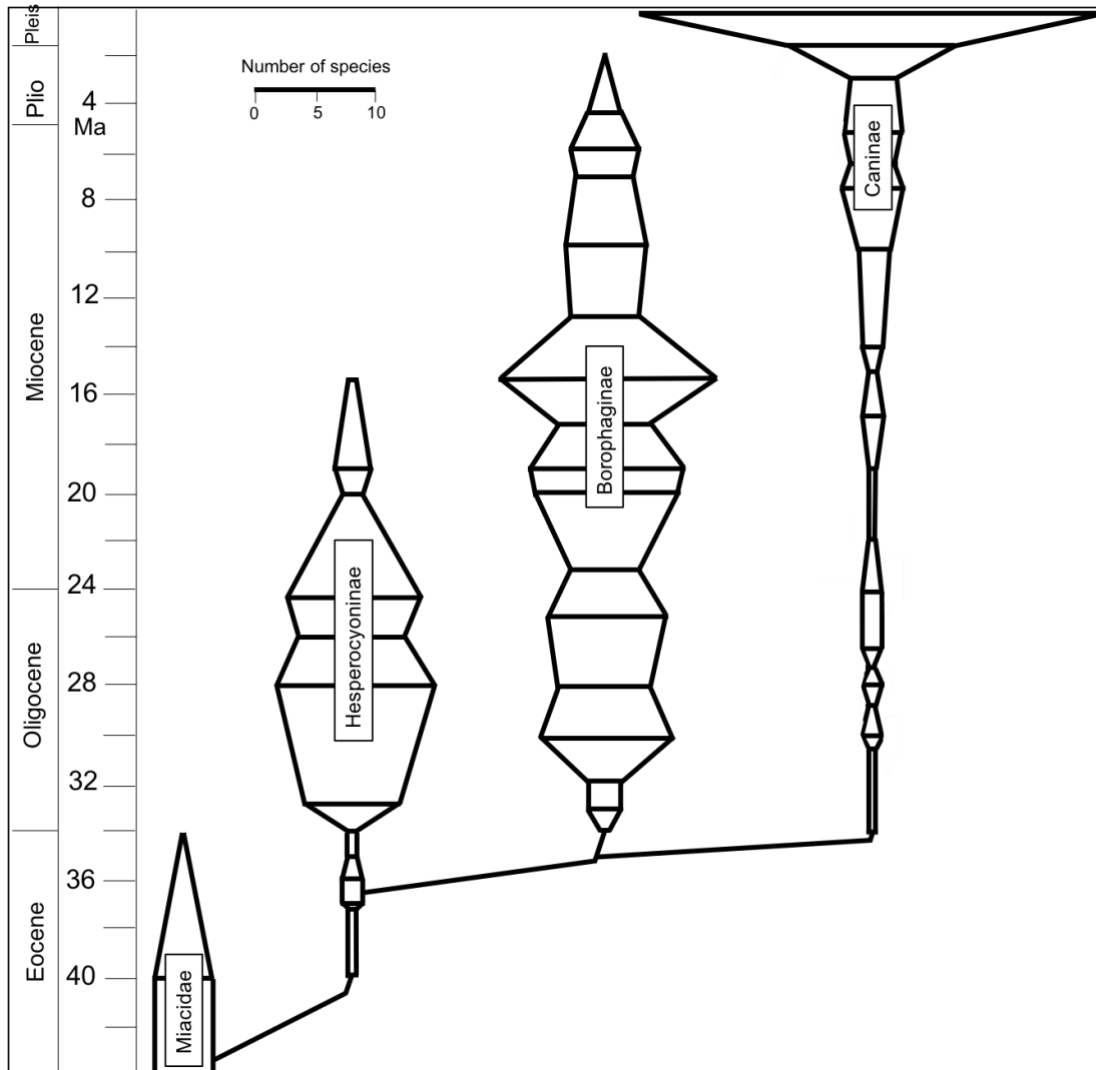


Figure 1.1 Diversity of species through time in the three subfamilies of Canidae, after Wang and Tedford (2010).

### 1.2.3 The rise of the Caninae

The subfamily Caninae originated from the North American landmass and remained confined to this continent for much of their history (Wang *et al.*, 2004; Prevosti *et al.*, 2009; Tedford, *et al.*, 2009; Sotnikova and Rook, 2010). Fossil evidence shows *Leptacyon*, the precursor to all modern canids, existing in various small weasel to fox sized forms from around 30 Ma to around 8 Ma (Van Valkenburgh, 1999; Wang and Tedford, 2010). With the opening up of ecospace previously occupied by the Borophagines, the Caninae began to flourish. At around 10 Ma the first major branch from *Leptacyon* developed into the *Vulpes* clade, and another branch soon after became the *Eucyon* clade, which later evolved to be the *Canis*

clade. *Leptocyon*, the first recognised member of the Caninae, became extinct around 9Ma. Around 8Ma the Caninae began to migrate beyond North America, and specimens start to appear in the fossil record in Europe, Africa and Asia (Hunt, 1996; Van Valkenburgh, 1999; Wang and Tedford, 2010). The timing of the sudden expansion of both the number of Caninae species and their geographical dispersal is complex and has caused much debate. The Bering strait land bridge existed long before canids dispersed to Europe, Africa and Asia, and yet they appeared not to have moved out of North America until the late Miocene (Wang and Tedford 2010). A number of related theories have been proposed. Firstly, the Bering region was highly forested and as such precluded early canids from moving into it as the contemporaneous felids dominated this type of environment. Another possibility is that the changing anatomy of the new Caninae species towards a more cursorial form (longer limbs with a reduced skeleton) allowed canids to cover greater distances and they began to utilise the new grassland landscapes that were opening up within the North American landmass (Van Valkenburgh, 1987; Van Valkenburgh, 1999; Andersson and Werdelin, 2003). Researchers have also proposed that canids were able to cross the Bering land bridge but were met with such strong competition from existing felids and hyaenids that they failed to gain any significant foothold, and it was only the decline in these species that allowed wide geographical dispersal of canid species (Wang and Tedford, 2010). As none of these theories are mutually exclusive, in all probability it was a combination of competitive and environmental factors that allowed for this great canid radiation into Europe, Asia and Africa. This complex scenario differed from the canid expansion into South America approximately 3Ma, which occurred as a result of the Panamanian land bridge opening due to global cooling (Wayne et al., 1997; Van Valkenburgh, 2007; Nyakatura et al., 2012; Tchaicka et al., 2016). Few large carnivores existed in South America before this time and the lack of competition from other sympatric species allowed multiple migrations of canids into South American where they quickly radiated and diversified into many environments (Berta, 1987;

Wozencraft, 1993; Van Valkenburgh, 1999; Sillero-Zubiri *et al.*, 2004; Perini *et al.*, 2010; Prevosti, 2010; Tchaicka *et al.*, 2016).

The mass radiation of canids happened over a relatively short period of time (Nyakatura *et al.*, 2012), which is one of the factors that makes categorisation of modern canids so difficult. To discriminate between closely related species a great quantity of genomic sequence is required to yield enough informative nucleotide sites for unambiguous reconstruction of phylogenetic trees (Lindblad-Toh *et al.*, 2005). For this reason, the current taxonomy of canids is, at least partially, unresolved, and most authors acknowledge that any detailed phylogenetic trees have some branches that are poorly supported by the evidence. However, some common themes populate the literature: it is widely supported that the grey foxes (*Urocyon*) are a basal clade that separated from the other modern canids early at the start of the last radiation and formed a sister group to all other extant canids. The remaining species fall into two groups - one of which contains *Otocyon megalotis*, *Nyctereutes procyonoides* and all of the *Vulpes* species, and one which contains all other species, including jackals, wolves and the South American foxes. (Wayne *et al.*, 1997; Zrzavý and Řičánková, 2004; Lindblad-Toh *et al.*, 2005; Agnarsson *et al.*, 2010; Perini *et al.*, 2010; Nyakatura *et al.*, 2012). Many authors agree that the South American canids form a monophyletic clade. However, divisions within the South American group are less clear. Some authors speculate that there are two groups - *Chrysocyon brachyurus* and *Speothos venaticus* form one group, and all of the South American foxes form the other group (Lindblad-Toh *et al.*, 2005; Perini, *et al.*, 2010). However, other studies (Bardeleben *et al.*, 2005; Lindblad-Toh *et al.*, 2005) consider that both *Chrysocyon brachyurus* and *Speothos venaticus* may be better aligned to other clades. Nyakatura places *Speothos* with *Lycaon pictus* as a sister clade to all remaining canini. Bardeleben considers that *Chrysocyon brachyurus* may be grouped with either the South American foxes, the wolf like canids or *Speothos venaticus*.

#### 1.2.4 Extant canid taxonomy

Order carnivora

Suborder caniforma

Superfamily cynoidea

Family Caninae

Tribes – canini and vulpini

There are 34 - 38 species within 10 - 14 genera of extant canid, all belonging to the subfamily Caninae (Wozencraft, 1993, 2005; Macdonald and Sillero-Zubiri, 2004; Nowak, 2005; MacDonald, 2009; Wang and Tedford, 2010). The uncertainty in quantifying the exact number of genera and species is accounted for in the ambiguity relating to their classification. This is occasionally due to new species being discovered and therefore not being recognised in older texts. However, it occurs more often due to the taxonomic revision of existing species. Revised species are often subsequently given new common and/or binomial names. The classification of species, even using advanced molecular techniques, is also often confounded by hybridisation between similar species who, by nature or human intervention, share the same geographic territory. Whether a group of related animals are a species or subspecies may also be contentious. Many recent examples highlight these confounding factors: the wolf may be classified as one species (*Canis lupus*) (Wilson and Reeder, 2005), two species (*Canis lupus* and *Canis rufus*) (Nowak, 2005), or three species (*Canis lupus*, *Canis rufus* and *Canis lycaon*) (Kyle *et al.*, 2006). Similarly, *Canis aureus lupaster*, the Egyptian Jackal, was formerly considered to be a subspecies of *Canis aureus*, the golden jackal. However, following work that highlighted morphological similarities between *Canis aureus lupaster*, and *Canis lupus* (Ferguson, 1981), further studies using molecular analysis of DNA, have confirmed that *Canis aureus lupaster* is closely related to *Canis lupus* (Rueness *et al.*, 2011; Koepfli *et al.*, 2015). As to whether this is now a subspecies of *Canis lupus* or a phylogenetically distinct species continues to be debated, as does the possibility of re-

naming (Sillero-Zubiri *et al.*, 2004; Koepfli *et al.*, 2015). Similarly the dingo (*Canis lupus dingo*) is described as either a subspecies of domestic dog (*Canis lupus familiaris*) (Nowak, 2005), or a subspecies of *Canis lupus*, possibly derived from the Indian wolf subspecies, *Canis lupus pallipes*, (Sillero-Zubiri, *et al.*, 2004; MacDonald, 2009). Further examples of taxonomic revision within the canid clade include the raccoon dog, *Nyctereutes procyonoides* which is arguably separable into two distinct species (Kauhala and Saeki, 2004), and *Vulpes zerda* which is named as *Fennecus zerda* when placed in its own genus, *Fennecus*, (Geffen *et al.*, 1992; Wayne *et al.*, 1997; Nowak, 2005), but called *Vulpes zerda* when placed within the *Vulpes* genus (Macdonald and Sillero-Zubiri, 2004; Sillero-Zubiri *et al.*, 2004). Similarly, the arctic fox has the binomial *Alopex lagopus* when placed in its own genus (*Alopex*) (Macdonald and Sillero-Zubiri, 2004; Nowak, 2005), or *Vulpes lagopus* when considered as belonging within the *Vulpes* genus

Notwithstanding ongoing taxonomic deliberations, for the purposes of this thesis I follow the categorisation and nomenclature from Wilson and Reeder (1993). The later edition (Wilson and Reeder, 2005) reclassifies *Alopex lagopus* as *Vulpes lagopus*. For detailed descriptions of species used in this study see 'Species details' in Appendix 1.

### **1.2.5 Phylogenetic trees**

Published phylogenetic trees of Caninae (Zrzavý and Řičánková, 2004; Lindblad-Toh *et al.*, 2005; Nyakatura *et al.*, 2012) have used molecular and morphological analyses to attempt to clarify the evolutionary history and relationships between the extant canids. Lindblad Toh *et al.*'s (2005) molecular analysis allows the canids to be grouped into four main clades: the red fox-like clade, the wolf-like clade, the South American clade and the grey fox-like clade (Figure 1.2). The more recent tree by Nyakatura *et al* (2012) concurs with these groupings with the exception of placing *Speothos venaticus* with the wolf like clade, rather than the South American clade (Figure 1.3). Zrzavý and Řičánková (2004) executed multiple tree

based on different datasets, both molecular and morphological, and concludes that *Speothos venaticus* is difficult to place, sometimes grouping with the South American subset, and sometimes with the wolf subset.

For all of the phylogenetic analyses within this study I used the tree published by Nyakatura *et al.* (2012), as this was an open source resource and is widely cited within the literature (Rolland *et al.*, 2014; Michaud *et al.*, 2018; Prevosti and Forasiepi, 2018; Rizzuto *et al.*, 2018; Wu *et al.*, 2018).

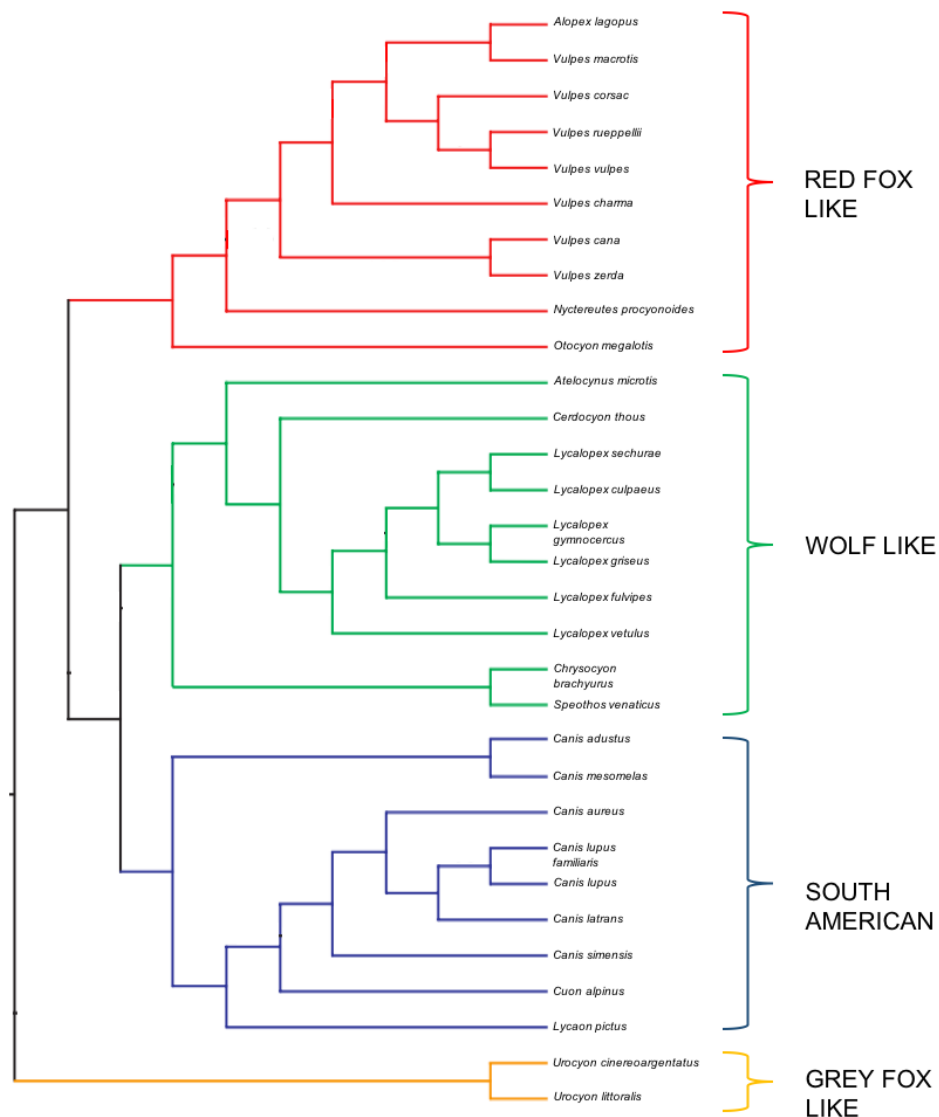


Figure 1.2. Phylogenetic tree of the extant Caninae from Lindblad-Toh *et al.* (2005).



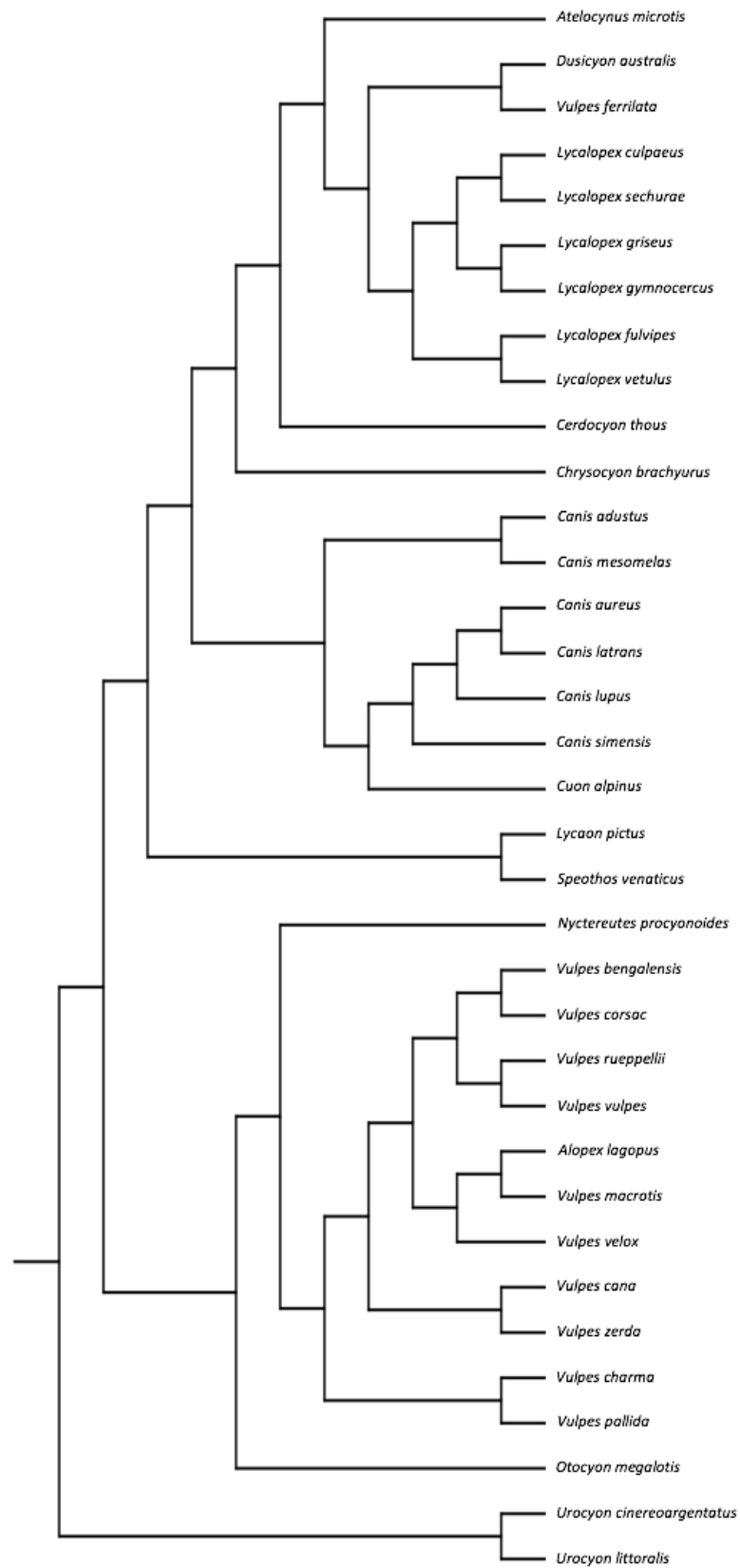


Figure 1.3 The complete downloaded tree from Nyakatura *et al.* (2012). This differs from the Lindblad-Toh *et al.* (2005) tree in the placement of *Speothos venaticus* with the wolf like species, rather than the South American species.

### **1.3 Canid anatomy.**

The focus of this thesis is the gross functional anatomy of the canid head, specifically the structure and function of the jaw adductor muscles and their relationship to the skeleton of the head. Jaw adduction plays a key role in acquisition and processing of food, and in drinking, panting and social behaviours such as grooming and vocalisation. This thesis focuses on jaw adduction in relation to masticatory function, that is, biting for food acquisition and processing. In order to contextualise the role of the head, I firstly consider the post cranial anatomy with regard to hunting and digestion. To highlight some of the salient anatomical adaptations I briefly compare the canids to their close carnivoran counterparts, felids, ursids and mustelids, plus some of their prey species, chiefly large and small herbivorous mammals. Carnivoran competitors must be well matched in the functionality of prey capture, killing and food processing, whilst herbivorous prey must be equalled in speed and manoeuvrability to ensure hunting success in at least some pursuits. In part 1.3.2 I describe the features of the generic mammalian head salient to this thesis, and focus on properties particular to canids.

#### **1.3.1 Post cranial form and function.**

Two important influences have shaped how the canids specialise and differ from the basic mammalian quadruped blueprint: that they, like nearly all carnivorans, are meat eaters, and that they, unlike most carnivorans, are adapted for cursorial hunting (Wayne 1986; Van Valkenburgh, 1987; Figueirido *et al.*, 2015). Cursorial animals have evolved to run both quickly and efficiently, often for sustained periods of time. These factors greatly influence both cranial and post cranial anatomy, and trade-offs in functionality, for example that the dexterity of the distal limbs is sacrificed for a reduced lightweight skeleton, are common. Such compromises often have consequent effects on cranial anatomy. For instance, species unable to use their forelimbs to apprehend prey must rely on their jaws and teeth to do so.

#### 1.3.1.1 Spine

The canid spine is made up of seven cervical, thirteen thoracic, seven lumbar, three sacral and up to twenty coccygeal vertebrae. The areas that exhibit the greatest flexibility are the cervical region, where flexion of the neck is important for obtaining and manipulating food and drink, plus it is essential for grooming, and the caudal thoracic and lumbar region (Getty, 1975; Evans and De Lahunta, 2013; Singh *et al.*, 2018). It is the great flexibility at the caudal thoracic and lumbar region that allows the alternating spinal flexion and extension seen in the fast gallop of canids. At such high pace the distal part of the hindlimbs may be placed alongside or in front of the distal forelimbs, greatly extending overall stride length, which is the goal of all cursors (Hildebrand *et al.*, 1995). One notable feature of the lumbar vertebral region is the relatively short transverse processes of the vertebrae which are reduced as they do not need to support the extensive musculature needed to contain a large abdomen as seen in herbivores. In addition, the articular processes of the lumbar vertebra do not display the pronounced 'interlocking' form that is frequently seen in herbivorous species (Dyce *et al.*, 2009; Getty, 1975). The interlocking processes create a strong, rigid and inflexible spine which is able to support the weight of the enlarged herbivore gastrointestinal tract, and so are not necessary in the canid. The intervertebral discs, the collagenous soft tissue structures that lie between the vertebrae and are not present when regarding skeletal material alone, are also diagnostic of spinal function. It is the relatively large size of the intervertebral discs in canids, especially in the cervical and lumbar regions that contributes towards enhanced flexion and extension in this region (Evans and De Lahunta, 2013). In ungulates the intervertebral discs account for around 10% of the overall spine length, but they make up around 16% in dogs (Dyce *et al.*, 2009). In carnivores, the deeply lobed appearance of the viscera lying within the central part of the trunk i.e. the lungs in the thorax and the liver in the abdomen, also reflect the increased degree of spinal movement as this allows the individual lobes to slide over one another during ventral flexion, rather than

become compressed. In contrast, the straight-backed ungulates have only shallow or even absent divisions between the lobes of their lungs and liver.

#### 1.3.1.2 Neck

The neck of the canids distinguishes them from other carnivorans. Within the neck the nuchal ligament runs from the first cervical vertebra, the axis, to first thoracic vertebra and is continuous with the supraspinous ligament. It is a thick elastic structure and helps support the weight of the head, whilst conserving muscular effort (Hildebrand *et al.*, 1995; Dyce *et al.*, 2009; Evans and De Lahunta, 2013). Within the extant carnivorans, only canids possess a nuchal ligament, and within the canid guild it is only the extant subfamily, the Caninae, that do so (Wang and Tedford, 2010). Inference from fossil remains suggests that the nuchal ligament was absent in both the extinct Hesperocyoninae and Borophaginae families. Felids too lack a nuchal ligament, which has led to speculation it acts as a compensatory device to offset the longer neck, and hence the longer lever arm, of canids (Hildebrand *et al.*, 1995). Not only is the canid neck relatively longer than that of the felid, it also has relatively less muscle mass, and so is weaker (Dyce *et al.*, 2009). The short well-muscled neck of the felids allows for more powerful control over their prey during the kill (Macdonald, 1992). Fossil evidence shows that the extinct canid families also had shorter stockier necks and may have hunted and killed in a similar way to modern felids (Wang and Tedford, 2010; Andersson, 2005). Felids, and extinct canids, had shorter faces, and hence shorter nasal cavities, which may imply less of a reliance on olfaction, and a greater reliance on sight for hunting. Wang and Tedford (2010) posit that the longer length of the canid neck is needed to follow scent trails that are located primarily on the ground, and that the lengthening of the neck may have been particularly necessary due to the lengthening of the limbs that is seen in the Caninae subfamily.

The relative weakness of the long slender canid neck is not disadvantageous when hunting small prey (Macdonald, 1992; Wang and Tedford, 2010). As hypercarnivory evolved in the Caninae, individuals formed packs to disarm and kill large quarry. Neck strength may be one of the morphological constraints of modern canids that consigns them to a pack hunting lifestyle. Hildebrand (1952) notes that the modern hypercarnivorous canids, *Canis lupus*, *Cuon alpinus* and *Lycaon pictus*, do have slightly shorter necks than predicted for canids of their body mass, and so maybe are evolving towards more hypercarnivorous forms.

#### 1.3.1.3 Limbs

Morphological cursorial adaptations of the limbs are less pronounced in canids than in their large herbivorous prey. Although predator and prey species must be well matched to maintain a sustainable ecological equilibrium, canids have the advantage of a flexible spine, something that the herbivores, with their large rounded abdomens, are unable to achieve (Getty, 1975; Hildebrand *et al.*, 1995; Singh *et al.*, 2018). Ungulates, constrained by their relatively rigid spine, demonstrate extreme cursorial adaptations of the limbs, whilst canids demonstrate only a moderate elongation of the limbs (Getty, 1975; Hildebrand *et al.*, 1995). The different anatomical adaptations which are allied to dietary constraints, ensure that the top running speeds of large prey species such as bison (*Bison bison*), wildebeest (*Connochaetes*) and zebra (*Equus zebra*) are well matched to that of their hypercarnivorous pursuers such as *Canis lupus*, *Cuon alpinus* and *Lycaon pictus*. In his review paper of mammalian running speeds, Garland (1983) describes *Canis lupus*, *Lycaon pictus* and *Canis mesomelas* as all exceeding running speeds of 60km/h. Their prey, such as bison (*Bison bison*), zebra (*Equus zebra*) and various Cervidae, are recorded as having similar maximum speeds of between 56-65km/h (Mech, 1970; Garland, 1983). A defining feature of the limbs of the cursorial mammals is the simplified range of movement to simple protraction and retraction, with little or no rotational or abduction movements, especially in the forelimbs

(Van Valkenburgh, 1987). Although the proximal limbs demonstrate some cursorial adaptation they retain relatively large and robust bones to accommodate the muscle masses required to move the limbs (Getty, 1975; Hildebrand *et al.*, 1995; Singh *et al.*, 2018). The more distal segments of the limbs are elongated with reduced skeletal and muscular components (Hildebrand *et al.*, 1995). Specific limb related cursorial adaptations are discussed below.

### Forelimb

The lateral compression of the ribcage is a key anatomical trait seen in cursorial mammals. It allows the scapulae to be positioned on the lateral aspect of the thorax, and so act as a functioning part of the limb (Hildebrand *et al.*, 1995; Kardong, 2015). This is in contrast to more primitive species or those that are adapted for climbing, where the scapulae lie on the dorsal or posterior surface of a dorsoventrally flattened thorax (Hildebrand *et al.*, 1995; Kardong, 2015). The scapulae in cursorial mammals are enabled to protract and retract, effectively lengthening stride length (Hildebrand *et al.*, 1995). In form, the cursorial scapulae are simplified and the bony prominences such as the coracoid and acromion are vestigial or absent (Hildebrand *et al.*, 1995; Kardong, 2015; Singh *et al.*, 2018). In extreme cursors such as equids, the dorsal border of the scapula is also extensively enlarged by an unossified rigid cartilaginous process which increases the long axis of the scapula, in effect lengthening limb length and thus stride length (Hildebrand *et al.*, 1995; Getty, 1975). Canid scapulae demonstrate only small acromial, coracoid and hamate processes, and lack the suprahumeral process found in felids (Getty, 1975; Evans and De Lahunta, 2013; Singh *et al.*, 2018). The reduced form of the cursorial scapula reflects their limited range of motion. Although the glenohumeral joint retains the ancestral ball and socket morphology, functionally it acts as a hinge joint allowing only fore and aft movements to any degree. The strong tendons of insertion of the subscapularis, supraspinatus and infraspinatus muscles act

as collateral ligaments running proximodistally across the joint to restrict any lateral or rotational shoulder joint movements (Evans and De Lahunta, 2013). The clavicle is absent or vestigial in cursors (Oxnard, 1968; Hildebrand *et al.*, 1995). In the equids and bovids, no trace remains, whereas in the canid, a small tendinous line indicates the ancestral position and in some specimens this may ossify in later life (Getty, 1975; Dyce *et al.*, 2009; Thrall and Robertson, 2015). The effect of losing or reducing the clavicle has two major implications. Firstly, there is no fixed bony connection of the shoulder region to the axial skeleton, and freed from such constraints, the shoulder joint may be drawn extensively cranially or caudally, considerably increasing stride length. Secondly, the muscles attaching to the clavicle, cleidomastoideus, cleidocervicalis and cleidobrachialis, unite to become one long straplike muscle, brachiocephalicus (Evans and De Lahunta, 2013). This extensive muscle runs from the caudal skull and dorsal neck to the distal cranial surface of the humerus, and is a powerful protractor of the forelimb. Felids retain a small bony clavicle, and although it does not articulate with any other part of the skeleton and is skeletally functionally obsolete, it serves to clearly delineate the individual muscles of brachiocephalicus (Getty, 1975; Evans and De Lahunta, 2013; Singh *et al.*, 2018). The more complex shoulder anatomy of felids, with more prominent scapula processes and a bony clavicle, reflects the wider range of shoulder movement which is utilised during grappling prey and climbing (Getty, 1975; Evans and De Lahunta, 2013; Singh *et al.*, 2018). Within the carnivorans, forelimb anatomy is also characteristic of specific hunting methods (Van Valkenburgh, 1985; Van Valkenburgh, 1987; Andersson, 2004). Current literature cites three methods of hunting that are allied to forelimb morphology: ambush, pounce/pursuit and pursuit (Andersson and Werdelin, 2003; Janis and Figueirido, 2014; Figueirido *et al.*, 2015). The humeral component of the elbow joint in particular, is diagnostic of predatory habit (Andersson and Werdelin, 2003; Janis and Figueirido, 2014; Figueirido *et al.*, 2015). Ambush predators, have wide (from medial to lateral) elbow joints, capable of a large degree of pronation and supination in the

antebrachium, an action used for grappling prey and climbing (Andersson, 2004). Ambush predator elbow morphology is considered to be the generalised condition and is found in all early forms of carnivores, including the early Caninae. Ambush predators are seen extensively in the extant felid ursid and mustelid families where the laxity of the joint allows for the forelimbs, with their sharp claws, to be used tackling prey (Andersson and Werdelin, 2003). No ambush predator elbow morphologies are found within the extant canid species, as these were superseded by more cursorial forms from the late Miocene (Andersson and Werdelin, 2003).

Around 7Ma pounce/pursuit elbow morphologies began to appear in the Caninae lineage, followed at around 2Ma by the most derived form, the pursuit predator elbow morphology (Figueirido *et al.*, 2015). Pursuit hunters have a narrow (from medial to lateral) elbow joint which is relatively fixed in the prone position, allowing only very limited rotation of the distal limb (Andersson, 2005). The distal condyle of the humerus, composed of the capitulum and trochlea, that articulate with the radius and ulna respectively, is much narrower than in the ambush predators (Andersson and Werdelin, 2003). This form limits rotation, increases stability, and enables the elbow to function primarily as a hinge joint, which is of great benefit to efficient sustained trotting and running. Canid pursuit hunters are represented by the modern species *Canis lupus*, *Cuon alpinus* and *Lycaon pictus* (Janis and Figueirido, 2014; Figueirido *et al.*, 2015) who specialise in long distance pursuit and endurance hunting. All other extant canids are pounce/pursuit hunters, specialising in short distance sprinting and either grabbing prey by the neck or pouncing to restrain them with their forepaws. Pounce/pursuit hunters, have an intermediate morphology, with a moderately narrow humeral condyle.

The bones of the brachium and antebrachium are relatively long and slim and have a very congruent elbow joint to promote stability whilst running (Getty, 1975; Hildebrand *et al.*, 1995; Singh *et al.*, 2018). In canids and felids, the radius and ulna maintain their identity as



two separate bones, but they have become united and reduced in the ungulates. The ability to pronate or supinate the distal antebrachium or paw is still very evident in felids, much reduced in canids, and due to the fused nature of the antebrachial bones, completely absent in the ungulates. Muscles associated with rotation of the distal limb are correspondingly evident: in the cat, two supinators, brachioradialis and supinator, and two pronators, pronator teres and pronator quadratus, are clearly present. The canids usually possess all four muscles although the brachioradialis is very slight. Ungulates have none of these muscles, their function is obsolete and their mass would only add to the weight of the distal limb (Getty, 1975; Dyce *et al.*, 2009; Liebich *et al.*, 2009; Evans and De Lahunta, 2013). The bones of the carpus are reduced and simplified in all cursorial species. In canids and felids, the radial and intermediate carpal bones are fused. Equids variably lack a first carpal bone and ruminants lack a first carpal bone and the second and third carpal bones are fused (Dyce *et al.*, 2009; Liebich *et al.*, 2009). Range of motion at the carpal joint is largely confined to simple flexion and extension. The majority of canids and all felids have five metacarpal bones and associated phalanges, although the most medial is much reduced, and colloquially called the dew claw. The dew claw is vestigial and has little function but may play a small role in food manipulation. The first digit is lost altogether in *Lycaon pictus*, and the second and third digital pads are usually fused in this species. Both of these adaptations of reduction and simplification, have been associated with the very cursorial lifestyle of *Lycaon* (Sillero-Zubiri *et al.*, 2004; MacDonald, 2009). To aid the semi-aquatic lifestyle of the bushdog, *Speothos venaticus*, it has partially webbed feet (Zuercher *et al.*, 2004). Ruminant ungulates have fused metacarpal bones three and four, and digits two and four are represented by vestigial remnants. In equids, the most extreme cursorial limb adaptations are evident with digit three becoming the only weight bearing component, and vestigial remains of digits two and four evident as small splint-shaped bones.

Canids, with their moderate limb adaptations, deploy a digitigrade stance, where at normal standing position only the palmar or plantar aspects of the phalanges, or more accurately their footpads, are in contact with the ground. Ungulate species are, by definition unguigrade, that is, weight bearing on only the tips of the digits, protected by the structure of the horny hoof (Hildebrand *et al.*, 1995; Kardong, 2015, Singh, 2018). Ruminants bear weight on two hooves, and equids on one single hoof per limb. The canids have well developed digital and metacarpal/metatarsal footpads. These structures consist of a densely cornified epidermis covering a collagenous fatty pad. They act to cushion and protect the bony structures of the foot and their roughened appearance may aid grip in slippery conditions (Nickel *et al.*, 1981). Canid claws are blunt and non-retractile. Canids appear to have lost the ability to retract their claws early in their evolutionary history, with the fossil remains of the early *Hesperocyon* species showing reduced phalangeal lateral ridges that housed the retracted claws (Andersson, 2005; Wang and Tedford, 2010). The assumption follows that non-retractile claws are blunt as they are eroded by exposure to the ground. This indicates a move away from arboreal dwelling to ground dwelling as sharp claws help with climbing (Wang and Tedford, 2010). The function of blunt claws is to aid grip on even ground, scratching for parasite removal and for digging, either to unearth prey or to dig dens for shelter. They do not function as a weapon to catch prey or as grappling irons to aid tree climbing, both actions which are seen in the felids (Hildebrand *et al.*, 1995; Andersson, 2005; Wang and Tedford, 2010).

### Hindlimb

The ilium of the pelvis of the ungulates is relatively vertical. The effect of this is to bring the sacroiliac joint directly above the hip joint, which aids in carrying the heavy burden of the trunk (Getty, 1975). This is less important in the carnivore species as they have proportionally smaller and lighter abdomens, and consequently have a more obliquely orientated pelvis

with the sacroiliac joint cranial to the hip joint. The more oblique angle of the canid ilium increases the effectiveness of the abdominal muscles in flexing and extending the spine, which aids the bounding gait of the carnivores. Unlike the ball and socket arrangement of the shoulder joint, the ball and socket formation of the hip joint in carnivores is still capable of rotational movements, for example during squatting and leg cocking activities associated with urination and scent marking (Evans and De Lahunta, 2013). The range of movement at the hip joint in ungulates is much more restricted. Ruminant hip anatomy allows for a small amount of outward rotation, which allows the flexed stifle to avoid hitting the abdomen during fast gait (Dyce *et al.*, 2009). Equids possess an accessory ligament, which runs from near midline as a detachment of the prepubic tendon, and passes under the transverse tendon at the point of the acetabular notch, to insert on the femoral head. This effectively prohibits abduction or rotational movements of the equine hip, another example of their extreme cursorial adaptation (Getty, 1975; Dyce *et al.*, 2009; Liebich *et al.*, 2009). In both canids and ungulates, the femur is around one fifth longer than the humerus, to compensate for the lack of an elongate lateral girdle bone, as in the scapula in the forelimb. The skeleton of the distal hindlimb, like that of the forelimb is simplified in form and reduced in mass. The tibia and fibula are both present in the carnivores, although the fibula is very slight. In ruminants the fibula shaft is absent with only the proximal and distal extremities remaining. In equids the fibula is very slight and only the proximal half is present (Getty, 1975; Dyce *et al.*, 2009; Liebich *et al.*, 2009). As in the forelimb carpus, there is a similar pattern of bones in the tarsus, with fusion and reduction of certain bones, simplifying the overall arrangement. Bones, integumentary and soft tissue structures of the pes are very similar to those of the manus in all species.

#### 1.3.1.4 The gastrointestinal tract

The gastrointestinal tract is concerned with the acquisition, mechanical and chemical processing of nutrients, and the elimination of waste. As, in essence, it is a modified tube running from the mouth to the anus, the oral cavity is the first part of the tract. The masticatory apparatus, that is the structures involved in chewing within the oral cavity, include the jaws and their muscles, teeth, tongue and salivary glands. The remaining parts of the tract are the oesophagus, stomach and the small and large intestines. The jaws and the muscles that power them, are discussed extensively throughout this work, but here I briefly cover the gross anatomy of the remaining tract. Associated gastrointestinal structures (e.g. salivary glands, pancreas and liver) are not discussed.

The nutritional quality of the food plus the methods of procuring it all have a great impact on the morphology and relative size of the component parts of the gastrointestinal tract. Although I am unaware of any published studies comparing the gross anatomy of the gastrointestinal tract of different species of canid, from my personal observations of the digestive tracts of *Vulpes vulpes*, *Lycaon pictus* and *Cuon alpinus* I can remark that they are all grossly very similar to one another and also to that of the domestic dog. Meat is a very nutritious food source and requires relatively little processing to gain great nutrient resource, and consequently the gastrointestinal tract in carnivorans is relatively short and simple. This is in contrast with species that follow a herbivorous diet who must have greatly expanded fore or hindgut fermentation chambers to break down complex carbohydrates into easily absorbable simple starches. Ruminant species are foregut fermenters with a greatly enlarged stomach, and equid species are hindgut fermenters with a greatly enlarged large intestine (Dyce *et al.*, 2009). The poor nutritional quality of the herbivore diet also means that food must be consumed in great quantities to gain sufficient nutrition. The average combined length of the small and large intestine in the canid is around five times body length which in a large domestic dog would equal around five to six metres. In

comparison, the length of the intestines in the horse is around ten times the body length, equaling around 30 metres in a large horse, and in the ox the intestinal tract is around 20 times the body length, a total of up to 63 metres (Nickel *et al.*, 1979). The economical proportions of the canid tract are not its only advantage. Unlike herbivores that must eat for up to 18 hours per day and constantly process food to fuel their needs, carnivorans often exist in a 'feast or famine' regime, where large meals may be taken infrequently. The great distensibility and capaciousness of the carnivore stomach allows canids to make the most of any opportunity to gorge. The stomach of an average sized domestic dog has a capacity of up to 9L (Nickel *et al.*, 1979). When empty it lies completely within the intrathoracic part of the abdominal cavity, but when fully distended its caudal limit extends as far into the abdomen as the fourth lumbar vertebra (Nickel *et al.* 1979). It is this great distensibility that not only allows gorging on plentiful food supplies, for instance after a large kill, but also allows food to be transported back to the den to feed weaned offspring. A short, simple and often empty tract takes up considerably less room in the abdominal cavity than a large one that is constantly full (Getty, 1975; Evans and De Lahunta, 2013; Singh *et al.*, 2018). This has two advantages; it weighs less, which takes up less energy to carry around, and it allows for a dorsoventrally flexible spine (Hildebrand *et al.*, 1995). Although, to my knowledge, there are no studies comparing gut transit times in all canid species, studies have been done on domestic dogs, and less frequently on wolves, and due to the similarity in gross anatomy, it may be fair to extrapolate this data to the broader range of canid species. In brief, animal derived protein based diets in wolves and dogs have gut transit times of between eight and fifty-eight hours depending on content (Floyd *et al.*, 1978; Kreeger *et al.*, 1997; Iwanaga *et al.*, 1998; Bruce *et al.*, 1999; Boillat *et al.*, 2000; Lefebvre *et al.*, 2001; Rolfe *et al.*, 2002; Hernot *et al.*, 2005). Indigestible content such as hair, decreases transit time, and one theory is that wolves strategically consume the hair of large carcasses to accelerate gut transit time to permit them to quickly eat again from the same kill (Peterson and Ciucci, 2003). Wolves

may consume up to 10kg of meat per day (Mech and Boitani, 2003; Peterson and Ciucci, 2003). At the other dietary extreme, dogs also have the ability to survive with little or no meat content in their diet, allowing them to thrive in a wide variety of environmental conditions. At certain times of the year for example, the diet of the maned wolf consists of around 50 - 64% vegetable matter, and fruit, nuts and seeds make up large proportions of the autumnal diet of many foxes (MottaJunior *et al.*, 1996; Rodden, *et al.*, 2004; MacDonald, 2009). The ability to exist on a low meat diet is due to the canid's ability to synthesize taurine, an amino acid that is essential to virtually all body systems (Hand and Lewis, 2000). The potential for omnivory gives dogs an advantage over other carnivorans such as felids and mustelids, who, due to their inability to synthesize taurine must obtain it from ingested animal protein, and consequently are obligate carnivores (Sjaastad *et al.*, 2010; Miller and Fowler, 2014).

### **1.3.2. Anatomy of the head.**

The head is arguably the most complex region of mammalian anatomy, both morphologically and functionally. It houses the major component of the central nervous system, the brain, plus the special sensory organs associated with vision, olfaction, gustation, hearing and balance. It also houses the start of both the gastrointestinal and respiratory tracts. In this section I describe the anatomy associated with jaw adduction only, that is the bones of the skull and mandible, and the jaw adductor muscles, with reference to the work of previous authors.

#### **1.3.2.1. The skeleton of the head.**

All mammalian skulls follow a modified synapsid pattern with regard to the pattern of individual bones that contribute to the unified whole (Vaughan *et al.*, 2013; Kardong, 2015). It can be seen from the wide diversity of mammalian form that within this broad blueprint,

morphology is highly varied, reflecting the vast array of mammalian adaptations (Hildebrand *et al.*, 1995; Kardong, 2015). Accordingly, nomenclature varies between authors when describing the elements that make up the skull, and differences in classification occur, even within genera. In canids, some authors describe 11 paired bones, occurring on the left and right of the skull to make 22 bones, plus seven unpaired bones, which lie ventrally and medially, giving a total of 29 bones (Dyce *et al.*, 2009; Liebich *et al.*, 2009). Other authors (Getty, 1975; Evans and De Lahunta, 2013) describe 31 skull bones as they classify the dorsal and ventral nasal turbinate bones as separate entities rather than projections from the internal nasal and maxillary surfaces. The smaller bones associated with the skeleton of the head are the nine hyoid bones and six middle ear bones. See Figure 1.4 for labelled diagrams of bones of the skull.

The bones of the skull are joined to one another with sutures and synchondroses that variably ossify during life. The skull can broadly be divided into two regions or modules: the facial/palatine component consisting of the incisive (premaxilla), maxilla, vomer, nasal, zygomatic, palatine, lacrimal, and pterygoid bones, and the cranium consisting of the parietal, interparietal, frontal, temporal, basisphenoid, presphenoid, ethmoid and occipital bones. The mandible is the third major skeletal component of the head (Dyce *et al.*, 2009; Evans and De Lahunta, 2013). This is usually counted as one bone, but sometimes as two when classified as distinct left and right elements. Although morphologically distinguishable, the division between the three areas is not as well defined functionally, with many actions, (e.g. chewing, breathing and swallowing), utilising all three components simultaneously. Modularity of the skull is further discussed in Chapter Three, part 3.3.2.2.

#### Embryological origins of the bones of the skull.

Not all of the bones of the skull share the same embryological origin. The ventral bones of the skull are derived from three cartilaginous tissue types, all of which develop from neural

crest cells (Hall, 2005). The parachordal and trabecular cartilages fuse to form the chondocranium, which lies ventral to the brain, and the pharyngeal arch cartilage forms the hyoid apparatus, bones of the middle ear, the laryngeal cartilages and part of the mandible (Hall, 2005; Evans and De Lahunta, 2013). The bones forming the dorsal cranium arise from membranous tissue to form the desmocranium. The chondocranium and desmocranium unite to form the skull. Development of the mandible is complex with a cartilaginous rod, Meckel's cartilage, arising from pharyngeal arch one, and elongating and expanding to fuse rostrally at the mandibular symphysis (Evans and De Lahunta, 2013). Membranous bone subsequently forms around Meckel's cartilage, which itself also undergoes ossification (Stevens-Sparks and Strain, 2014). The mandible is therefore made of both cartilaginous and membranous derived bone.

Ossification of the membrane derived bones occurs before those derived from cartilage, and the maxilla, frontal nasal incisive, palatine, zygomatic, mandibular and parietal bones have begun to ossify by day 32 in the domestic dog embryo (Evans and Sack, 1973; Williams and Evans, 1978). Ossification of the cartilage derived bones begins to occur from day 35 to day 50 (Evans and Sack, 1973; Williams and Evans, 1978; Evans and De Lahunta, 2013). In the region of the dorsocaudal border of the mandible a secondary cartilage develops, ossifies and fuses with the main body of the mandible to form the condylar process. The final skeletal component of the skull to begin to ossify is the hyoid apparatus where ossification begins to occur from day one until two months after birth (Evans and Sack, 1973; Williams and Evans, 1978; Evans and De Lahunta, 2013).



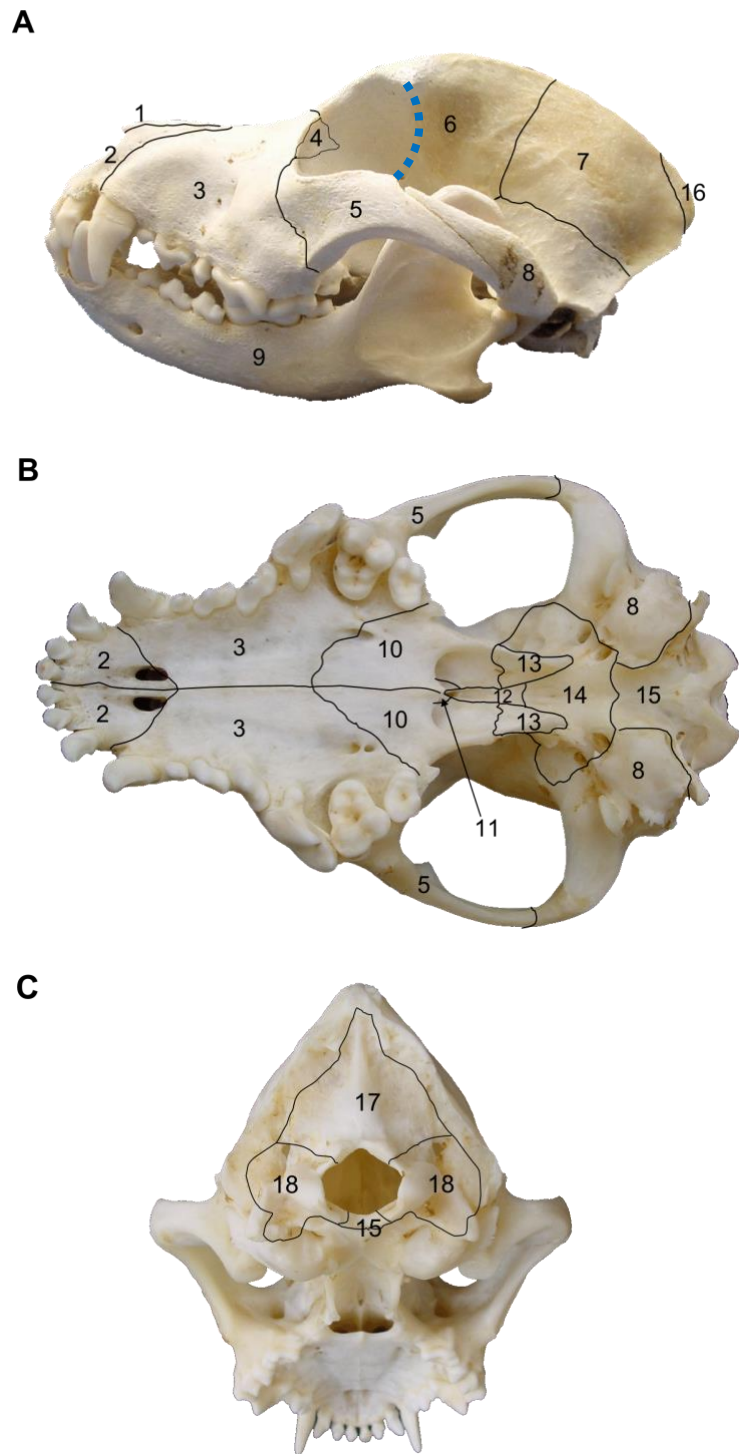


Figure 1.4 Bones of the skull. A, Lateral Skull and mandible, B, Ventral Skull, C, Caudal Skull. 1 nasal, 2 incisive, 3 maxilla, 4 lacrimal, 5 zygoma, 6 frontal, 7 parietal, 8 temporal, 9 mandible, 10 palatine, 11 vomer, 12 presphenoid, 13 pterygoid, 14 basisphenoid, 15 basioccipital, 16 interparietal, 17 supraoccipital, 18 exoccipital. The ethmoid bone is completely hidden from view in the intact skull. The dashed blue line indicates the position of the orbital ligament.

### Macroscopic structure of bone.

There are two categories of bone structure: compact bone and trabecular bone. Nomenclature varies between texts and compact bone is also referred to as cortical bone, and trabecular bone is also referred to as spongy or cancellous bone. Both cartilaginous and membrane derived bones can develop into either bone type. Compact bone consists of concentrically arranged densely packed lamellae arranged around neurovascular channels called Haversian canals. Compact bone forms the dense outer part of all bones. Trabecular bone is found within the bone cavity and consists of many small struts of bone attaching to the inner lamellae of the compact bone. The orientation of the trabecular struts chiefly follows Wolff's law, with many struts broadly reflecting the direction of the primary stresses the bone is subject to (Gefen and Seliktar, 2002; Mitchell and Peel, 2009; Young *et al.*, 2014).

### Shape of the bones of the skull

Most of the dorsal bones of the head are classified as flat bones, *ossa plana*. These consist of external and internal layers of compact bone, and an intermediate layer of trabecular bone called the diploë (Hall, 2005; Dyce *et al.*, 2009). However, none of the bones of the skull are entirely flattened, and even the 'flat' bones are curved and consist of often expansive and intricate projections. For example, the temporal bone is subdivided into three divisions: squamosal, petrous and temporal (Getty, 1975; Evans and De Lahunta, 2013; Singh *et al.*, 2018). In canids, only one part of the squamous division, the plate making up the caudolateral cranial vault is flattened (Evans and De Lahunta, 2013). Other parts of the bone make up the highly complex bony middle and inner ear structures, the caudal zygomatic arch and the mandibular fossa (Figure 1.4) (Getty, 1975; Evans and De Lahunta, 2013; Singh *et al.*, 2018). The ventral bones of the skull are termed irregular bones, *ossa irregulata*, to describe their complex form and various projections and processes (Getty, 1975; Liebich *et al.*, 2009).

## Diploë

In many mammalian species, the flat bones of the cranium consist of a trilaminar arrangement whereby diploë, areas of trabecular bone, lie between the innermost and outermost layers of compact bone. The diploë increase in volume nearer the centre of flat bones of the skull, away from the sutures (Mcelhane *et al.*, 1970). The structures of diploë in mammalian cranial bone appear to be highly varied with random patterns of trabecular struts throughout (Mcelhane *et al.*, 1970). Lynnerup *et al.* reported in studies of human cranial bone that diploe thickness related to overall cranial vault thickness, and did not differ relative to age, body mass or height in human subjects. Their study also found that the only region to demonstrate sexual dimorphism were the diploe within the frontal bone, where male diploe were thicker than those found in female specimens (Lynnerup *et al.*, 2005). Whilst a physiological role has been determined for the diploe, i.e. it houses bone marrow and thus contributes to haematopoiesis, the biomechanical function of the diploe is debated. Most authors acknowledge the diploe as a device to thicken the skull without adding excessive mass (Copes and Kimbel, 2016), and other authors also describe them as a way of creating a disparity between the inner surface area of the cranium and the outermost surface (Sharp and Rich, 2016). Other authors have also suggested that the diploe may also serve to act as an energy absorbing layer, reducing the impact of external forces, and to increase the bending strength of the cranium (Motherway *et al.* 2009; Rahmoun *et al.*, 2014).

## Cranial sutures and synchondroses.

Two types of joints separate the bones of the skull. Sutures are the fibrous joints between the membrane formed bones or between membrane formed bones and cartilage formed bones (Hall, 2005; Geiger and Haussman, 2016). Synchondroses are cartilaginous joints between the cartilage formed bones. In the immature animal, the sutures and synchondroses clearly demarcate the margins of the individual bones, but as the animal ages

most of the sutures ossify and unite adjacent bones. As the mammalian skull follows a similar basic pattern regarding the number and position of bones that make up the skull, it follows that the position and name of the sutures and synchondroses that lie between them are also broadly homologous. The degree of suture interdigitation between bones follows a standard arrangement: some sutures present relatively straight alignments with their neighboring bones as seen in the plane and limbous forms of the zygomaticotemporal and internasal sutures. These are associated with regions of skull that experience tension (Herring and Teng, 2010). Other sutures or synchondroses are arranged as tortuous interdigitations between opposing bones, as seen in the denticulate and serrate sutures of the fronto-maxillary and maxillo-palatine sutures, and are characteristic of compression resistance (Rafferty and Herring, 1999; Burn *et al.*, 2010). Within this broad pattern, and at a finer level of detail, species have particular and identifiable patterns of cranial suture arrangements (Brunner *et al.*, 2004; Wilson and Sánchez-Villagra, 2009). Species that can generate high bite forces, eat obdurate foodstuffs, or that compete through head-butting behaviors are shown to have a more complex interdigitated pattern suggesting an adaptive morphology to specific loading (Jaslow, 1990; Monteiro and Lessa, 2000; Byron, 2009;2018; Buezas *et al.*, 2017). The sutures and synchondroses perform three major functions. Firstly, to unite the bones of the skull whilst allowing for small measures of movement, notably during birth (Ogle *et al.*, 2004). Secondly, the synchondroses and sutures are the primary areas for bone formation in the skull during ontogeny and allow for areas of rapid interstitial growth (Opperman, 2000; Ogle *et al.*, 2004; Kolpakova-Hart *et al.*, 2008). This is particularly evident in the bones forming the calvarium to allow for brain expansion (Ogle *et al.*, 2004). Thirdly, they play a role in mechanical stress absorption (Jaslow, 1990; Herring and Ochareon, 2005; Curtis *et al.*, 2013; Goswami *et al.*, 2013; Geiger and Hausman, 2016). In particular the suture microstructure suggests that the orientation of the collagen fibres reflects their biomechanical function. Fibres with straight orientation are found in sutures

undergoing tensile forces, and fibres with oblique orientation are found in sutures undergoing compressive forces (Rafferty and Herring 1999; Kolpakova-Hart *et al* 2008).

The extent of and timing of closure of sutures varies within mammals. Fusion occurs when growth slows down or ceases, and varying heterochronous patterns are seen across mammalian genera (Rager *et al.*, 2014). Goswami *et al.* (2013) concluded that the caniform carnivorans displayed a greater number of heterochronous shifts in cranial suture fusion when compared to feliforms, which may account for the greater diversity of cranial shape in canids. In canids some sutures remain patent throughout life, most notably the zygomaticotemporal suture and the internasal suture (Goswami *et al.*, 2013; Thrall and Robertson, 2015). Landon *et al.* (1998) also report the basisphenoid/presphenoid synchondroses as late or never closing in the wolf. Whether this reflects a continued need to attenuate force, or a diminished need to transmit force in these regions is not established at present.

#### Paranasal Sinuses.

The paranasal sinuses are air filled diverticula of the nasal cavity that arise from the pneumatization of the diploe in post-natal development (Singh *et al.*, 2018). In bones where well-developed sinuses are present, the shape of the outer and inner surfaces of the bone may be significantly different (Singh *et al.*, 2018). Developmental expansion of the sinuses during ontogeny accounts for some of the differences in head shape between immature and mature animals (Getty, 1975; Evans and De Lahunta, 2013; Singh *et al.*, 2018). Individual paranasal sinuses are named after the bones that they invaginate, although they can extend into several other bones of the skull. In the canids, the maxillary sinuses have a wide communication with the nasal cavity and are often termed the paranasal recesses (Evans and De Lahunta, 2013). The sphenoidal sinus is small and lies within the presphenoid bone. The largest and most defined sinus in canids is the frontal sinus (Getty, 1975; Evans and De

Lahunta, 2013; Thrall and Robertson, 2015; Singh *et al.*, 2018). The presence of a frontal sinus is also used to recognise Canidae within the fossil record, and all major subfamilies of Canidae exhibit evidence of frontal sinuses throughout their lineage (Huxley, 1880; Tedford, *et al.*, 1995; Wang, *et al.*, 1999; Tedford *et al.*, 2009). The frontal sinuses lie between the inner and outer tables of the frontal bone and are subdivided by bony septa into three divisions. Each division communicates independently with the caudal nasal cavity. The functions of mammalian paranasal sinuses are not well understood. Many authors have speculated as to their function which I briefly summarise here. Firstly, that they may serve to alter head shape to enhance performance by enlarging areas of muscle attachment (Curtis and Van Valkenburgh, 2014). Secondly, they may help to dissipate stresses during biting (Bookstein *et al.*, 1999; Prossinger *et al.*, 2000; Farke, 2008; Tanner *et al.*, 2008; Curtis and Van Valkenburgh, 2014). Thirdly that they may offer thermal or mechanical protection to the deep skull contents (Davis *et al.*, 1996). Fourthly that they may have a role to play in respiratory physiology as proposed by Lundberg *et al.*, after their discovery that nitrous oxide (NO) is produced within the paranasal sinuses. The role of NO is to enhance pulmonary oxygen intake as it acts as a vasodilator (Lundberg *et al.*, 1994). Or finally, as several authors suggest (Márquez, 2008; Rae and Koppe, 2008; Zollikofer and Weissmann, 2008; Curtis and Van Valkenburgh, 2014) they may simply act as biological ‘spandrels’, in effect simply filling spaces between functionally meaningful structures. The concept of spandrels was first posited by Gould and Lewontin and considers the viewpoint that not all anatomical differences must have adaptive significance, and many morphologies arise as a result of incidental spaces or structures due to incongruities between regions of functional significance (Gould and Lewontin, 1979).

### Mandibular symphysis.

The lower jaw consists of the left and right mandibles. In carnivorans the degree of fusion between the two mandibles at the mandibular symphysis varies widely. Scapino (1981) studied 23 genera of carnivorans and classified them as having one of four types of mandibular symphysis. Type I showed very little unification, with a fibrocartilage pad between the two halves and a relatively high degree of independent mobility. At the other extreme, Type IV showed complete bony fusion and no independent movement. Scapino also noted that symphysis type appeared to be independent from other morphological and behavioural factors such as dentition, temporomandibular joint shape, body mass, diet and feeding behaviour.

Scapino (1985) defined all genera of canids except for *Speothos*, as Type I. He noted that *Speothos* has much higher degrees of fusion, and classified the single *Speothos* specimen in his study as Type IV. I conducted a brief review of freely available online CT scans of *Speothos* specimens and concur that in this species the mandibular symphysis is usually well fused. The specimen used in this thesis was not fully dissected at the mandibular symphysis but CT reconstructions show a closely united linear division between left and right halves, so may have not been fully fused, although this may have been as a consequence of immature age, which was unrecorded in this specimen.

The advantage of semi-independent mandibles may be to allow for subtle realignment of teeth during biting, possibly to orientate them to advantage or to protect their sectorial surfaces. Scapino describes the widening of the posterior part of the mandibular symphysis to aid in aligning upper and lower carnassial teeth during unilateral carnassial biting (Scapino, 1965). Movement at the symphysis may also allow the joint to act as a shock absorber under duress, and limit forces transmitted to the skull (Gans, 1961).

The cost of having semi-independent hemi mandibles is that forces transmitted to one side of the mandible are not readily transferred to the other. Transference of force may be

advantageous during unilateral biting where high force is required. Therefore, if the masticatory muscles are powerful enough to allow for required force to be recruited on one side, fusion is not required and is lost at the expense of mobility.

#### Orbital ligament

The morphology of the lateral orbit of the eye is diverse in mammals (Cox, 2008; Jasarevic *et al.*, 2010). Most mammals display the primitive condition with a collagenous structure, the postorbital ligament, extending from the zygomatic process of the frontal bone to the frontal process of the zygomatic bone. This is the condition found in canids. The postorbital ligament makes up approximately one quarter of the circumference of the orbit in the domestic dog (Evans and De Lahunta, 2013). The role of the postorbital ligament is unclear. Its position, bridging the gap between the zygomatic arch and the frontal bone, implies it may have a functional use during mastication. As the masseter contracts and displaces the arch ventrally, forces may be transmitted across the post orbital ligament, in effect supporting the zygomatic arch (Buckland-Wright, 1978, Herring *et al.*, 2011). However, other authors dispute this and speculate it may protect the orbit of the eye from injury (Prince, 1953; Simons, 1962), or help to stabilize the eye during temporalis contraction (Cartmill, 1970, 1980). The biomechanical role of the post orbital ligament is explored further in Chapter Five.



### 1.3.2.2 Dentition

In all mammals, the form of the rostral part of the skull reflects the requirements of the dental apparatus. The dentition of the canids is specialised to reflect their carnivorous diet but retains much of the basic mammalian plan. The typical eutherian mammal has 44 teeth, with each quadrant of the jaw having three incisors, one canine, four premolars and three molars (Hildebrand *et al.*, 1995; Kardong, 2015). Most evolutionary adaptations away from the primitive condition are a reduction in the number of teeth, with the exception of cetaceans, one canid and one armadillo species, who all demonstrate increased numbers of teeth (Armfield *et al.*, 2013). Unlike some other families of carnivorans, most notably felids and ursids, the cursorial specialisation of the canid distal limbs renders them ineffective for prey apprehension, and consequently the dentition is used for capture, submission and killing of prey and for food processing. In this section I describe the general dentition of *Canis lupus familiaris*, as this takes the form of the generic canid and is well documented in the literature. Species specific differences are described in the next section. All canids demonstrate diphyodont, brachydont and heterodont dentition (Gorrel, 2004; Tutt *et al.*, 2006; Dyce *et al.*, 2009; Evans and De Lahunta, 2013). Diphyodont dentition is the replacement of the deciduous teeth seen in juveniles, with the permanent teeth of adults. The embryological derivation of the teeth is from the ectoderm and mesoderm of pharyngeal arch one. Tooth enamel is formed from the ectoderm, and the dentine and cementum from mesoderm. In domestic dogs, the deciduous dentition of puppies erupts between day 20 and 35 after birth, although the teeth have become calcified from day 55 of gestation (Evans and De Lahunta, 2013). Deciduous teeth start to be shed and replaced by the permanent dentition from two months, and all permanent teeth have fully erupted by around seven months (Williams and Evans, 1978; Gorrel, 2004; Gioso and Carvalho, 2005; Tutt *et al.*, 2006; Dyce *et al.*, 2009; Evans and De Lahunta, 2013). Adults have more teeth than pups: the first premolar erupts late and is not replaced, but remains throughout life, and all of the molars

have no deciduous counterpart and are only present in the permanent adult dentition. The generic canid dental formula is:

Deciduous I3/3, C1/1, PM3/3 x2 = 28

Permanent I3/3, C1/1, PM4/4, M2/3 x 2 = 42 (Figure 1.5)

I – incisors, C – canines, P – premolars, M – molars

Brachydont dentition describes the condition where the crown of the tooth is fully erupted by adulthood and is entirely covered with enamel. The overall form of the teeth can be described as tuberculosectorial, with all teeth except the canines exhibiting greater or lesser degrees of tubercles, and all teeth having a sectorial or cutting component (Getty, 1975; Tutt *et al.*, 2006; MacDonald, 2009; Evans and De Lahunta, 2013). All carnivorans exhibit distinct heterodont dentition, with four categories of teeth, each specialising in particular tasks. The individual tooth morphologies are particularly distinct in the canids (Figure 1.5) (Peterson and Ciucci, 2003). The incisors are adapted for grooming and nibbling, and in young adults the unworn upper incisors take the form of a tri-lobed crown, and the lower ones a bi-lobed crown. This incisive formation usually reduces to a simple peg form with age and wear (Gorrel, 2004; Tutt *et al.*, 2006; Dyce *et al.*, 2009). The large canine teeth curve caudally and have no lobes or tubercles. They are well designed for stabbing and gripping prey. The length of the canines impacts on the space between the upper and lower jaws, i.e. the size of prey that can be accommodated and killed, and so a trade-off must occur between canine tooth length and functional gape width. Canine teeth have the longest crown of any teeth, and their root is even more extensive at nearly twice the length of the crown (Gorrel, 2004; Dyce *et al.*, 2009; Evans and De Lahunta, 2013). The roots of the canine teeth are usually wider and more massive below the gum line, an arrangement that, along with their caudally curved shape, keeps them securely anchored within their alveoli during prey capture and food

processing (Gorrel, 2004; Dyce et al., 2009; Evans and De Lahunta, 2013). The first premolars are single cusped and single rooted. The second and third premolars of the upper arcade, and premolars two, three and four of the lower arcade are double rooted, and the fourth upper premolar has three roots, reflecting its greater bulk (Getty, 1975; Evans and De Lahunta, 2013). The premolar tooth roots tend to diverge within the mandible and maxilla, and are often longer than the crowns, making them very well anchored for grappling and processing prey (Gorrel, 2004; Dyce et al., 2009; Evans and De Lahunta, 2013). The first lower molar is very large with correspondingly massive roots (Gorrel, 2004; Dyce et al., 2009; Evans and De Lahunta, 2013). The remaining molars are much smaller with a flattened tubercular appearance to the crown. Both upper molars and lower molars one and two have short diverging roots, whilst lower molar three is single rooted (Gorrel, 2004; Dyce et al., 2009; Evans and De Lahunta, 2013). Lower molar one (LM1) and upper premolar four (UPM4) constitute the carnassial dentition that is particular to carnivorans, which together act as a shearing blade to slice skin and meat from carcasses (Gorrel, 2004; Gioso and Carvalho, 2005; Dyce et al., 2009; Evans and De Lahunta, 2013). There is some overlap of function between the premolars and molars, with the carnassial teeth variably exhibiting both slicing and crushing functions (Getty, 1975; Evans and De Lahunta, 2013). LM1 in particular, exhibits a wide variety of morphological variation between canid species, and is indicative of diet (Ewer, 1973; Van Valkenburgh, 1991; Biknevicius and Ruff, 1992; Van Valkenburgh and Koepfli, 1993; Van Valkenburgh, 1996; Macdonald and Sillero-Zubiri, 2004; Sillero-Zubiri *et al.*, 2004; MacDonald, 2009).

### Dental occlusion

Unlike herbivorous mammals, carnivoran dentition does not exhibit an extensive flat occlusal 'table', as the teeth are not used as a grinding surface. Normal occlusion in the canids protects and maintains the enamel and sharp cutting surfaces of the teeth and follows a

complex and precise arrangement. The crowns of the upper incisors are positioned rostral to the crowns of the lower incisors, the tips of the crowns of the lower canines lie rostral and medial to the tips of the crowns of the upper canines within an interdental space. As the mandibular dental arcade is anisognathic, being narrower and shorter than that of the upper arcade, the lower cheek teeth lie medial to their upper counterparts. The sharp cusps of the first three upper premolar teeth interdigitate with the spaces between the premolar teeth of the lower arcade. The upper premolar teeth do not contact the lower premolar teeth but instead a small gap is maintained at occlusion, often referred to as the carrying space (Hobson, 2005; Tutt *et al.*, 2006; Dyce *et al.*, 2009; Evans and De Lahunta, 2013). The lower carnassial tooth lies medial to the upper carnassial tooth at occlusion, creating a shearing pair during biting. The largest process of the lower carnassial tooth fits into a small fossa on the hard palate at occlusion (Evans and De Lahunta, 2013). The relatively flat molars maintain contact with their upper or lower counterparts at normal occlusion (Hobson, 2005; Evans and De Lahunta, 2013). This arrangement preserves the sharp cutting edge of the large teeth used for killing prey and processing meat, the canines, premolars and carnassials. An important factor in protecting teeth by moderating chewing patterns and bite force is the proprioceptive feedback modulation mechanism. Mechanoreceptors within the periodontal ligament associated with the alveolus of each tooth detect forces acting upon the teeth and provide sensory feedback to the brain via the trigeminal nucleus. This mechanism regulates bite force to provide an appropriate amount of bite force and ensure that the tooth cusps are not brought into occlusion too rapidly or too strongly (Lund, 1991; Piacino *et al.*, 2017).

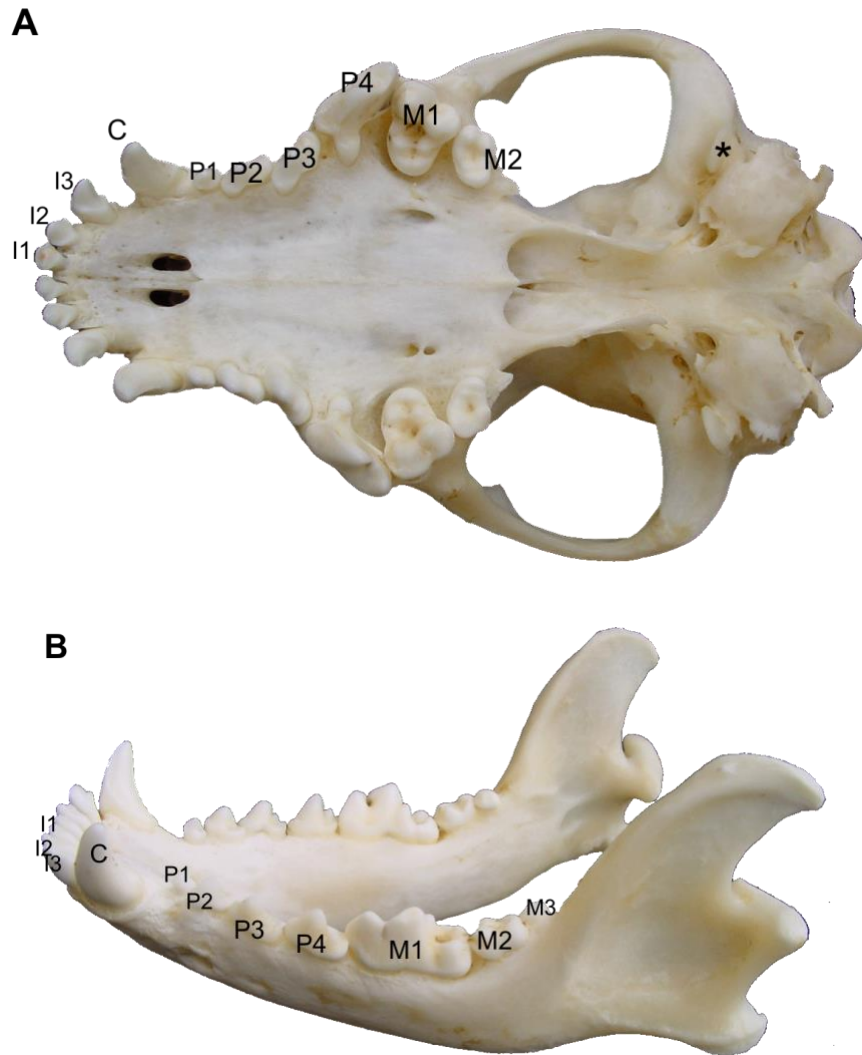


Figure 1.5 Generic canid dentition. A, ventral aspect of skull, B, Dorso-lateral aspect of mandible. I – Incisor, C – Canine, P = Premolar, M- Molar. The asterisk marks the retroglenoid process of the temporal bone. Normal dental occlusion can be seen in Figure 1.4A.

#### Species specific dental adaptations and variations

The dentition of some of the canid species diverges from the generic description in two ways: firstly, the number of teeth, and secondly the form of the individual teeth. The form of the teeth describes both their size and shape. All of these factors affect the functionality of biting. Size and shape determine how the teeth interact with foodstuffs, and their placement within the jaws relative to the TMJ, influences the force with which they can come together.

Three of the hypercarnivorous species, *Cuon alpinus*, *Lycaon pictus* and *Speothos venaticus* have evolved an entirely slicing function of the LM1, elongating the cutting blade and replacing the caudal basin-shaped talonid with a sharpened edge, the trenchant heel (Ewer, 1973; Van Valkenburgh and Koepfli, 1993). The fourth hypercarnivore, *Canis lupus*, has an intermediate form of talonid, lying between the three other hypercarnivores and all other canid species (Ewer, 1973; Van Valkenburgh and Koepfli, 1993). It is this feature that confounded early taxonomists who erroneously classified these species as close relatives. However, molecular analyses conclude that this feature has evolved separately in all four lineages, and demonstrates convergent evolution (Zrzavý and Řiřáňková, 2004; Lindblad-Toh *et al.*, 2005; Nyakatura *et al.*, 2012). Two of the hypercarnivorous species have reduced dentition: *Cuon alpinus* has only two lower molar teeth instead of the usual three, and *Speothos venaticus* has only one upper molar and two lower molars (de Mello Beisiegel and Zuercher, 2005), reducing the total number of teeth to 38. As the molars lie at the most caudal end of the dental arcade, reducing either their size or number has the effect of shortening the muzzle and bringing both the canine and carnassial teeth closer to the TMJ, which in turn increases the force of the piercing and slicing apparatus respectively. However, a trade-off must occur between bite force and gape (Dumont and Herrel, 2003; Slater and Van Valkenburgh, 2009; Perry *et al.*, 2011). Teeth nearer to the TMJ have more power driving them, but the space between the upper and lower teeth at wide gape needs to be such that it allows sizeable pieces of food to be processed. Pack hunters are often in competition for their kills, with either other pack members or different species, and food must be removed from the carcass, chewed and swallowed with great haste. Excessive reduction of either the number or size of the post carnassial teeth would therefore restrict the functionality of the jaw. In small prey and generalist dentition, lower molar one has a shorter cutting blade rostrally, a distinct talonid basin caudally, and the molars are relatively larger (Ewer, 1973; Macdonald and Sillero-Zubiri, 2004; MacDonald, 2009). The enlarged bunodont formation

of the molars provides a greater crushing and grinding surface for tackling a wide variety of foodstuffs (Ewer, 1973; Macdonald and Sillero-Zubiri, 2004; MacDonald, 2009). In one species, *Urocyon megalotis*, whose diet consists almost solely of invertebrates, the molars are not only increased in number (variably three or four upper molars and four or five lower molars), but also zalambdodont in shape, even the carnassial teeth, which indicates a diet high in coarse material (Sillero-Zubiri *et al.* 2004). Lengthening the tooth row also has the effect of positioning the teeth that catch prey, the canines, further from the TMJ. As in the third-class lever model this lessens the force that can be generated at the canine bite point but increases the speed with which the canines can come together, an advantage in catching fast moving prey.

#### 1.3.2.3 Movement of canid jaws.

There are four major requirements for movement of the canid jaw. Firstly, the ability to close the jaws with sufficient force to capture and subdue struggling prey and process tough food. Forces of struggling prey are chiefly ventrally and rostrally and must be opposed by caudal and dorsal bite forces (Maynard-Smith and Savage, 1959; Greaves, 2012). Secondly, a stable temporomandibular joint is required to restrict lateral and rostrocaudal jaw movements. This is achieved by the bony components that make up the TMJ, with the cylindrical form of the condylar process of the mandible neatly fitting into the transversely elongated gully of the mandibular fossa of the temporal bone. This congruent arrangement limits any translational movements and protects the tooth enamel from any potentially damaging malocclusion (Getty, 1975; Evans and De Lahunta, 2013; Singh *et al.*, 2018). There is also a pronounced bony retroglenoid process that prevents caudal luxation of the TMJ (Figure 1.5A). The very prescribed occlusal closing arc allows the carnassial teeth to shear past each other for effective biting, and the congruent TMJ also allows for the jaws to close with great strength without the risk of dislocation. This is especially important when dealing

with struggling prey and tough foodstuffs (Getty, 1975; Smith, 1993; Greaves, 2012). Thirdly, a wide gape is required to allow sufficient space between upper and lower canine teeth when apprehending and killing prey, and to allow sizeable chunks of food to be inserted laterally into the oral cavity and be processed by the carnassial teeth. Not only do the jaws need to be able to attain a wide gape, but they must also maintain a powerful bite force whilst doing so (Greaves, 1983; Smith, 1993). Lastly, the jaws need the capacity for fast closing (Maynard-Smith and Savage, 1959; Smith, 1993). This is more important in species that hunt by lone stealth. Stealth hunters surprise their quarry, and as such their prey may have the energetic capacity to outrun them if not overpowered quickly. Long jaws are advantageous in allowing the rostral most teeth to come together at great speed, and hunters of small prey have longer jaws than those that hunt large prey (Slater *et al.*, 2009). Large prey specialists hunt in packs and aim to exhaust and overpower individual prey during a long pursuit, and the fast snapping shut of jaws may not be of such importance (Radinsky, 1981; Macdonald and Sillero-Zubiri, 2004; Sillero-Zubiri *et al.*, 2004).

#### The carnivoran jaw as a modified third-class lever.

In its most simplified representation the mammalian jaw acts as a lever to obtain and process food. In species where some or all of the masticatory muscle attachment lies cranial to the most caudal teeth, for example rodents and primates, biting at the most caudal tooth points represents a second-class lever system (Turnbull, 1970; Mansour and Reynik, 1975; Cox 2017). In carnivoran species biting at all tooth points along the the jaw has been described as a third-class lever, where force is applied between the load and the fulcrum. That is, the muscle force inserts on the vertical ramus of the mandible which lies between the bite points (the load) and the temporomandibular joint (the fulcrum). In this model, bite forces increase toward the TMJ, with the highest forces experienced at the most caudal tooth points. Clearly the three-dimensional biological condition is more complex than simple geometric lever



mechanics implies. The most influential factor to increase complexity of the model is to unite the two halves of the mandible into one functioning unit, as is the case in all mammals. This transforms the simple bar lever to a triangle consisting of two fulcrums, the TMJs, and one shared rostral apex, the mandibular symphysis. When muscle forces are bilaterally and equally applied the resultant single vector that represents muscle force lies at point approximately half way between the rostral most and caudal most points on the midline.

Greaves goes some way to describing the consequences on bite force of this more complex geometry the generalised carnivore jaw (Greaves, 1983; 1985; 2012). He refers to a triangle of support consisting of both TMJs and the particular tooth bite point. When the bite point is unilaterally on an incisor, canine or premolar tooth the triangle of support contains the midline resultant muscle force. As the bite point moves caudally the midline resultant force point lies outwith the triangle of support. In this condition, the balancing side muscle forces are reduced to prevent dislocation at the temporomandibular joint. The consequence is a lower than expected bite force at the caudal end of the dental row. This finding was also supported in later work on primates by Spencer (Spencer, 1997). In carnivores this is of little biological consequence as strong bites at the very caudal part of the dental row are limited in function as the gape between upper and lower arcades is so narrow. Using his model, Greaves was able to identify a region approximately halfway along the carnivoran mandible as the most powerful bite position when loaded with idealized forces. Carnassial teeth are sited here, allowing for maximum bite force and relatively wide gape.

Greaves model is however, still limited to describing the functional shape of the lower jaw as a triangular plane and a series of straight intersecting lines within it. The morphology of the skull and individual tooth shapes is far less straightforward. The mandible is curved both dorsally and medially, and the irregular profile of the teeth mean that the true condition cannot be captured by simple geometric calculations.

### Jaw adductor muscle anatomy

The muscles that close the jaws are comprised of three muscle groups: the temporalis, the masseter and the pterygoids. Embryologically they are all derived from the first pharyngeal arch and are innervated by the mandibular division of the trigeminal nerve (Evans and De Lahunta, 2013; Singh et al., 2018). Muscle classification and the nomenclature of the subdivisions within each muscle varies between authors. For this study I broadly follow the plan of Druzinsky (Druzinsky *et al.*, 2011). Throughout the text I use the anglicised versions of muscle names, rather than their Latin counterparts. The basic mammalian plan is described below. More detailed descriptions of the jaw adductor muscles of the species used in this study are given in Chapter Two.

### Temporalis

The temporalis muscle arises from the lateral bones of the calvarium and lies within the temporal fossa, a shallow depression behind the orbit. In species with a relatively small temporalis the origin chiefly covers the temporal and sphenoidal bones with only a small amount of the muscle originating from the parietal and frontal bones. In species with a more powerful temporalis the origin is more extensive and covers most of the parietal and occipital bones, in effect covering most of the lateral cranium. The temporalis muscle is subdivided into three divisions: the suprazygomatic, superficial and deep bellies. Druzinsky *et al.* (2011) states that the primitive condition for temporalis is the presence of all three of these divisions, but either one or both of the suprazygomatic and superficial parts are lost in many taxa. All three divisions are present in canids (Evans and De Lahunta, 2013). All parts of the temporalis insert onto the dorsal, medial and lateral surfaces of the vertical ramus of the mandible and its action is to draw the mandible dorsally and caudally.

## Masseter

The morphology of the masseter is complex in mammals and this is reflected in the varied nomenclature used to describe its subdivisions across academic texts. It is a multi-layered muscle, arising from the ventral and medial aspects of the zygomatic arch. In some taxa, the origin extends as far rostrally as the maxilla. It consists of at least three distinct muscle bellies, arranged as three broad flat layers, with their muscle fascicles running in opposing directions. Some authors describe the three layers as superficial, middle and deep masseter (Getty, 1975; Liebich *et al.*, 2009; Evans and De Lahunta, 2013). However, the deepest part of the masseter complex is more often described as a separate muscle, zygomaticomandibularis, with the remaining two layers named deep and superficial masseter (Davis, 1964; Turnbull, 1970; Druzinsky *et al.*, 2011). This is the classification used within this thesis, with the entire complex referred to as the masseter. All bellies insert onto the caudal lateral mandible at the masseteric fossa. In addition, the most superficial belly also covers the most ventral aspect of the mandible to insert on the medial aspect of the mandible and by way of a tendinous raphe, onto the pterygoid muscle. The action of masseter is to close the jaw, and in species capable of translational jaw movements, to work in conjunction with the contralateral pterygoid to draw the mandible to the working side. The more specific functional roles of each subdivision are less clear. Studies on pigs, rabbits and humans describe how the differently orientated fascicles of the masseter are recruited at different times throughout the masticatory cycle (Hannam *et al.*, 1981; Tonndorf *et al.*, 1989; Herring *et al.*, 1991; Widmer *et al.*, 2003). Fascicles that contract simultaneously have the same nerve supply and so belong to the same functional neuromuscular units. However, all of these species are capable of translational movements of the jaws, and many of the muscular sub-units are associated with lateral or rostro-caudal movements of the mandible. No work to date has been published regarding how the subdivision of the masseter function within the bite cycle of carnivorans, as due to the congruent nature of the carnivoran

temporomandibular joint, translational or rostrocaudal jaw movements are not possible. Other authors argue that a different functionality may explain the subdivision of the masseter. In their 2011 paper Druzinsky *et al.* (Druzinsky *et al.*, 2011) speculate that the separation of the masseter into smaller subdivisions may not be allied to complex translational jaw movements but may be related to the production of large bite forces at specific points along the dental arcade. They noted that some genera capable of translational jaw movements such as Suidae and Primates had relatively minimal amounts of masseteric subdivision, whereas some species capable of exerting large bite forces at the rostral teeth, such as Glires, carnivorans and many ungulates, had well defined superficial masseters.

#### Pterygoids

The pterygoids consist of two muscles, the small lateral pterygoid and the much larger medial pterygoid. In some species, including humans, the lateral pterygoid is reported to be further subdivided into a superior and inferior belly (Turnbull, 1970; Koolstra *et al.*, 1988; Endo *et al.*, 2003; Liu *et al.*, 2016; Melke *et al.*, 2016). Both pterygoid muscles originate from the pterygoid plate of the skull and insert on the caudomedial surface of the vertical ramus of the mandible, with some fibres from the medial pterygoid inserting onto the tendinous raphe of the superficial masseter. The function of the medial pterygoids appears to be consistent amongst mammals. Most authors are in accordance that they adduct the mandible and in species capable of translational or rostrocaudal jaw movements, they move the mandible laterally and rostrally, when working in conjunction with the contralateral masseter. The function of the lateral pterygoids appears to be more controversial, or at least unresolved. In some species, notably many primates, the lateral pterygoid abducts the mandible (Madeira and de Oliveira, 1979; Hylander and Johnson, 1994; Murray, 2012). In species with two distinct lateral pterygoid bellies, such as man, the actions of the two divisions may

oppose each other with the superior division active during jaw closing and the inferior division active during jaw abduction. The opposing actions are facilitated by the fascicles running in different orientations, the superior head fascicles run caudoventrally and the inferior head fascicles run caudodorsally (McNamara, 1973). During electromyographic studies the superior head has been shown to adduct the jaw whilst the inferior head is only active during jaw opening (Gibbs *et al.*, 1984; Juniper, 1984).

Whilst the carnivoran masticatory muscle arrangement broadly adheres to the basic mammalian plan it is noticeable for the dominance of temporalis as the main jaw closer, whereas herbivorous mammals tend to favour the masseter complex (Turnbull, 1970; Cox, 2008). Surprisingly few empirical reports exist regarding the soft tissue structures of non-human mammalian heads, and those that do tend to focus largely on primates (Perry *et al.*, 2014; Taylor *et al.*, 2015, 2018; Terhune *et al.*, 2015; Dickinson *et al.*, 2018; Hartstone-Rose *et al.*, 2018), or rodents (Satoh and Iwaku, 2006; Abe *et al.*, 2008; Hautier and Saksiri, 2009; Williams *et al.*, 2009; Cox and Baverstock, 2016; P-H Fabre *et al.*, 2017). Veterinary anatomy text books cover the anatomy of domestic species, and descriptions of domestic dog morphology, as a subspecies of *Canis lupus* are a valuable resource (Getty, 1975; Dyce *et al.*, 2009; Liebich *et al.*, 2009; Evans and De Lahunta, 2013). Descriptions of the musculature in wild species of carnivoran are greatly underrepresented in the literature. Within the ursid family Davies describes the masticatory apparatus of both *Tremarctos ornatus* (Davis, 1955), and *Ailuropoda melanoleuca* (Davis, 1964), and Endo *et al* describe the masticatory apparatus of *Ailuropoda melanoleuca* and *Ursus thibetanus* (Endo *et al.*, 2003). Turnbull (1970) describes the jaw adductors of the domestic cat (*Felis silvestris*) to illustrate the condition found within the 'carnivore-shear' mammals (Turnbull, 1970). His description of the masseter muscle within this text is based in the main from a translation of Toldt's earlier work (Toldt, 1904 in Turnbull, 1970). However, even within this single species the two

authors disagree on some findings. Toldt describes the superficial masseter as being divided into four distinct lobes, whereas Turnbull, disputes this. Turnbull also reports differences on the position of the insertion of the superficial masseter, the degree of division of the deep temporalis from zygomaticomandibularis, and the morphology of the lateral pterygoid muscle. A later work on felid masticatory musculature by Hartstone-Rose *et al.*, describes the jaw adductors in nine species of wild felid, and disagrees with some of the findings of both previous authors (Hartstone-Rose *et al.*, 2018). This serves to illustrate the difficulty in establishing the true arrangement of soft tissue structures. Reported differences may be attributed to variation within the sample set, alternative dissection techniques or variance in the interpretation of findings.

### Muscle architecture

Skeletal muscles consist of elongate contractile cells, described as fibres, which are bound together by collagenous supporting tissue into small bundles, called fascicles. Fascicles are surrounded by a collagenous support tissue, the perimysium. Spaces within the perimysium lying between the individual fibres are also filled with collagenous support tissue, the endomysium. Fascicles are grouped together to form a muscle mass, which is invested in a dense collagenous sheath, the epimysium. Blood vessels, nerves and lymphatic vessels run within the epimysium, perimysium and endomysium at sequentially smaller diameters to eventually supply individual fibres (Mitchell and Peel, 2009; Young *et al.*, 2014). Although individual muscle fibres are large enough to be visible to the naked eye it is easier and more conventional to measure the fascicles when considering the gross anatomy of muscle architecture, as they are easy to identify and easy to separate from neighbouring fascicles (Anapol and Barry, 1996; Taylor *et al.*, 2018). Physiological cross-sectional area (PCSA) is a measure of how many individual fascicles, and therefore fibres, a muscle has. PCSA calculations are a refinement of simple cross-sectional area calculations as they take into

account not just the volume of the muscle but also the arrangement of the fascicles within the space that it occupies. PCSA is proportional to the maximum force that a muscle can generate and muscles with a high PCSA are capable of producing more force than those with a low number of fascicles and a low PCSA (Powell *et al.*, 1984; Lieber and Friden, 2000). Muscles where the fascicles are arranged running parallel to the long axis of the muscles have greater contractibility, whereas those with fibres running obliquely to an internal tendon, have greater force. This is because the muscles with internal tendons can accommodate more (but shorter) fascicles, thereby increasing their PCSA (Gans, 1982; Sacks and Roy, 1982; Van Eijden *et al.*, 1997). In the carnivoran jaw adductor muscles the masseter and temporalis both have internal tendons, whereas the pterygoid muscle fascicles run in parallel to the axis of the muscles, and no internal tendon is present. Muscle architecture is further discussed in Chapter Two part 2.4, and PCSA is further discussed in Chapter Four, part 4.2.3.

## **1.4 Canid Diet and hunting strategies**

### **1.4.1 Diet**

A carnivorous diet has many advantages. Meat is highly nutritious and easy to digest which means that only a simple gastrointestinal tract is required to process it. Simple gastrointestinal tracts are smaller and shorter than complex gastrointestinal tracts and take up less space, especially as, due to infrequent meals they are often empty, and so weigh less (Hildebrand *et al.*, 1995; Dyce *et al.*, 2009). However, the food is often perilous to obtain, and may involve great risk to chase, kill and guard against thievery. Dependency on prey species means that hunters are in turn, dependent on the fortunes of their prey, and any environmental factors that affect the diet of prey species will impact on the success of sympatric carnivores. For instance, in African grasslands, in years where there is a lower than average rainfall, vegetation fails to grow and the species that feed on it fail to prosper (Owen-Smith, 1990; Ogutu *et al.*, 2008; Gandiwa, 2016). If herbivore mortality rates are high, birth rates are low and the impact on predator success may affect not only the current year but also a number of subsequent years (Mech and Peterson, 2003; Mech and Boitani, 2003; Macdonald and Sillero-Zubiri, 2004; Sillero-Zubiri *et al.*, 2004). In evolutionary timescales, long term global climatic changes have led to widespread changes in vegetation, and subsequent changes in the morphology of herbivorous mammals. One example of this is the decline of the rainforests and opening up of the grass lands in the late Oligocene period. Many previously short legged leaf browsers evolved to become long legged grazers, who were able to quickly cover the open grasslands (Janis, 1993). Consequentially, the canid predators of grassland species evolved cursorial anatomical adaptations to be able to pursue their fleeing prey (Figueirido *et al.*, 2015). Energy expended during unsuccessful hunting is energy wasted, and predators must be able to assess the likelihood of success before starting the chase. Accurate scientific data of hunting behaviours is scarce and often hard to categorise, for example when is a pack actually hunting, rather than assessing prey, and how



much food needs to be gained per individual per hunt for it to be deemed successful? Notwithstanding the nuances of observational studies, several have shown the success rate of hunts to be less than 50%. Packs of *Lycaon pictus* have a mean 47% success rate (Creel and Creel, 1995), *Canis lupus* a success rate of between 10-49% (Peterson and Ciucci, 2003) and the maned wolf a success rate of 21% (Rodden *et al.*, 2004).

Protein derived from animal prey need not mean, and in most cases, does not mean, large mammalian quarry. The majority of extant canid species routinely hunt prey smaller than themselves, and in many cases also consume plant material. Of the small prey, not all of it is mammalian, with the opportunistic taking of birds (and their eggs), fish, reptiles, amphibians and invertebrates. *Otocyon megalotis* preferentially hunts invertebrates particularly dung beetles and termites (Nel, 1978; Maas, 1993; Klare *et al.*, 2011). Many species vary their diet throughout the year, as food stuffs become more, or less, available. Many species have been shown to have a reliance on fallback foods, that is nutritional resources that are only utilised when preferential foods are unavailable (Marshall and Wrangham, 2007; Ungar *et al.*, 2008; Marshall *et al.*, 2009). Several authors have found the incidence of tooth fractures increases in carnivorans when poor resources lead to increased utilisation of prey material. That is, in times of duress, carnivorans that may optimally select soft tissue foodstuffs, are driven to consuming skeletal material (Mech and Frenzel, 1971; Carbone *et al.*, 1997; Vucetich *et al.*, 2012; Mann *et al.*, 2017). These pinch points in an animal's life may act as a selective pressure on morphological traits to allow for survival success.

Seasonal changes to diet may be due to the migration of large quarry, such as caribou and wildebeest, or fluctuations in small quarry populations, such as lemmings and ground squirrels. Many species that live near coastlines seasonally hunt marine mammals that come ashore to breed and give birth, such as seals and walruses, or survive on seabird eggs and young during the breeding season (Sillero-Zubiri *et al.*, 2004). Species that take fruit and

berries will also take advantage of seasonal gluts. In species living in cold climates the autumn fruit and berry glut allows individuals to increase their subcutaneous and intraperitoneal fat reserves to endure the cold climate. For example, *Alopex lagopus* increase their body mass by 50% in the autumn to survive the cold winter (Prestrud, 1991). In *Nyctereutes procyonoides* this behaviour is even more extreme, as individuals not only greatly increase their body weight, but also undertake periods of decreased activity or even hibernation (Nowak, 2005; Kitao *et al.*, 2009). Even within one species, dietary and hunting specialisms exist. For example, *Vulpes vulpes* may exist on earthworms and human refuse in built up urban areas (Doncaster *et al.*, 1990; Bateman and Fleming, 2012; Vuorisalo *et al.*, 2014) or rabbits and sheep carrion in agricultural areas (Forbes-Harper *et al.*, 2017). *Canis mesomelas*, usually thought of as hunters of small mammals, have been seen to tackle antelope, although this is usually undertaken when hunting in pairs (Nowak, 2005; MacDonald, 2009). Small canids are opportunistic eaters of carrion and will readily consume large prey that they have had no part in chasing or killing. *Vulpes vulpes* for example, are keen followers of *Canis lupus* and often consume the remains of moose carcasses (Peterson and Ciucci, 2003), and all species of jackal will take carrion from the kills of apex predators such as *Panthero leo* or *Lycaon pictus* (Yarnell *et al.*, 2013).

Competition also occurs between sympatric species, although resource partitioning of either food, habitat or time allows species living in the same environment to co-exist. In this way dietary choice is often determined by the presence of potential competitors, as well as the availability of prey. For example, in Scandinavia the *Alopex lagopus* and *Vulpes vulpes* dietary niches overlap. As *Vulpes vulpes* is the larger species it dominates the lowland environment. However, it is less well adapted to high altitude mountainous environments and it is here that the *Alopex lagopus* thrives. An alternative strategy is food resource partitioning, where available prey are divided into distinct niches. The dominant species, usually the species with the larger body mass, consumes the prime prey species, whilst the subdominant species

take food items of lower nutritional value. Dividing of resources has allowed for example, *Vulpes corsac* and *Vulpes vulpes* to co-exist in Mongolia (Murdoch *et al.*, 2010), and *Vulpes macrotis* and *Canis latrans* to co-exist in North America (Cypher and Spencer, 1998; Kozlowski *et al.*, 2008).

Despite the variation in diet, seasonally, geographically and opportunistically, it is possible to categorise canids into three broad dietary categories. For this I follow Slater *et al.* (Slater *et al.*, 2009):

- Hypercarnivores: prey species that are 50% larger than their own body mass and make up at least 70% of their diet.
- Small prey specialists, also often referred to as mesocarnivores: prey species that are smaller than 50% of their own body mass constitute 50% or more of the diet.
- Generalists or omnivores: invertebrates, amphibians, fish, plant matter and carrion make up over 50% of the diet.

#### **1.4.2 Hunting strategies**

##### **1.4.3.1 Hunting large prey**

Pursuing large mammalian prey, requires observation, fearlessness, speed and endurance. In open landscapes, keen eyesight is used to spot and observe prey, but in dense cover or areas of tall grass, olfaction maybe more important. Nocturnal or crepuscular hunting relies heavily on hearing and olfaction. When hunting individuals within a herd, the canid pack aims to provoke them into fleeing. Sustained chases may cover several kilometres, and the initial aim is to identify a weaker individual within the heard, usually one that is young, old or injured, and then pursue and kill it (Mech and Peterson, 2003; Mech and Boitani, 2003; Peterson and Ciucci, 2003). The tactic of chasing prey also allows the pack to attack from behind, a less risky strategy with large ungulates who often have horns or antlers and may use aggressive head butting in combat. By selecting weaker individuals, the chase is likely to

be shorter, so conserving energy, and the close contact with the prey animal at the point of killing is less dangerous to the pack. Even strong confident canid packs tend to avoid confrontation with fully grown, fit prey individuals (Mech and Peterson, 2003). Prey is chased and run to the point of exhaustion, whereupon it is quickly dispatched. Canids overpower large prey with multiple pack members inflicting many sustained bites. First contact may be with the back or hindquarters of the animal and then one or more individuals will grasp the prey by the nose, and several other individuals will attack the ventral abdomen and flanks with the aim of eviscerating the prey. Death occurs due to shock through blood loss (Creel and Creel, 1995, 2002; Sillero-Zubiri *et al.*, 2004; MacDonald, 2009). The nature of smaller predators attacking larger quarry is often treacherous, and, when cornered, large ungulates will defend themselves, and their young, using their strong kicking hooves, horns or antlers (Mech and Peterson, 2003). Mortality among canids due to wounding by large prey, although not commonly reported, does occur, and presumably non-life-threatening injuries are more frequent (Mech and Nelson, 1990; Weaver *et al.*, 1992). Pack hunting as a strategy, is demonstrably successful. As measured by kilograms of meat per individual, the gains are higher than if hunting alone (Creel and Creel, 2002). When feeding, canids gorge on food and remove meat from the carcass and swallow it as quickly as possible. The liver, heart intestines eaten first, then muscle, then bones and hide. Larger packs can not only tackle larger prey species, but packs can better defend their kills against scavengers (Fanshawe and Fitzgibbon, 1993; Creel and Creel, 2002).

The canid method of killing large prey differs from the felid approach. Large felids will tackle sizable prey alone, and death usually follows an ambush or a short pursuit. Capture and restraint uses the claws of the forelimbs, as well as teeth, and death is by a sustained ventral neck bite causing suffocation. The choice of the ventral neck limits the possible interaction of canine teeth against the bony skeleton of the prey animal, which could damage the teeth,

and the great power of the bite quickly asphyxiates, and immobilises prey (MacDonald, 1992; Van Valkenburgh, 2007; MacDonald, 2009).

#### 1.4.3.2 Hunting small prey

Small mammals, birds, fish, reptiles and invertebrates constitute much of the diet for the mesocarnivores or small prey hunters. All fox diets appear to be similar in potential and are only limited by local availability of foodstuffs (MacDonald, 2009). The hypercarnivorous species will also opportunistically take these foodstuffs, especially when their usual large prey are hard to come by (Ewer, 1973; MacDonald and Sillero-Zubiri, 2004; Sillero-Zubiri *et al.*, 2004; Nowak, 2005). The method of hunting for small prey differs greatly to that when hunting for large prey. Many small mammals and reptiles have subterranean burrows or dens and a long pursuit would allow them to escape underground. Similarly, birds and fish can usually evade capture by taking to the air or swimming beyond reach, if not quickly ambushed. The small size of the prey, usually less than 50% of the predator canid body mass, means that it will be easily overpowered, and collaborative group hunting is not necessary. It is more energy efficient, even for canid species that live communally, for individuals to hunt alone (Sillero-Zubiri *et al.*, 2004). Small prey hunters therefore hunt singly and covertly, often under the cover of dark or the low light conditions found at dawn and dusk. Even those that hunt in daylight, may be doing so 'blind' as their quarry may be hidden from sight. For example, during the long arctic winter *Alopex lagopus* chases voles within their snow covered runs and burrows, and, on the African plains *Otocyon megalotis*, listens for termites within their mounds. Keen eyesight and enhanced senses of olfaction and hearing are key to success for the small prey hunters. They hunt by stealth, lying low and observing or listening before executing a short quick pursuit or high arcing pounce. The pounce allows the hunter to land forefeet first, trapping their prey, before killing it with a bite, seen for example in *Canis mesomelas* and *Alopex lagopus* when hunting mice and voles. Chasers usually attempt to

catch their prey by the back of the neck, before shaking it vigorously to break the spinal cord, for example when *Vulpes vulpes* tackles rabbit or hare. The high pounce is usually deployed for very small prey such as rodents, whereas the short pursuit is used when hunting lagomorphs or juvenile cervids (MacDonald and Sillero-Zubiri, 2004; Rodden *et al.*, 2004; MacDonald, 2009). Many species of canid are adept at several hunting techniques and adapt their strategies to either pursue larger prey or pounce on small rodents (Martín-Serra *et al.*, 2016). Most canids have been known to carry food away from the kill site to either cache it for future use, eat quietly away from scavengers, or give to pups back at a den (Peterson and Ciucci, 2003).

### **1.5 Summary**

The aim of this thesis is to contribute toward the understanding of cranial morphology and masticatory biomechanics in the Canidae. Canids are ideal for this study as their evolutionary history is well documented, and many extant forms survive today. Despite their 40-million-year evolution, for most of their history the only extant subfamily, the Caninae, remained geographically and morphological restricted. Their current wide diversity, in terms of body mass, diet and geographical dispersal are a result of several recent adaptive radiation events occurring in the late Pleistocene. This is evidence of their ecological adaptability and morphological plasticity, and many adaptive traits such as muzzle length and dental form have been identified by previous authors. The roles of interspecific differences in head shape however, are not always clear. This thesis uses empirically derived data to explore the interaction of the previously under-reported soft tissue structures with the bony morphology of the skull. I build on previous findings to determine the function and constraints of some of the traits associated with the masticatory apparatus. I hypothesise that the morphological differences between canid species reflect dietary specialisms, and that hypercarnivorous species have relatively greater bite forces and more robust skulls than

small prey or generalist hunters. In addition, it is hoped that the findings from this study may help inform methodologies in future comparative morphological studies.

## **Chapter Two. Sampling, Imaging and Dissection**



## **2.1 Introduction**

In a bid to minimise repetition, in this chapter I review the techniques used and report the methodological details common to many subsequent chapters regarding sampling, ethics, imaging and dissection. I also describe the gross anatomy of the jaw adductor muscles. Techniques, methodologies and statistical tests specific to individual chapters are discussed within the relevant chapters.

## **2.2 Sampling**

### **2.2.1 Review of species and numbers used in previous studies.**

Previous studies exploring canid head shape and bite force have varied widely in sample size, from a single specimen (Wroe *et al.*, 2007; Bourke *et al.*, 2008) to in excess of 800 (Damasceno *et al.*, 2013) (Table 2.1). The number of canid species within each study is accordingly varied, ranging from one to 34. All of the previously reported canid bite force studies have been performed using dry skull specimens (Wroe *et al.*, 2005; Christiansen and Adolfssen, 2005; Christiansen and Wroe, 2007; Wroe *et al.*, 2007; Bourke *et al.*, 2008; Slater *et al.*, 2009; Tseng and Wang, 2010; Damasceno *et al.*, 2013). Dry skull studies have several shortcomings. Firstly, often little is known about individual specimens regarding age, sex and body mass, as specimens tend to come from natural history museum collections, where such information is inconsistently recorded. Secondly, soft tissue structures are missing from dry skull material. With regard to studies considering bite force, of particular pertinence are the details of the jaw adductor muscles, i.e. the muscles that close the jaw to seize, kill and process prey. Muscle details can include not only the mass of the muscles but also information regarding their sites of attachment and the structure of their internal architecture. Attachment sites influence biomechanical function, and knowledge of the muscle architecture is important to calculate muscle force capabilities (Chapter Four). Thirdly, in studies working directly with specimens, for example when measuring bone stress

or strain, the nature of dried material does not reflect the material properties seen in the live condition.

**Table 2.1. Comparison of sample size with previous studies.**

<b>Source</b>	<b>1</b>	<b>2</b>	<b>3</b>	<b>4</b>	<b>5</b>	<b>6</b>	<b>7</b>	<b>8</b>	<b>This study</b>
<b>Type of study</b>	Muscle force and dry skull bite force	Muscle force and dry skull bite force	Muscle force and dry skull bite force	Muscle force and FEA bite force	Muscle force and FEA bite force	Muscle force and FEA bite force	Muscle force and FEA bite force	Muscle force and dry skull bite force	Muscle force and FEA bite force
<b>Wet(W) or dry(D) skulls</b>	D	D	D	D	D	D	D	D	W
<i>Alopex lagopus</i>	*	1	**					37	1
<i>Atelocynus microtis</i>			**					21	
<i>Borophagus secundus</i> †							1		
<i>Canis adustus</i>			**					30	
<i>Canis lupus</i>	*	1	**				1	30	3
<i>Canis lupus dingo</i>	*			1	1			33	
<i>Canis lupus hallstromi</i>	*							6	
<i>Canis aureus</i>	*		**					30	
<i>Canis dirus</i> †									
<i>Canis familiaris</i>			**						
<i>Canis latrans</i>			**					30	
<i>Canis mesomelas</i>			**			1		30	1
<i>Canis rufus</i>								6	
<i>Canis simensis</i>						1		8	
<i>Cerdocyon thous</i>		1	**					32	
<i>Chrysocon brachyusus</i>		1	**					22	1
<i>Cuon alpinus</i>	*	1	**					20	1
<i>Epicyon haydeni</i> †							1		
<i>Hesperocyon gregarius</i> †									
<i>Lycalopex gymnocercus</i>		1	**				1	30	
<i>Lycalopex culpaeus</i>			**					31	
<i>Lycalopex fulvipes</i>								2	
<i>Lycalopex griseus</i>			**					30	

Source	1	2	3	4	5	6	7	8	This study
<i>Lycalopex sechurae</i>								30	
<i>Lycalopex vetulus</i>			**					18	
<i>Lycaon pictus</i>	*	1	**			1		30	4
<i>Mesocyon coryphaeus</i> †							1		
<i>Microtomarctus conferta</i> †							1		
<i>Nyctereutes procyonoides</i>		1	**					30	1
<i>Otocyon megalotis</i>		1	**					30	1
<i>Speothos venaticus</i>		1	**					21	1
<i>Urocyon cinereoargenteus</i>	*		**					39	
<i>Urocyon littoralis</i>								30	
<i>Vulpes bengalensis</i>			**					10	
<i>Vulpes chama</i>			**					19	
<i>Vulpes corsac</i>									4
<i>Vulpes ferrilata</i>			**						
<i>Vulpes macrotis</i>								21	
<i>Vulpes pallida</i>			**					19	
<i>Vulpes rueppelli</i>			**					30	
<i>Vulpes velox</i>			**					14	
<i>Vulpes vulpes</i>	**	1	**					32	23
<i>Vulpes zerda</i>		1	**					30	1
<b>TOTAL</b>	<b>49</b>	<b>12</b>	<b>609</b>	<b>1</b>	<b>1</b>	<b>3</b>	<b>6</b>	<b>831</b>	<b>42</b>
<i>Number of species</i>	<i>9</i>	<i>12</i>	<i>28</i>	<i>1</i>	<i>1</i>	<i>3</i>	<i>6</i>	<i>34</i>	<i>12</i>

**Table 2.1. Comparison of sample size with previous studies.**

1. Wroe *et al.*, 2005, 2. Christiansen and Adolfssen, 2005, 3. Christiansen and Wroe, 2007, 4. Wroe *et al.*, 2007, 5. Bourke *et al.*, 2008, 6. Slater *et al.*, 2009, 7. Tseng and Wang, 2010, 8. Damasceno *et al.*, 2013.

† extinct.

\* This study did not break down specimen numbers to individual species. 49 specimens representing 39 carnivoran species. 11 species were from the Canidae family.

\*\* This study did not break down specimen numbers to individual species. 609 specimens representing 150 carnivoran. 28 species were from the Canidae family.

### 2.2.3 Description of sample

Dry skull specimens were not used for this thesis as this work considered the relationship of soft tissue structures to the bony skeleton. Wet specimens, that is those with the soft tissues still intact, were used for all work reported in this thesis. Wet specimens allowed for the acquisition of empirical specimen specific muscle data, and the material properties of the skeletal components more closely reflected the conditions found in live animals. In particular, specimen specific data was used to explore scaling of muscle mass and force, the accommodation of muscles on the cranium, to build *in silico* models to determine bite force, stress and strain within the skull and to conduct *ex vivo* laboratory experiments to explore the role of the orbital ligament during biting.

In order to avoid preservation artefacts such as tissue drying or shrinking, only fresh or fresh/frozen specimens were used. All specimens with the exception of *Canis lupus familiaris*, *Cuon alpinus* 1 and 2, *Lycaon pictus* 2 and *Vulpes vulpes* 1-8 arrived at the University of Liverpool in a frozen condition. The *Vulpes vulpes* specimens 9- 24 were supplied by the Animal and Plant Health Agency (APHA) had been frozen shortly after post mortem sample collection and not been defrosted since. The samples supplied by the National Museum of Scotland (Table 2.2) were initially donated to them via several zoos and safari parks, and the precise number of freeze thaw cycles is unknown. Several of the fresh specimens were frozen soon after arrival (Table 2.2). All frozen specimens were defrosted once, and scanned and dissected within 24 hours of defrosting. Table 2.2 details the number of freeze thaw cycles where known. The difficulty in acquiring such rare specimens resulted in a limited sample size of 47 specimens (Table 2.2). Shortcomings of having small data sets are the concomitant increase in standard deviation values (SD), standard error of the mean (SEM) values and consequentially, broader confidence interval (CI) ranges. This in turn can lead to an increase of Type II errors, where significant differences are masked by the wide CI range (Vinyard *et al.*, 2003; Button *et al.*, 2013). However, small sample sizes are

unavoidable in studies using rare specimens, and this is widely acknowledged and demonstrated within the literature (Gittleman, 1991; Abouheif and Fairbairn, 1997; Wang *et al.*, 1999; Huber, 2005; Christiansen and Wroe, 2007; Anapol *et al.*, 2008; Rae and Koppe, 2008; Christiansen, 2008; Cox, 2008; Drake and Klingenberg, 2008; Pierce *et al.*, 2009; Huq *et al.*, 2015; McIntosh and Cox, 2016; Burrows, 2018). Five specimens were rejected for further analysis due to damage sustained at the time of death or post mortem and are not reported again. The remaining sample set consisted of 42 individuals, covering nine of the 13 genera and 12 of the 36 species within the canid family. Not all of the specimens were used in all parts of the study. Details of specimen allocation are reported in Table 2.2. Canid diversity was further reflected in the sample set by the wide range of body masses spanning two orders of magnitude (1kg to 36kg), and the broad range of dietary specialisms that it encompassed. All four of the hypercarnivorous species were represented (*Canis lupus*, *Cuon alpinus*, *Lycaon pictus*, *Speothos venaticus*), plus five small prey specialists (*Alopex lagopus*, *Canis mesomelas*, *Chrysocyon brachyurus*, *Vulpes corsac*, *Vulpes vulpes*) and three generalists (*Nyctereutes procyonoides*, *Otocyon megalotis*, *Vulpes zerda*). In addition, specimens came from the three major canid clades: the fox-like clade, the wolf like clade and the South American clade. Only the grey-fox clade, consisting of only two species, was unrepresented in the sample set.

**Table 2.2 Details of specimens used in this thesis.**

Specimen	Donor institution	Remarks on sample/condition	Freeze/thaw cycles	Sex	Body mass (kg)	Mean body mass (kg) from literature <sup>1,2</sup>	Condylbasal length from specimen (mm)	Condylbasal from literature (mm)	Parts of the study
<i>Alopex lagopus</i> 1	National Museum of Scotland	Unusable - shot through head.	unknown	M	Not known	5.2	Not measured	114.7-132.5 <sup>3,4,9,14,16</sup>	x
<i>Alopex lagopus</i> 2	National Museum of Scotland	Good, head only, skinned.	unknown	M	6.5	5.2	130.1	114.7-132.5 <sup>3,4,9,14,16</sup>	C, D, E
<i>Canis lupus</i> 1	National Museum of Scotland	Subspecies <i>signatus</i> . Good, head only, skinned	unknown	F	32.6	36.5	205.7	182-285 <sup>4,9,13,14,16</sup>	C, D.
<i>Canis Lupus</i> 2	National Museum of Scotland	Subspecies <i>chanco</i> . Head only, skinned. Fair condition, slight damage to zygomatic arch	unknown	M	32.4	36.5	215.3	182-285 <sup>4,9,13,14,16</sup>	C, D, E
<i>Canis Lupus</i> 3	National Museum of Scotland	Subspecies <i>chanco</i> . Head only, skinned	unknown	M	33.2	36.5	229.8	182-285 <sup>4,9,13,14,16</sup>	C, D.
<i>Canis lupus familiaris</i>	University of Liverpool	Good, entire.	0	M	Not measured	x	Not measured	x	A
<i>Canis mesomelas</i>	National Museum of Scotland (Hamerton Zoo)	Good, head only, skinned.	unknown	M	7.9	9.7	152.6	140.9-160 <sup>9,14,17</sup>	C, D, E
<i>Chrysocon brachyusus</i>	National Museum of Scotland (Port Lympne)	Good, head only, skinned.	unknown	F	22.5	25.0	209.8	198 - 235 <sup>4,9,12,14</sup>	C, D, E
<i>Cuon alpinus</i> 1	Twycross Zoo	Unusuable - calvarium and temporalis partially removed, brain removed	1	F	Not known	14.0	Not measured	161.7-171.4 <sup>4,7,9,14</sup>	X
<i>Cuon alpinus</i> 2	National Museum of Scotland	Head only, skinned	unknown	F	26.9	14.0	171.0	161.7-171.4 <sup>4,7,9,14</sup>	C, D, E
<i>Lycaon pictus</i> 1	Chester Zoo	Poor - temporalis removed. Not used.	0	F	30.0	26.5	Not measured	185 -198 <sup>4,9,14,15,16</sup>	x
<i>Lycaon pictus</i> 2	Twycross Zoo	Good. Entire specimen.	1	M	Not known	26.5	185.9	185 -198 <sup>4,9,14,15,16</sup>	C, D.

Specimen	Donor institution	Remarks on sample/condition		Sex	Body mass (kg)	Mean body mass (kg) from literature <sup>1,2</sup>	Condylbasal length from specimen (mm)	Condylbasal from literature (mm)	Parts of the study
<i>Lycaon pictus</i> 3	West Midlands Safari Park	Good - entire but GI tract removed	1	M	27.4	26.5	194.7	185 -198 <sup>4,9,14,15,16</sup>	C, D, E
<i>Lycaon pictus</i> 4	National Museum of Scotland	Good, head only, skinned.	unknown	F	30.3	26.5	185.1	185 -198 <sup>4,9,14,15,16</sup>	C, D.
<i>Nyctereutes procyonoides</i>	National Museum of Scotland	Good. Head only, skinned.	unknown	Not known	Not known	6.5	120.8	108.9-125.7 <sup>4,9,14,16,18</sup>	C, D, E
<i>Otocyon megalotis</i>	National Museum of Scotland	Good. Head only, skinned	unknown	M	4.9	4.2	109.7	104-121 <sup>4,5,9,14,16</sup>	C, D, E
<i>Speothos venaticus</i>	National Museum of Scotland (Port Lympe)	Good. Head only, Skinned	unknown	F	6.5	6.5	131.5	120 -133 <sup>4,7,9,14,16</sup>	C, D, E
<i>Vulpes corsac</i> 1	National Museum of Scotland (Paradise Wildlife Park)	Good. Head only, skinned	unknown	M	Not known	2.9	109.5	103-111 <sup>6</sup>	C, D.
<i>Vulpes corsac</i> 2	National Museum of Scotland	Good. Head only, skinned	unknown	M	3.0	2.9	108.8	103-111 <sup>6</sup>	C, D, E
<i>Vulpes corsac</i> 3	National Museum of Scotland	Good. Head only, skinned	unknown	M	2.7	2.9	110.5	103-111 <sup>6</sup>	C, D.
<i>Vulpes corsac</i> 4	National Museum of Scotland	Fair condition some slight damage to skull	unknown	Not known	3.5	2.9	108.1	103-111 <sup>6</sup>	C, D.
<i>Vulpes corsac</i> 5	National Museum of Scotland	Unusable - damage to skull	unknown	F	Not Known	2.9	Not measured	103-111 <sup>6</sup>	X
<i>Vulpes vulpes</i> 1	Gamekeeper	Good. Entire specimen.	0	M	6.1	8.5	141.1	127.6-150 <sup>2,7,9,12,14</sup>	C, D, E
<i>Vulpes vulpes</i> 2	Gamekeeper	Good.	1	M	8.5	8.5	Not measured	127.6-150 <sup>4,9,11,14,16</sup>	B
<i>Vulpes vulpes</i> 3	Gamekeeper	Good.	1	F	4.7	8.5	Not measured	127.6-150 <sup>4,9,11,14,16</sup>	B



Specimen	Donor institution	Remarks on sample/condition		Sex	Body mass (kg)	Mean body mass (kg) from literature <sup>1,2</sup>	Condylbasal length from specimen (mm)	Condylbasal from literature (mm)	Parts of the study
<i>Vulpes vulpes</i> 4	Gamekeeper	Unusable. Shot through head	1	M	Not measured	8.5	Not measured	127.6-150 4,9,11,14,16	x
<i>Vulpes vulpes</i> 5	Gamekeeper	Good.	1	M	6.3	8.5	Not measured	127.6-150 4,9,11,14,16	B
<i>Vulpes vulpes</i> 6	Gamekeeper	Good.	1	M	8.0	8.5	Not measured	127.6-150 4,9,11,14,16	B
<i>Vulpes vulpes</i> 7	Gamekeeper	Good	1	M	8.7	8.5	Not measured	127.6-150 4,9,11,14,16	C, E,
<i>Vulpes vulpes</i> 8	Gamekeeper	Good.	1	F	5.9	8.5	Not measured	127.6-150 4,9,11,14,16	F
<i>Vulpes vulpes</i> 9-24	Animal and Plant Health Agency (APHA)	Good.	1	Not known	Not known	8.5	Not measured	127.6-150 4,9,11,14,16	F
<i>Vulpes zerda</i>	National Museum of Scotland	Good. Head only, skinned.	unknown	F	1.0	1.1	85.2	80-88 <sup>4,9,10</sup>	C, D, E

1. Macdonald and Sillero-Zubiri (2004), 2. Nowak (2005), 3. Audet *et al.* (2002), 4. Christiansen and Adolfsen (2005), 5. Clark (2005), 6. Clark *et al.* (2009), 7. de Mello Beisiegel and Zuercher (2005), 8. Elmhagen *et al.* (2000), 9. Gittleman (1991), 10. Larivière (2002), 11. Larivière and Pasitschniak-Arts (2018), 12. Mazzolli (2009), 13. Pocock (1935), 14. Van Valkenburgh and Ruff (1987), 15. Van Valkenburgh (1996), 16. Van Valkenburgh *et al.* (2014), 17. Walton (2018), 18. Ward and Wurster-Hill (1990).

A. MRI sensitivity study, *Canis familiaris* (n=1), this chapter B. Muscle mass MR/dissection validation *Vulpes vulpes* (n=4), this chapter, C. Dissection, all species (n=20), this chapter, D. Shape analysis, all species (n=19), Chapter Three, E. Finite element analysis models, all species plus one extra *Vulpes vulpes* (n=13), Chapters Four and Five, F. Strain Gauge experiments, *Vulpes vulpes* (n=17), Chapter Five.

All specimens in this study, with the exception of the *Vulpes vulpes* samples, came from the UK zoo and safari park population, and were captive bred and maintained. I am unaware of any studies describing the effects of captivity on the morphology of wild canid species. Other mammalian species are better documented, and captive animals are often reported to have better body condition and live to a greater age than their wild counterparts (Kitchener *et al.*, 1998; Ange *et al.*, 2001; Schwitzer and Kaumanns, 2001; O'Regan and Kitchener, 2005; Clauss and Hatt, 2006; Mason, 2010; Mason and Veasey, 2010; Müller *et al.*, 2010). It is also likely that many of the older specimens may have experienced some degree of sarcopenia, that is, muscle loss related to ageing, but this has not been widely explored in canid species to date, and no data on likely muscle loss currently exists. Several of the canid specimens, notably *Cuon alpinus* 2, had a greater body mass than that reported in the literature. This is in agreement with the International Species Information System (ISIS) for *Cuon alpinus* which reports greater body mass values for captive animals than those expected in the wild population (Appendix 2). In a study comparing body mass in wild and captive individuals of the primate *Chlorocebus aethiops sabaesus*, the authors found that the ready availability of high quality food, lack of competition and reduced activity rates of the captive animals resulted in their greater body mass, even when other variables such as genetic history and seasonality were kept constant. The authors found that morphological measures of length (forelimb, hindlimb and torso) were not statistically different between the wild and captive populations, but measures of girth (waist, thigh, upper forelimb) were, with the higher values reported in the captive animals. This indicates an increase in soft tissue such as muscle or adipose tissue (Turner *et al.*, 2016). In three further studies of primates the authors found that the weight gain seen in captive animals was due to a gain in adipose tissue resultant of their free access to food and their sedentary lifestyle (Altmann *et al.*, 1993; Pereira and Pond, 1995; Schwitzer and Kaumanns, 2001). As an additional measure to check if the specimens in this study fell within normal morphological range, and that any increased or decreased

body masses could be accounted for by body condition, I also measured condylobasal length. Condylobasal length measures the distance from the prosthion to the caudal border of the occipital condyle of the skull. It can be considered as a measure that is independent from body mass as it is unaffected by body condition, or changes in body condition. All condylobasal lengths fell within the parameters reported for wild caught specimens in previous studies (Table 2.2). Five specimens (*Cuon alpinus* 2, *Vulpes vulpes* 1,3, 5 and 8) had body mass values were markedly different, that is greater the 20%, from the normal reported body mass range, but as their condylobasal lengths fell within the normal parameters the differences were attributed to increased or decreased body condition.

Some degree of sexual dimorphism has been documented in many canid species, but the literature concurs that it is very modest, and that overall body size is the greatest differential factor (Ewer, 1973, MacDonald and Sillero-Zubiri, 2004; Nowak, 2005). Males often have a slightly greater body mass and larger overall proportions than females, however there appears to be a significant amount of overlap in body mass data between the largest female and smallest males (MacDonald and Sillero-Zubiri, 2004; Sillero-Zubiri *et al.*, 2004; MacDonald, 2009; Wang and Tedford, 2010). Several species have also been shown to exhibit some sexual dimorphism relating to dentition, although canids, along with hyaenids, are noted to be the least dimorphic in this respect of all of the carnivorans (Sillero-Zubiri *et al.*, 2004; Macdonald, 2009). Where species have been shown to exhibit dental dimorphism, males typically have 8-15% longer canines, but this is thought to relate to behavioral displays and is not correlated to body mass or skull length (Gittleman and Van Valkenburgh, 1997; Kim *et al.*, 2012).

#### **2.3.4 Ethical approval.**

No specimens were specifically euthanised for this thesis, and all were collected post mortem. Non-native British species were donated to the study from several sources: Chester

Zoo, Knowsley Safari Park, Twycross Zoo, West Midlands Safari Park and the National Museum of Scotland. Specimens that came from the National Museum of Scotland had been donated to them by other organisations including Port Lympne Wild Animal Park and Hamerton Zoo. These details, where known, are stated in Table 2.2. The wild British species specimens, *Vulpes vulpes*, were supplied by a gamekeeper and via the Animal and Plant Health Agency (APHA) York. The domestic species specimen, *Canis lupus familiaris*, was donated by a dog rescue organisation via the University of Liverpool Institute of Veterinary Science. All specimens used were covered by the University of Liverpool Ethical Approval Regulations (Reference: RETH000553 and VREC 480), and in addition, some of the outside agencies also required ethical approval forms, which were filled in before specimens were donated.

### **2.3 Imaging**

Digital imaging of specimens is widely used in morphological studies. It provides a long term record of biological material which would naturally degrade under normal conditions, and data can be digitally examined and reconfigured into virtual three dimensional models used to further explore form and function. The work in this thesis uses two imaging modalities, computed tomography (CT) and magnetic resonance (MR).

#### **2.3.1 Computed Tomography (CT)**

CT imaging is non-invasive, relatively quick and inexpensive to perform and the equipment required is widely available in both clinical and research settings. CT captures detail of the bony morphologies of the specimen whilst preserving the surrounding tissues, and can be performed on both living and *ex vivo* specimens. A great advantage of CT imaging is that it allows for all aspects of the specimen to be visualised, not just the external surfaces as seen in photographic or surface scanning techniques. Unlike conventional radiography, where a

two-dimensional image of a three-dimensional (3D) object is produced, CT allows for the imaging of individual body slices and virtual 3D rendering of scanned specimens (Hsieh, 2009; Seeram, 2009). The image produced is spatially accurate with no superimposition of overlying structures. Some studies use direct measurements from CT scans (Herring, 2007; Drake *et al.*, 2017), whilst others use them as a basis for further analyses, for example to recreate the bony morphologies for finite element techniques (Kupczik *et al.*, 2007; Cox *et al.*, 2011; Smith *et al.*, 2013 Toro-Ibacache *et al.*, 2016).

CT uses multiple X-rays to generate a composite radiographical image. During scanning an X-ray source rotates around the specimen producing many separate beams that pass through the specimen at different angles. The energies of the X-rays exiting the specimen are recorded by multiple detectors (Buzug, 2008; Hsieh, 2009). The degree to which the X-rays are attenuated by biological tissues is determined by their material density. The specimen is scanned in sequential slices. Each slice is made up of a square grid of pixels. As each pixel has a third dimension, the depth of the slice, it is referred to as a voxel, which describes a volume rather than an area. The sum of the attenuation of the X-rays is calculated for each voxel of the specimen. Computer software converts this information into a digital image for each slice. Regions of high density, such as bone, appear white, whilst regions of low density, such as gas appear black, with all potential intensities of density appearing as gradations in between. In this way, an image is produced for each slice. As each slice is made up of many voxels, it is possible, if the voxels are isometric, to reslice the data into alternative orthogonal and oblique views, allowing for visualisation from different aspects of the specimen (Wolbarst *et al.*, 2013). Serial slices can be reconstructed to re-assemble the entire morphology (Carver and Carver, 2012). Using segmentation software, tissues of similar densities can be identified and reconstructed to enable virtual three-dimensional models to be built (Chapters Three, Four and Five). Contrast resolution describes the ability to distinguish between tissues with similar grayscale values. Spatial resolution refers to the

degree to which different structures can be differentiated due to the number of pixels per slice. Signal to noise ratio (SNR) is a measure of noise (McNitt-Gray, 2006). SNR is a measure of the true signal from the specimen compared to the level of background noise originating from pixels that deviate from normal levels. There is a trade-off between spatial resolution and SNR. High SNR is desirable as it indicates lower levels of noise on the image. Thicker CT slices give a higher SNR but increasing slice thickness decreases spatial resolution in the Z axis. For high spatial resolution images, thin slices and a high number of pixels per slice are required.

There are two potential disadvantages to using CT imaging. The first is the high levels of radiation exposure generated during scanning, although this is only a concern when using this modality to image live patients and is not pertinent to this work (Carver and Carver, 2012; Mazonakis and Damilakis, 2016). The second disadvantage is that the detail of skeletal muscle and other soft tissue structures is not well differentiated using CT imaging. This is due to the similar X-ray attenuation properties of muscle, fascia, tendon and ligament.

### **2.3.2 Magnetic resonance imaging.**

In order to obtain more detailed electronic images of the jaw adductor muscles and postorbital ligaments, Magnetic Resonance (MR) scanning was performed. As with CT scanning, MR scanning captures internal and external structures of the specimen. The advantage of MR images over CT images is that they can distinguish between soft tissues, and MR is the modality of choice for imaging muscle, tendon, ligament and neurovascular tissues. However, due to the low water density and fast signal decay in skeletal material, MR images are less well able to reflect the fine detail of the bony structures (Hashemi *et al.*, 2010; Farncombe and Iniewski, 2013; Wolbarst *et al.*, 2013; Dale *et al.*, 2015; Miller, 2015). MR is another imaging modality that produces images of sequential slices of spatially positioned biological material. Again, each serial slice is made up of many voxels, which, providing they

are isometric, can be reconfigured to view different slice views or segmented to reconstruct volumes. Instead of using X-rays, MR depends upon the magnetic properties of the single protons of the hydrogen atom nuclei within the tissues of the specimen (Hashemi *et al.*, 2010; Wolbarst *et al.*, 2013; Dale *et al.*, 2015). The higher density of hydrogen protons in soft tissue structures results in enhanced soft tissue structure resolution. Conversely, the lower density of hydrogen protons in skeletal material results in poorer resolution of bony material. In the initial stages of scanning a powerful external magnetic force is applied to the outside of the specimen. This force is applied by the MR scanner to the sample within the scanner tube. The hydrogen atoms within the specimen align, either parallel or antiparallel, relative to the magnetic field. The hydrogen atoms then precess, that is they rotate around the axis of the magnetic field. However, they do not precess simultaneously and are said to be out of phase. The frequency of the precession in a given magnetic field is named the Larmor frequency. A second magnetic field is then locally applied via a coil perpendicular to the first, at the same frequency as the Larmor frequency. This is the radiofrequency pulse. The hydrogen nuclei realign to the coil force as it is switched on. As the hydrogen nuclei alter their net alignment they transmit energy which is detected, recorded and spatially located. The computer analysis of the signal between both conditions is the basis for the magnetic resonance image. The different characteristics of tissues are utilised to run different imaging sequences with different weightings. T1 or T2 weighted images describe the magnetic characteristics of the hydrogen nuclei, and the rate at which they realign to their original spin orientation as the coil force is switched off. Proton density weighted images discriminate between the differing densities of protons within each tissue.

### **2.3.3 Method**

To capture details of both soft tissue and bony morphologies, most specimens in this thesis were scanned using either or both computer tomography (CT) and magnetic resonance (MR)

modalities. CT scanning was used to capture the detailed bony morphologies of the head and allowed for differentiation of cortical bone, trabecular bone and dental tissues. CT scanning was performed on fully defrosted specimens. Specimens were scanned at the University of Liverpool either at the Small Animal Teaching Hospital using a Siemens Somatom Volume Zoom (Siemens AG, Munich) or a Toshiba Prime Aquilion (Toshiba Medical Systems, Europe), or at the Philip Leverhulme Equine Hospital using a GE Lightspeed Plus (GE Medical Systems, Milwaukee). Current and voltages used were 120 kV and 200 mA.

MR was used to capture the details of the jaw adductor muscles and the postorbital ligament. MR scanning was performed on fully defrosted specimens. Specimens were imaged using a 3T Siemens Trio (Siemens Medical Solution, Erlangen, Germany) magnetic resonance scanner at the Liverpool Magnetic Resonance Imaging Centre at the University of Liverpool. CT and MR slice thickness and pixel spacing used in this thesis are reported in Table 2.3. Scanning was performed before dissection occurred to ensure soft tissues as well as bony elements were scanned, and that no artefacts were created during the manual manipulation of the specimens. The specimens that did not undergo imaging were the 16 *Vulpes vulpes* specimens used in the *ex vivo* strain gauge experiments (Chapter Five).

**Table 2.3 Image slice thickness and pixel spacing for all scanned specimens.**

Specimen	MR slice thickness mm	MR pixel spacing	CT slice thickness	CT pixel spacing
<i>Alopex lagopus 2</i>	1.00	0.424	0.5	0.194
<i>Canis lupus 1</i>	1.00	0.424	0.5	0.417
<i>Canis Lupus 2</i>	1.00	0.424	0.5	0.357
<i>Canis Lupus 3</i>	1.00	0.424	0.5	0.34
<i>Canis lupus familiaris</i>	1.00	0.424	x	x
<i>Canis mesomelas</i>	1.00	0.5	0.625	0.283203
<i>Chrysocon brachyusus</i>	1.00	0.424	1.25	0.388672
<i>Cuon alpinus 1</i>	1.00	0.424	0.5	0.283
<i>Lycaon pictus 1,2</i>	1.00	0.424	1	0.29296875
<i>Lycaon pictus 3</i>	1.00	0.424	0.5	0.3203125
<i>Lycaon pictus 4</i>	1.00	0.424	0.5	0.333
<i>Nyctereutes procyonoides</i>	1.00	0.424	0.5	0.177
<i>Otocyon megalotis</i>	1.00	0.424	0.5	0.177



<i>Speothos venaticus</i>	1.00	0.424	1.25	0.292969
<i>Vulpes corsac 1</i>	1.00	0.424	0.625	0.187500
<i>Vulpes corsac 2</i>	1.00	0.424	0.5	0.172
<i>Vulpes corsac 3</i>	1.00	0.223	0.5	0.192
<i>Vulpes corsac 4</i>	1.00	0.223	0.5	0.162
<i>Vulpes vulpes 1,2,3,5,6</i>	1.00	0.424	0.5	0.203125
<i>Vulpes vulpes 7</i>	1.00	0.424	x	x
<i>Vulpes zerda</i>	1.00	0.223	2.0	0.136

### 2.3.4 Muscle imaging and validation

To determine which MR protocol was best able to distinguish between muscle masses, a short study was performed. One specimen was scanned (*Canis lupus familiaris*) using three different protocols (T1 weighting, T2 weighting and Proton density), and the resultant scans visually assessed. The proton density (PD) sequence gave the best signal intensity for collagenous tissues such as fascia, ligament and tendon, and consequently allowed the different divisions of the muscles to be more clearly identified (Figure 2.1). Consequently, all specimens were scanned using the PD sequence.

Previous studies have demonstrated a strong correlation with gross cadaveric findings of human skeletal muscle mass with those reconstructed via MR imaging (Mitsiopoulos *et al.*, 1998; Sanal *et al.*, 2009; Balius *et al.*, 2013; Storey *et al.*, 2016; Pinares Toledo *et al.*, 2018). To verify if this is also applicable in canid masticatory apparatus and that individual muscles could be correctly identified and measured, a validation test was performed. Four *Vulpes vulpes* specimens were scanned using MR. One of the specimens was subsequently frozen and bandsawed into approximately 1cm axial slices. Slices were compared with the corresponding specimen's MR axial images to identify the individual muscle masses of temporalis, masseter and the pterygoids (Figure 2.2 A, B). The three other *Vulpes vulpes* MR datasets were loaded into Seg3D software (CIBC, 2016), and individual muscles identified and reconfigured as muscle volumes (Figure 2.2.C). Volumes were converted into mass using the values of 1.056g cm<sup>3</sup> for mammalian muscle (Murphy and Beardsley, 1974). These three specimens were then dissected to determine jaw adductor muscle masses. Reduced major

axes (RMA) regression tests and *t*-tests were performed to establish any differences in mass between the two sample groups. RMA regression analyses were used to account for possible errors in both variables.

### Validation results

Muscle masses reported from dissections and calculated from MR scans are reported in Table 2.4. RMA regression slope was 1.02 ( $r^2$  0.99, CI 0.98, 1.04) (Figure 2.3) and not statistically different to the expected slope of 1. The *t*-test *t* value between the dissection and MR derived values was -0.07108 the *p*-value was 0.944217. The result was not significant. Both of these statistical tests imply that muscle masses determined from MR reconstructions were statistically indistinguishable than those determined by gross dissection techniques, and that either method is reliable for determining muscle mass values.

### **2.3.5 Combined computer tomography and magnetic resonance scans.**

Several easily distinguishable bony landmarks that were common to both the CT and MR datasets were selected and used to co-register both datasets using Avizo software (FEI Systems, Oregon, USA). This combined both imaging modalities into one series, which enabled the visualisation of muscles and other soft tissue structures relative to the reconstructed skull (Figure 2.4). This allowed for identification of muscle attachment sites (Chapter Three, part 3.3.3) and was also further explored to consider if landmarking the muscle boundaries could be used for shape analysis of muscles (Chapter Three, part 3.3.2.1). This technique was performed for each species in the dataset. Where more than one specimen represented the species, the individual identified as being closest to the mean shape was chosen (Chapter Three, part 3.3.2.3).

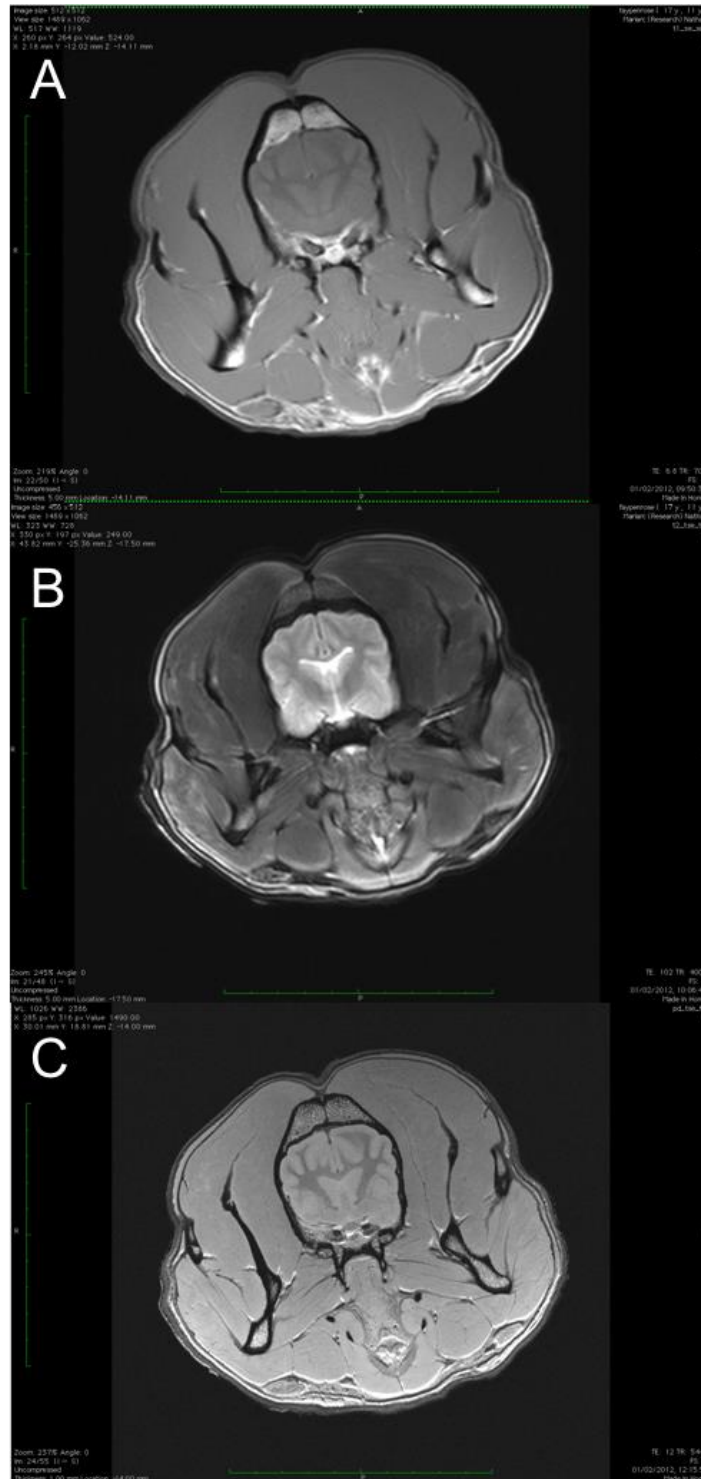


Figure 2.1 MR axial slices of *Canis lupus familiaris*, A, T1 weighted sequence, B, T2 weighted sequence, C, PD weighted sequence.

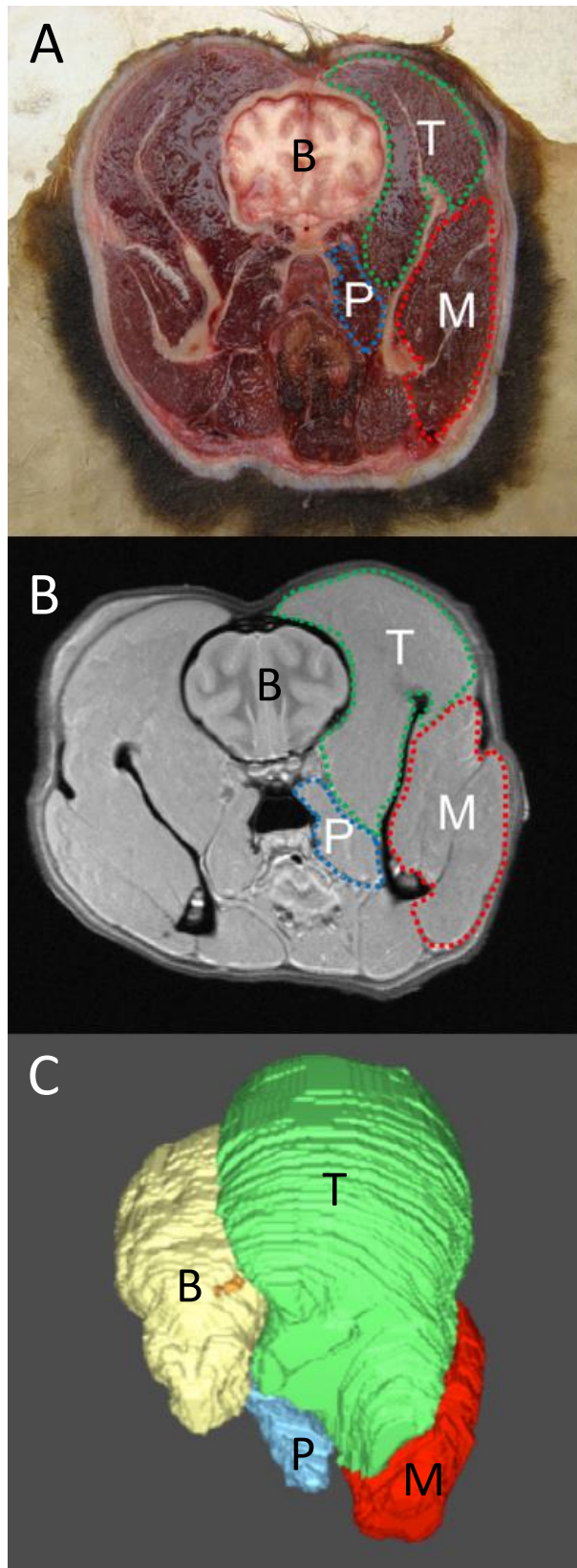


Figure 2.2 *Vulpes vulpes*. A: Bandsawed axial section, B: MR axial slice, C: Individual MR muscle slices reconfigured to render jaw adductor muscle volumes. T: temporalis, M: masseter, P: pterygoids, B:brain.

**Table 2.4. MR and dissection muscle volumes validation study.**

Specimen	Muscle	Voxels (individual voxel volume 7.63285E-05cm <sup>3</sup> )	Volume cm <sup>3</sup> from MR	Mass(g) from MR	Mass(g) from dissection*
<i>Vulpes vulpes</i> 2 Male 8.5kg	Temporalis	801798	61.2	64.6	66.1
	Masseter	300969	23.0	24.2	22.9
	Pterygoids	78480	6.0	6.3	7
<i>Vulpes vulpes</i> 3 Female 4.7kg	Temporalis	420517	32.1	33.9	35.9
	Masseter	147553	11.3	11.9	11.1
	Pterygoids	50955	3.9	4.1	4.9
<i>Vulpes vulpes</i> 5 Male 6.3kg	Temporalis	586172	44.7	47.2	48
	Masseter	212125	16.2	17.1	19.3
	Pterygoids	64606	4.9	5.2	5.7

\* Calculated from values in Murphy and Beardsley (Murphy and Beardsley, 1974).

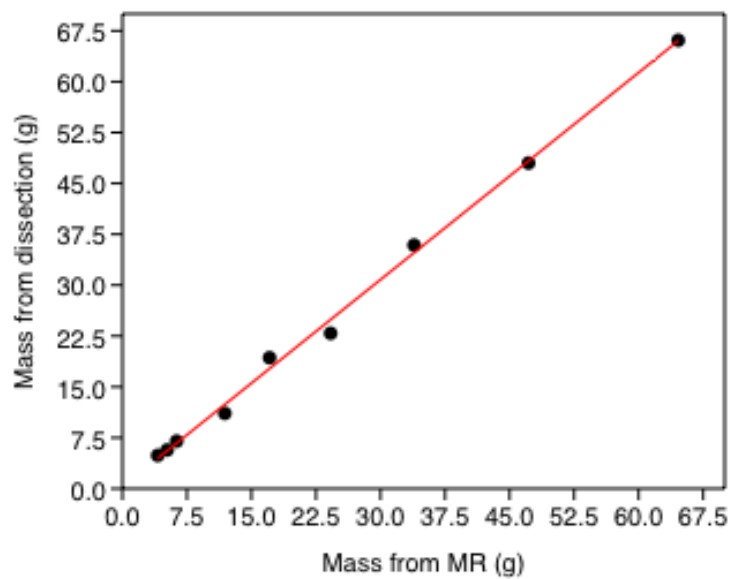


Figure 2.3 RMA regression of mass from MR vs Mass derived from dissection.

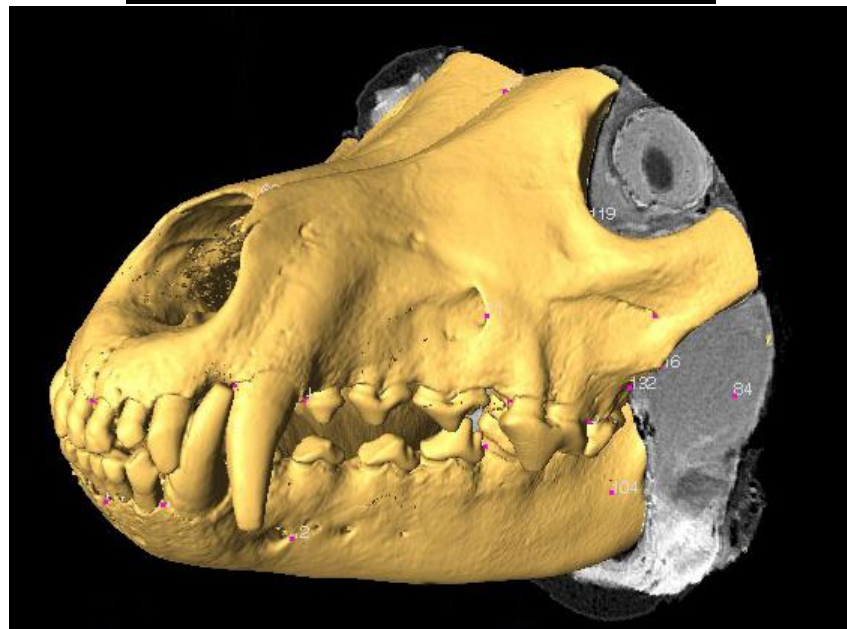
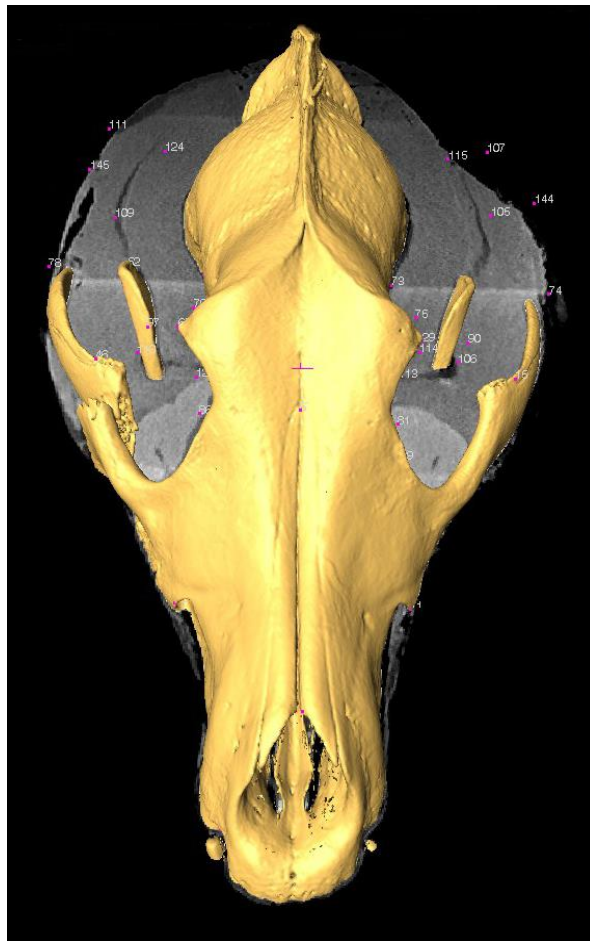


Figure 2.4 *Canis lupus*, co-registered MR and reconstructed skulls from CT scans. Pink dots and numbers indicate landmark placement sites.

## **2.4 Dissection and the gross anatomy of the jaw adductor muscles.**

### **2.4.1 Review**

Dissection, the structured dismantling of cadavers, has long been used in morphological studies to document and explore the form of biological material (Hildebrand *et al.*, 1995). It has two main advantages. Firstly, that empirical data is gathered (Jones, 1997; Budras *et al.*, 2007; Evans and De LaHunta 2016). This is may be used as a primary source for further analysis, or to validate other studies. Secondly, dissection also brings the understanding that the complexity of real anatomy cannot be summarised into numerical data, and it is only with close examination of real specimens that true biological condition can be described. However, access to real specimens also brings an understanding of how errors in acquisition or recording of samples are easily made. For example, muscle fascicle lengths vary greatly within a single muscle and it cannot be ignored that muscle samples naturally includes other tissues such as tendon, fat, fascia and neurovascular tissue. Dissection also revealed how the fascia in particular has a structural and unifying role in supporting the muscles and uniting them with their neighboring structures (Korf *et al.*, 2008).

Dissection has three major disadvantages. Firstly, it can only be performed on *ex-vivo* specimens, which limits the number of available specimens. Secondly, it must be performed in a sequential order, running from superficial to deep, which has the potential to overlook key topographical relationships. Thirdly, it is by nature destructive and no specimen can be dissected twice. It is essential that detailed notes and photographs are kept throughout the process.

In this thesis a combination of observations from both imaging modalities and dissection were used to integrate anatomical knowledge to inform further analyses, for example when calculating the muscle attachment surface areas (Chapter Three) or describing the muscle attachment sites in the finite element models (Chapter Four).

## 2.4.2 Method

This part of the thesis describes the gross anatomy of the jaw adductor muscles found in twelve species of Caninae. This is the most extensive descriptive work on wild canid species masticatory muscle to date. A total of 23 heads were dissected to determine the anatomy of the jaw adductors (Table 2.2). At least one representative from each of the species used in this thesis was dissected. After removal from the body, all heads were stored in either refrigerators or freezers. In some specimens, the fur and skin were present on receipt of the sample (Figure 2.5), whilst in other samples they had been removed, but no underlying tissues were disturbed. No fixative solution was applied to any specimen, that is they were all fresh or defrosted from frozen. Consequently, they were expected to suffer from minimum amounts of shrinkage, unlike specimens that have been stored in alcohol, formalin or other preserving fluids (Fox *et al.*, 1985; Tolhurst and Hart, 1990; Brenner, 2014; Hayashi *et al.*, 2016). Frozen specimens were defrosted before any analyses. Specimens were dissected on one side, either left or right, where necessary avoiding any pre-existing damage. No individual was judged to have a preferential working side judging from dental wear. Specimens were photographed throughout the dissection process to capture the details of morphology that cannot be reduced to numerical observations. These included the extent and thickness of the fascial coverings, the tendinous components of the muscles and the complexity of the layers of the muscles. Photography was performed using a digital camera (Sony DSC-H200) that in most cases was positioned approximately perpendicular to the sagittal, axial and coronal planes of each specimen. Oblique views were also used to capture deeper structures, or to cover several aspects of the areas of interest.

The masticatory muscles were photographed in situ and then removed. During the dissection, any large amounts of fat or connective tissue were removed from any muscles, but I acknowledge that small quantities of these and other tissue types, for example tendons,



fascial sheets and neurovascular bundles, also contribute to the muscle mass. Details observed and measured from the muscle architecture were used in physiological cross sectional area calculations (Chapter Four, part 4.2.3.2), and as with other studies using this method, the non-muscular components are not taken into account in this thesis. As each muscle and its subdivisions were removed, the origin and insertion points were recorded photographically. Individual muscles were wrapped in damp cloth and stored in labelled polythene bags to prevent dehydration. Individual muscles and their constituent subdivisions were subsequently weighed using Redwag WPS600/C/2 digital scales, accurate to 0.001g, and dissected for further analyses. The dissection photographs in this chapter represent a small number of the many taken and aim to give a representative overview of the diversity of the material.

Each specimen was skinned, and the muscles of facial expression and superficial connective tissue and fascia removed (Figures 2.6 and 2.8). The digastricus muscle, a jaw abductor was removed and was not used in any part of this study (Figure 2.7). The masseter was the first of the jaw adductor muscles to be dissected and removed as this partially covered both the temporalis and pterygoid muscles. The temporalis was removed next as this then enabled the pterygoids to be visualised and accessed. Muscle masses and muscle subdivision masses are reported in Table 2.5.



Figure 2.5 *Lycaon pictus*, intact head, with fur, skin and superficial structures in place.



Figure 2.6 *Lycaon pictus*, fur and skin removed. Any superficial non- masticatory muscles such as platysma, interscutularis, occipitalis and zygomaticus were removed.



Figure 2.7 *Lycaon pictus*. The digastric muscle (white asterisk) was dissected and removed. As a jaw abductor this muscle, although associated with mastication, was not included in any part of this study.



Figure 2.8 *Canis mesomelas*. The superficial layer of temporal fascia was contiguous with that covering the masseter and also ran forward to the maxillary region. This was photographed and then removed. The deep layer of fascia was more robust and was dissected with the temporalis muscles (see Figures 2.18 and 2.19).

### 2.4.3 Dissection notes on the masseter muscle.

The masseter muscle is the second largest of the jaw adductors in carnivorans (Getty, 1975; Evans and De Lahunta, 2016; Singh et al., 2018). The mean mass of the masseter in the specimens dissected in this study contributed 30% to the total jaw adductor mass. The masseter/zygomaticomandibularis system was the most morphologically complex part of the jaw adductor muscles. For further details on masseter muscle nomenclature see Chapter One, part 1.3.2.3. The masseter was subdivided into three layers, superficial, deep and zygomaticomandibularis, although the division between the superficial and deep layers was often unclear, particularly in the larger species where many additional leaflets were observed. All layers were to some extent merged with those that lay next to them, and so definitive boundaries of each muscle belly were not always possible to ascertain. In these instances, the boundaries were determined by observing the orientation of the fascicles: the superficial muscle fascicles ran in a caudoventral orientation, whilst those of the deep masseter ran more ventrally, and the zygomaticomandibularis fascicles had a rostroventral orientation. Although the specific architecture of each of the masseteric subdivisions was recorded (Table 2.5) all calculations, regarding mass and reduced physiological cross-sectional areas were calculated using the sum of the individual parts of the masseter, as the divisions were very indistinct. Turnbull describes similar observations relating to the masseter complex of the domestic cat, *Felis silvestris* (Turnbull, 1970). He noted that even when subdivisions of the muscles appear clearly separated at their origin, they soon merged with each other and the intermingling of fibres, occurred throughout all layers of the masseter. In addition, many fascicles were muscular at one end, and tendinous at the other. In these instances, the tendinous portion could be at either the origin or insertion. As morphological descriptions tend to oversimplify structures there may be no ideal method to accurately capture the complexity of this muscle.

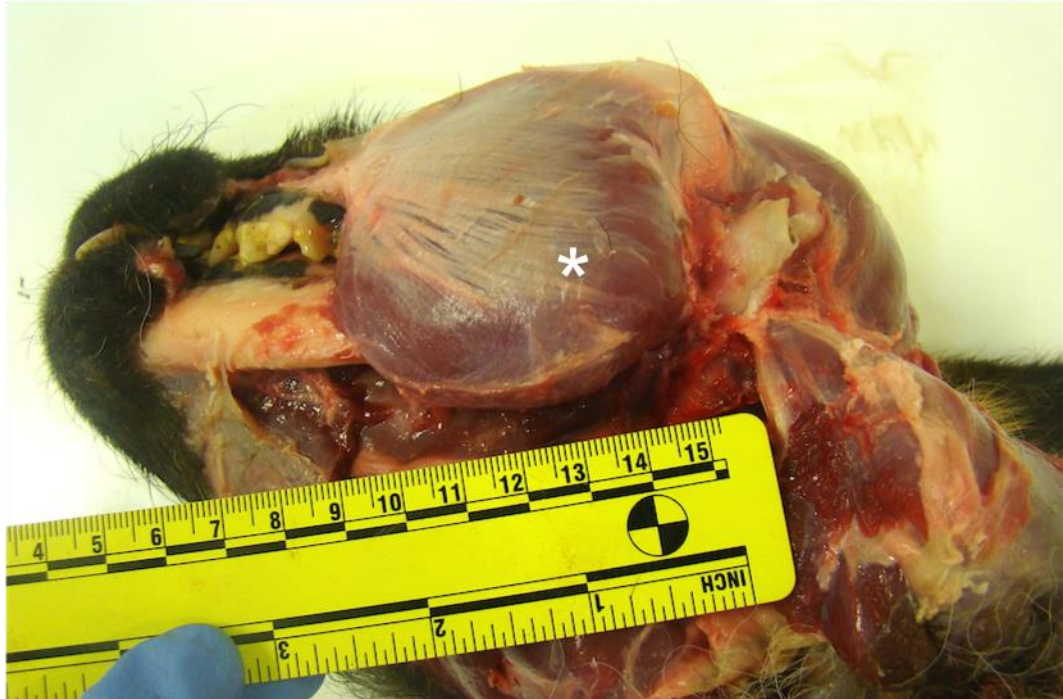


Figure 2.9 *Lycaon pictus*. Superficial masseter (white asterisk) caudoventral aspect. The fibres of superficial masseter run caudoventrally and insert partially on the lateral surface of the caudal mandible, whilst other fascicles run around the ventral border to insert on the ventromedial surface of the caudal mandible and the tendinous raphe of the pterygoids.



Figure 2.10 *Lycaon pictus*. Superficial masseter (white asterisk), lateral aspect.



Figure 2.11 *Nyctereutes procyonoides*. The origin of superficial masseter is by way of a robust tendon of origin (white asterisk) from a small bony prominence on the maxilla, dorsal to UM2. In all species muscle fibres also arose from the rostral half of the ventral zygomatic arch.

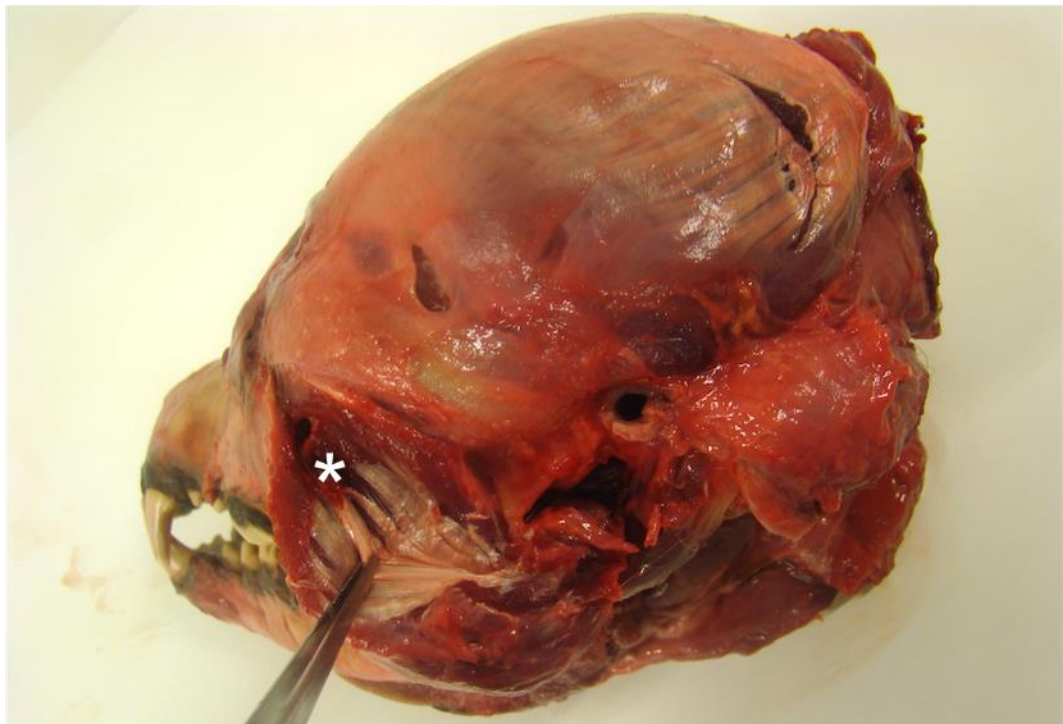


Figure 2.12 *Canis lupus*. Division of the superficial masseter. All species dissected revealed more than one easily identifiable layer of the superficial masseter. The muscle has a significant tendinous component, which although visually evident, was difficult to separate from the muscular element. In some of the larger species (*Canis lupus*, *Cuon alpinus*, *Lycaon pictus*, *Chrysocyon brachyurus*) the superficial leaflet of the superficial masseter folds back on itself (white asterisk).



Figure 2.13 *Canis lupus*. Showing the complex arrangement of superficial masseter leaflets (white asterisk). The muscle fascicles ran in many different directions and many had a great amount of tendinous component, particularly toward the muscle insertion on the angular process of the mandible.

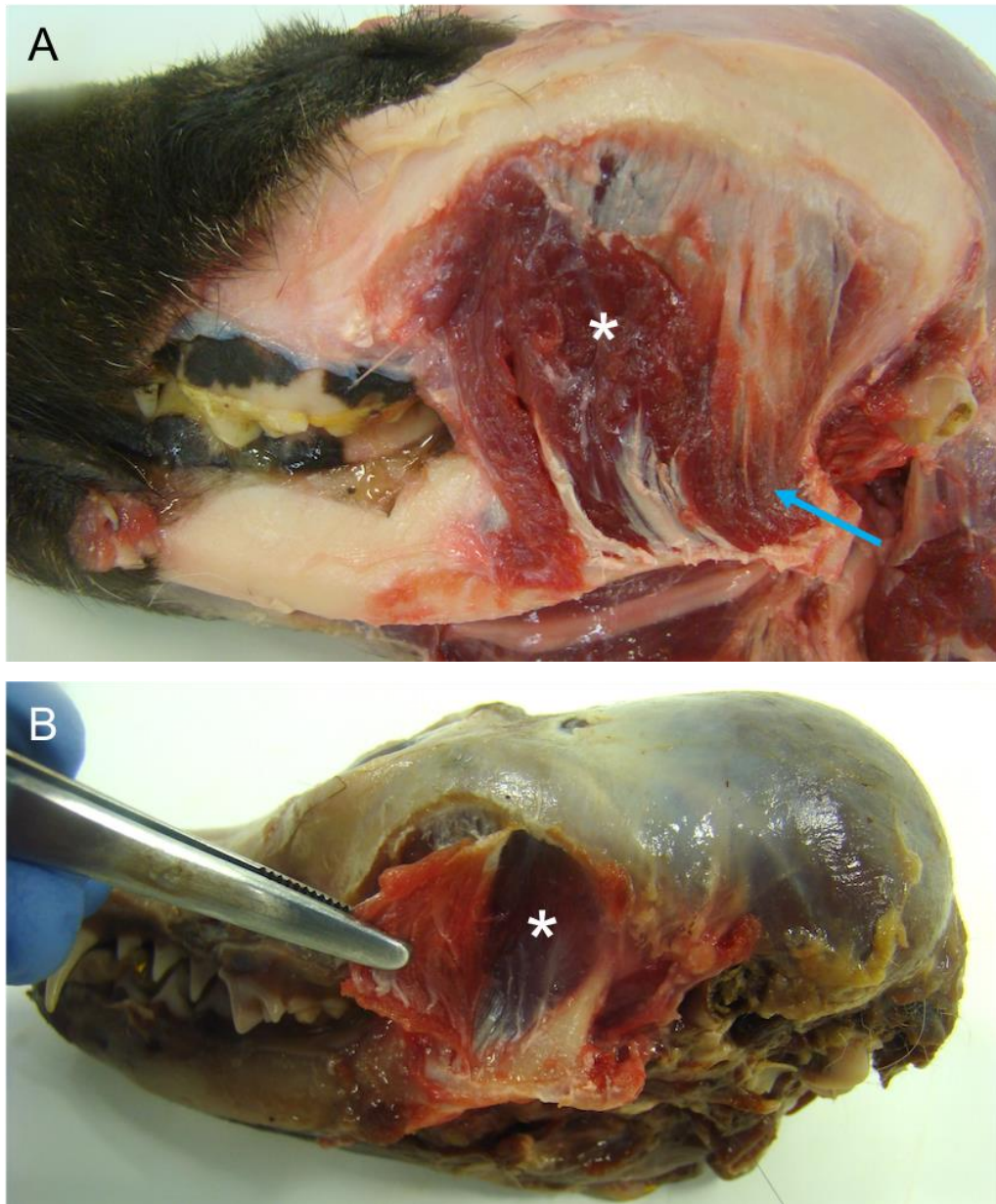


Figure 2.14 The deep masseter was complex, and all species revealed more than one easily identifiable layer (white asterisk). The deep masseter arises from the ventral zygomatic arch and inserts onto the lateral caudal mandible. There were many leaflets of muscle, which were especially evident in the larger species (Figure 2.14A, *Lycaon pictus*). The smaller species appeared to have a more straightforward arrangement of layers (Figure 2.14B, *Vulpes corsac*). Some leaflets arose from the arch and inserted by way of aponeuroses, onto other divisions of the muscle. Many of the muscle fascicles of such subdivisions were notably short (Figure 2.14A, blue arrow).



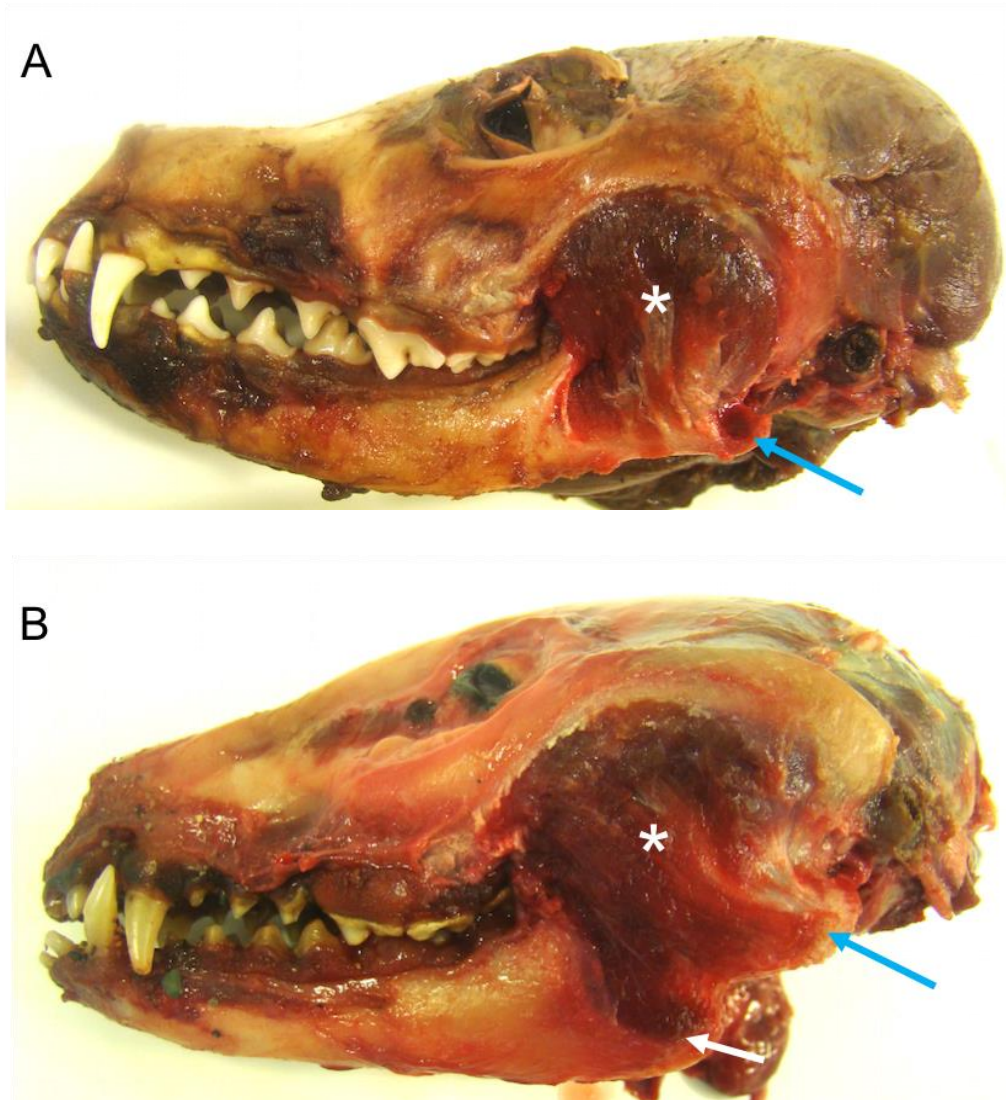


Figure 2.15. In two species, *Otocyon megalotis* and *Nyctereutes procyonoides*, the mandible exhibits a preangular process to which some of the fascicles of the deep masseter insert. Figure 2.15A illustrates the usual canid condition with no preangular process (*Alopex lagopus*), and 2.15B shows the pronounced preangular process in *Nyctereutes procyonoides*, a similar sized species. The white asterisk indicates the deep masseter, the blue arrow indicates the angular process and the white arrow indicates the preangular process. This extra prominence has the effect of lengthening the fascicles of this part of the masseter and re-orientating them into a more vertical position. This may reflect some functionality of the masseter, as an expanded area for the insertion on the caudal mandible is the condition seen in herbivorous mammals, who are more accustomed to utilising crushing and grinding actions of the cheek teeth.

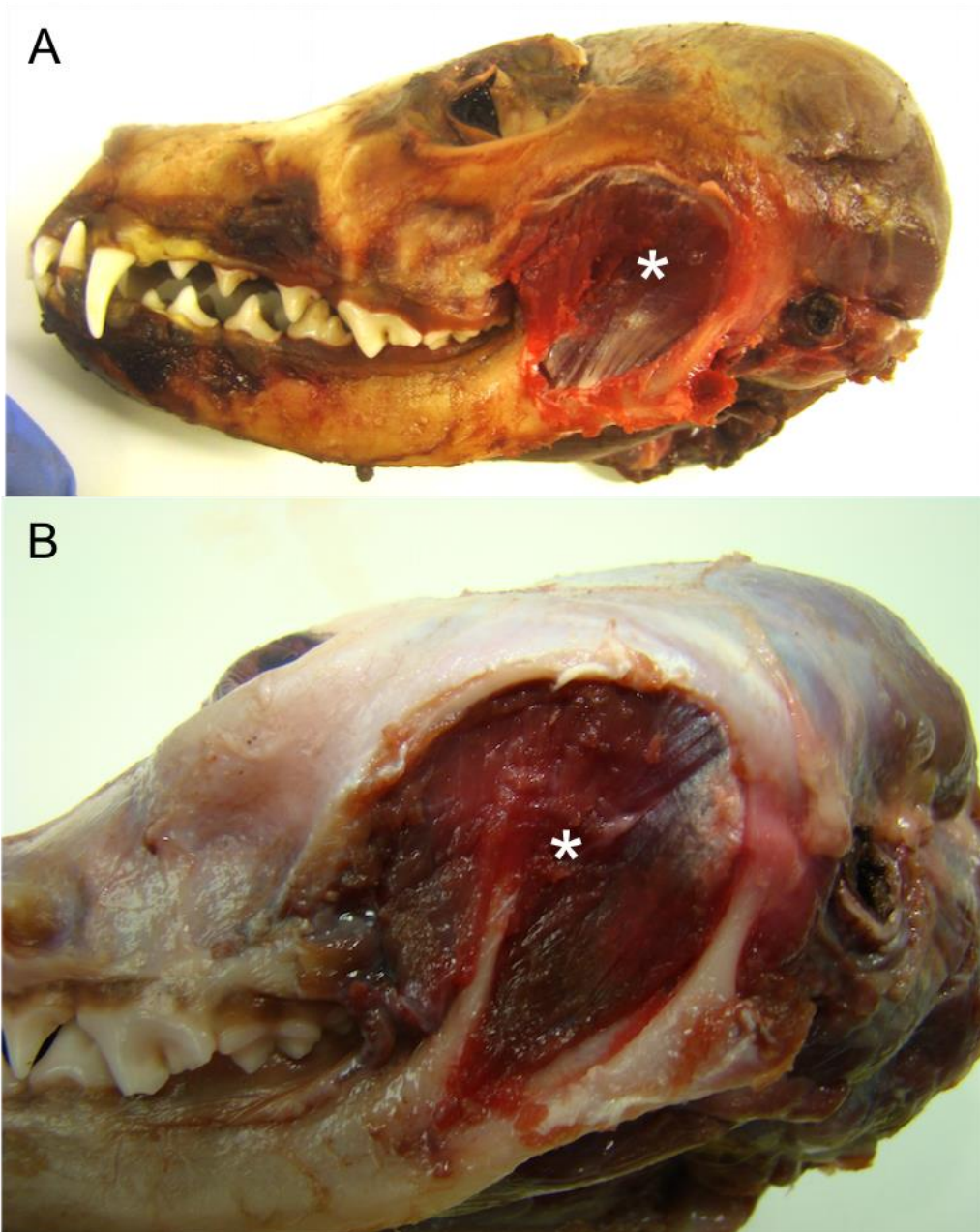


Figure 2.16A, *Alopex lagopus*, and B *Canis mesomelas*. The zygomaticomandibularis muscle (white asterisk), arises from the medial and caudal zygomatic arch and inserts onto the masseteric fossa and the area just ventral to this. At its origin, the fascicles can be difficult to isolate from those of the temporalis and, as the muscle runs rostroventrally some of its fascicles become blended with those of the deep masseter.

#### **2.4.4 Dissection notes on the temporalis muscle**

The temporalis muscle is the largest of the jaw adductors in the carnivorans (Getty, 1975; Evans and De Lahunta, 2016; Singh et al., 2018). The mean mass of the temporalis in the specimens dissected in this study contributed 62% to the total jaw adductor mass (Table 2.5). Its large area of origin covers most of the lateral cranium, arising from the parietal, temporal frontal and occipital bones. In larger species the left and right temporalis muscles originate at midline, but in the smaller species there is a marked sagittal space on the skull that is free of all overlying muscle (Figure 2.17). Temporalis inserts onto the coronoid process and medial vertical ramus of the mandible. The arrangement of the temporalis muscle, with its long fascicles, is less efficient at force production than the more lateral and ventrally sited masseter, but it has the advantage of not restricting jaw opening, and so is favoured in animals that require a wide gape (Gans, 1982; Eng *et al.*, 2009; Santana 2016). In all samples, the division of the temporalis into three discrete parts was clear.

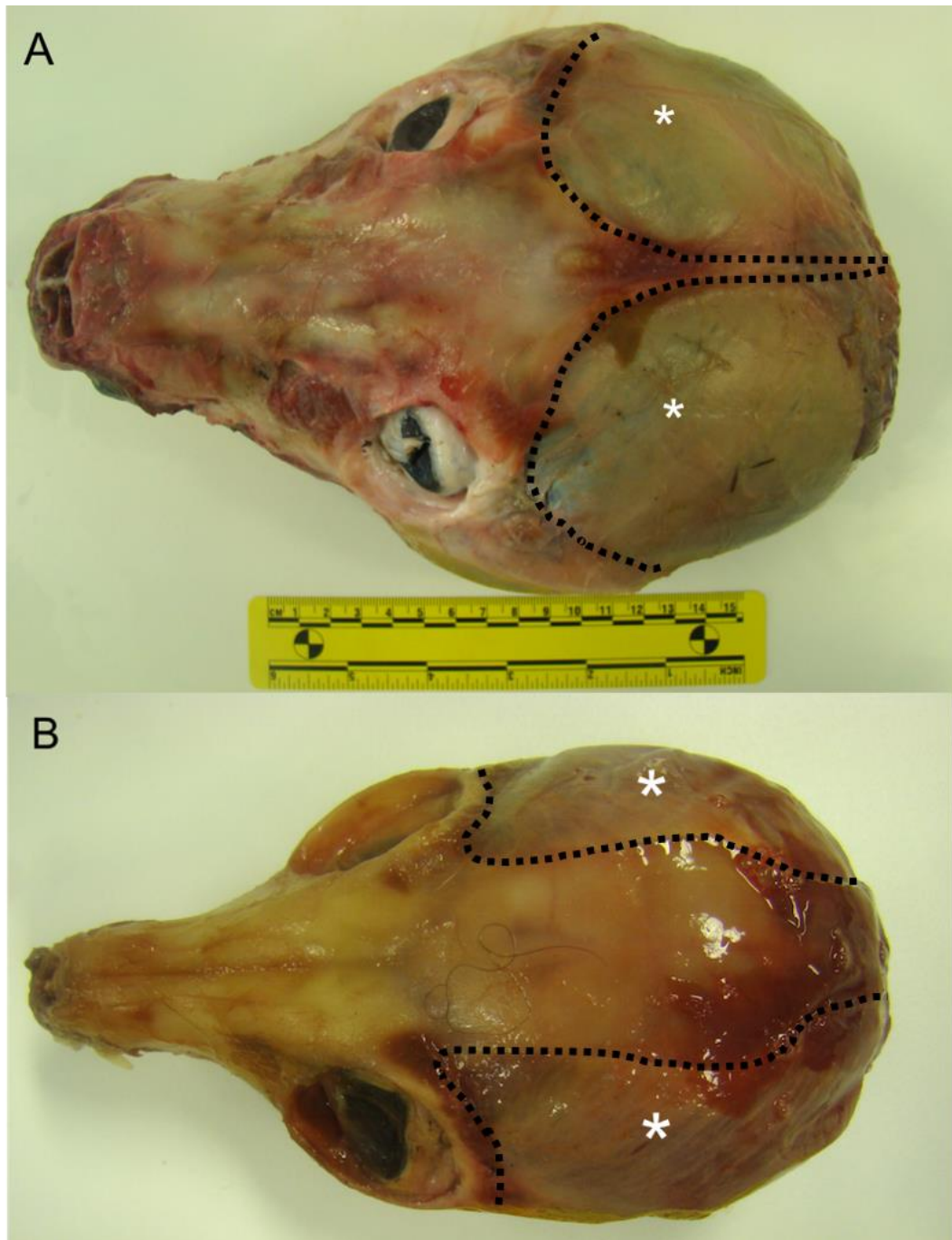


Figure 2.17 The extent of temporalis (white asterisk and black dotted lines) occupying the temporal fossa in A, *Lycaon pictus* and B, *Vulpes zerda*. In the three smallest species (*Vulpes zerda*, 1150g, *Vulpes corsac* 2850g and *Otocyon megalotis*, 4200g) the temporalis originated lateral to midline. In all other species the temporalis originated at midline. In species over species over 10kg, a pronounced sagittal crest was present, and increased the surface area available for the origin of temporalis.

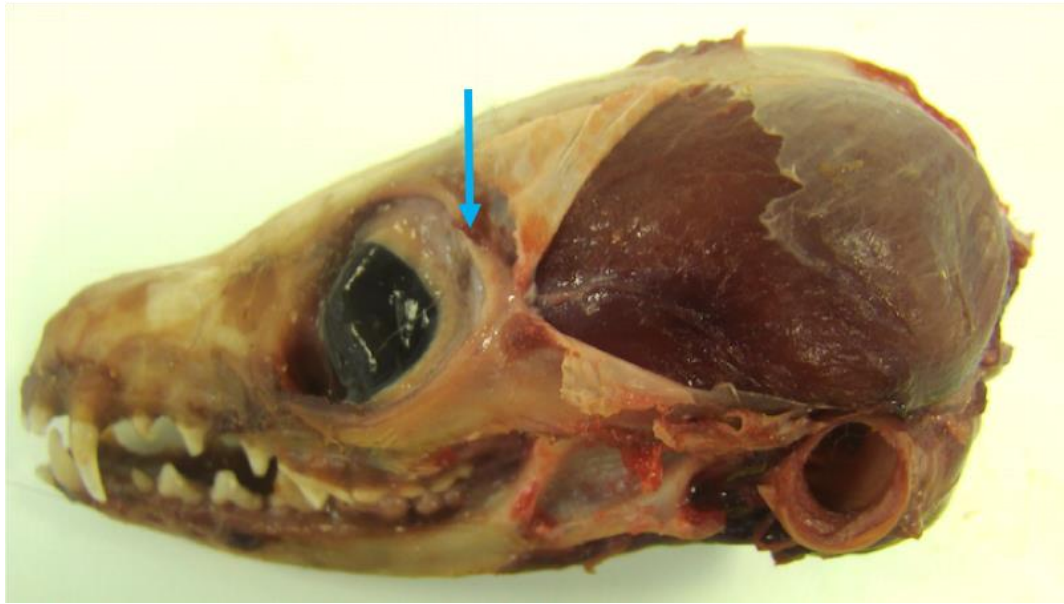


Figure 2.18 The substantial deep temporal fascia was seen in all species, even the tiny *Vulpes zerda*. It arises from the midline sagittal crest, the nuchal crest, the dorsal zygomatic arch and is contiguous with the orbital ligament (blue arrow).

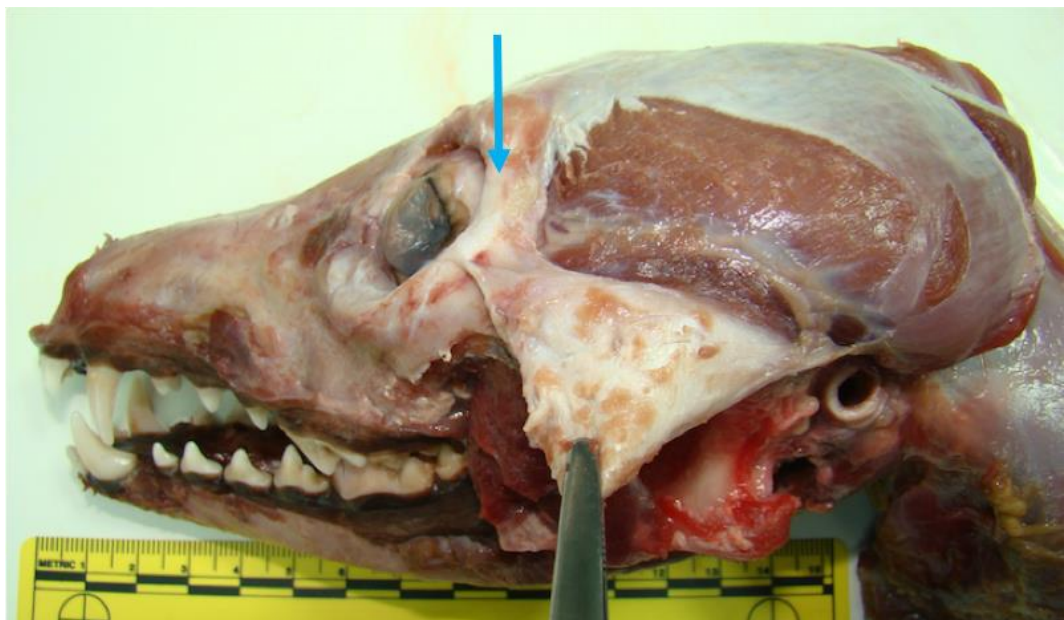


Figure 2.19 *Canis mesomelas*. The deep temporal fascia is much more substantial than the superficial layer, and some of the muscle fascicles of temporalis originate from it. In this way, fascia is linked to the action of the muscle and the fascicles can be shorter (and therefore more efficient) than if they arose from bone. This arrangement is also reported in the ursid species and felids (Davis, 1964; Turnbull, 1970). The orbital ligament is identified by the blue arrow.



Figure 2.20 *Lycaon pictus*. Temporal fascia removed to reveal the extent of the temporalis muscle.



Figure 2.21 *Vulpes vulpes*. In this specimen the zygomatic arch has been removed to reveal the extent of the suprazygomatic division of the temporalis muscle (white asterisk). This is the smallest division of temporalis and originates from the base of the zygomatic process of the temporal bone.



Figure 2.22 *Lycaon pictus*. The suprazygomatic division of temporalis (white asterisk) inserts the most laterally and cranially of any of part of temporalis, on the rostral vertical ramus of the mandible. It has the longest muscle fascicles of any of the jaw adductor muscles.



Figure 2.23 *Nyctereutes procyonoides*. The suprazygomatic division of temporalis has a tendinous component on its medial aspect (white asterisk).

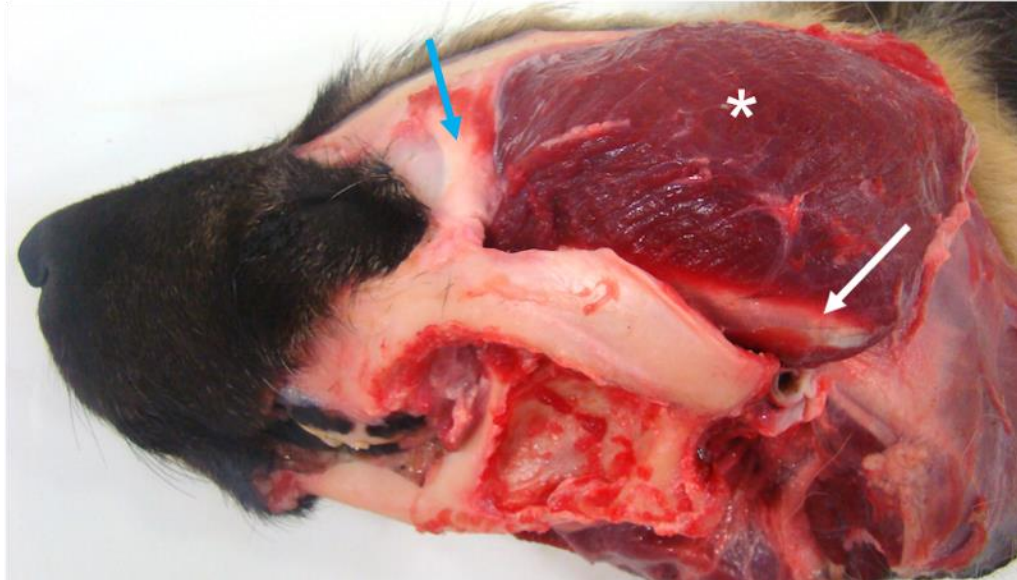


Figure 2.24 *Lycaon pictus*. Superficial temporalis (white asterisk). A large and extensive muscle originating from as far medially as midline and as far caudally as the nuchal line of the supraoccipital, parietal and temporal bones. Rostrally the limit of superficial temporalis is the orbital ligament (blue arrow). The origin is limited to a relatively narrow strip around the margins of the lateral calvarium as it overlies the deep temporalis. Insertion is limited to a relatively small area on the coronoid process of the mandible, chiefly on the dorsal medial aspect but also to a small area on the most dorsal lateral aspect. The muscle is broadly fan shaped. A proportion of the superficial temporalis, especially the part near its origin on the maxilla and zygoma, is made up of tendinous material (white arrow).



Figure 2.25 *Alopex lagopus*. Superficial temporalis, reflected. This figure shows the thickness of the superficial temporalis (white asterisk) and the extent of its coverage of deep temporalis (black arrow).



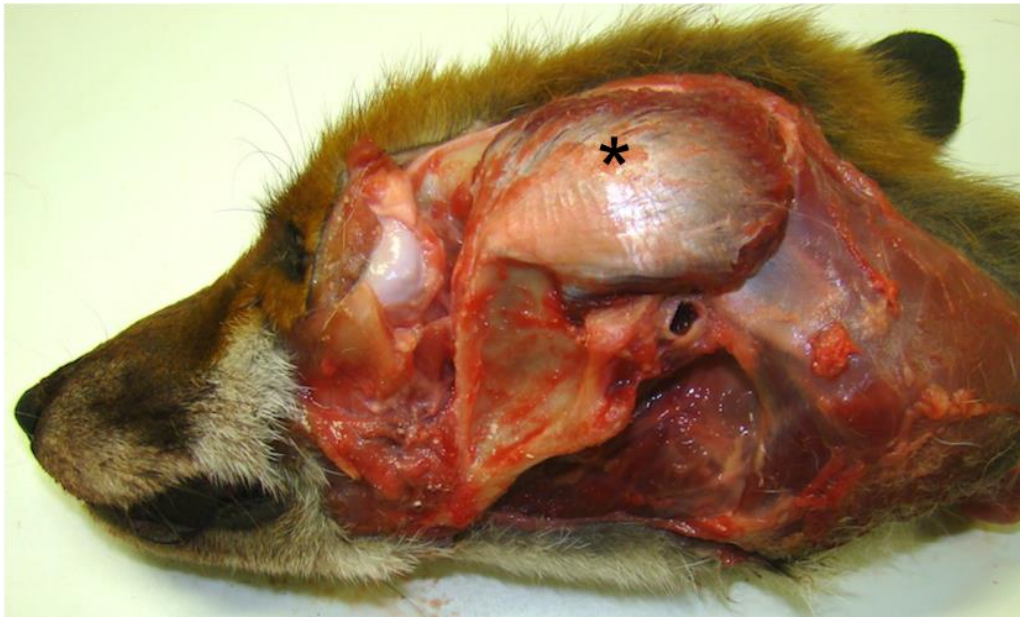


Figure 2.26 *Vulpes vulpes*. The deep temporalis (black asterisk). A fan shaped muscle, with its origin more ventral and lateral than that of the superficial temporalis. It arises from the lateral cranium and inserts onto the medial vertical ramus of the mandible as far ventrally as the level of the ventral extent of the masseteric fossa. In some of the larger species a number of fascicles from deep temporalis merge with those of both zygomaticomandibularis ventrolaterally, and pterygoids ventromedially. There is a large tendinous component to the muscle which becomes more pronounced towards its insertion.

#### 2.4.5 Dissection notes on the pterygoid muscles

The pterygoid complex consists of two muscles, the larger and more extensive medial pterygoid, and the much smaller lateral pterygoid (Figure 2.28 and Figure 2.29). The medial pterygoid muscle originates on the pterygoid, palatine and sphenoid bones, and the lateral pterygoid muscle originates from part of the sphenoid bone (Figure 2.30). Both insert on the caudal medial mandible. One specimen (*Vulpes vulpes* 7) was dissected to determine the contribution of the lateral pterygoid to the total pterygoid mass. Dissection values found that the lateral pterygoid made up approximately 3% of the total pterygoid mass in *Vulpes vulpes* (lateral pterygoid 0.28g, medial pterygoid 8.71g), and 0.27% to the total jaw adductor muscle mass. In some mammals the lateral pterygoid is reported as having two distinct heads, superior and inferior (Grant, 1973; McNamara, 1973; Gibbs *et al.*, 1983;

Murray, 2012), but I found no clear distinction in any of the canids dissected. This finding is in accordance with previous authors (Getty, 1975; Ström *et al.*, 1988; Tomo *et al.*, 1995; Gioso and Carvalho, 2005; Evans and De Lahunta, 2013). The mean mass of the combined medial and lateral pterygoids in the specimens dissected in this study contributed 9% to the total jaw adductor mass (Table 2.5). In both the medial and lateral pterygoid, the fascicles run caudoventrally and laterally from their origin on the pterygoid, sphenoid and palatine bones, to insert onto the medial aspect of the caudal part of the mandible. The medial pterygoid also has some fascicles inserting onto the tendinous raphe of the superficial masseter (Figure 2.27). The action of the medial pterygoid is to adduct the jaw. However, the action of the lateral pterygoid in the carnivorans is unclear and somewhat disputed. Some authors describe it as a jaw adductor or probable jaw adductor due to the orientation of the fascicles and close association with the medial pterygoid (Tomo *et al.*, 1995; Evans and De Lahunta, 2013; Singh *et al.*, 2018). Other authors describe it as a possible jaw protractor or joint stabilizer (Kawamura *et al.*, 1968, Turnbull 1970). All concur that its role is likely to be insignificant due to its small size and the bony constraints of the temporomandibular joint (Turnbull, 1970; Ström *et al.*, 1988; Herring, 2007; Hartstone-Rose *et al.*, 2012). Throughout this thesis, the medial and lateral pterygoid muscles were considered and referred to as one muscle, the pterygoids.

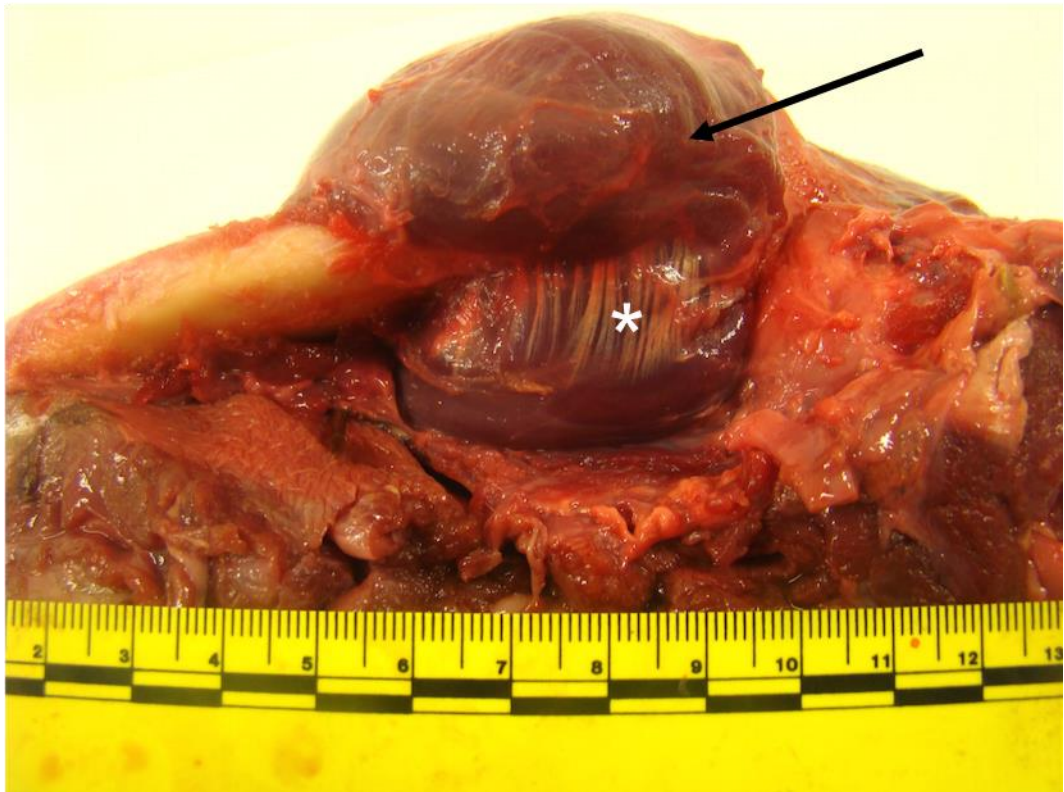


Figure 2.27 *Canis lupus*. The pterygoids (white asterisk) insert partly onto the medial aspect of the caudal mandible, and partly onto the tendinous raphe of the superficial masseter (black arrow).

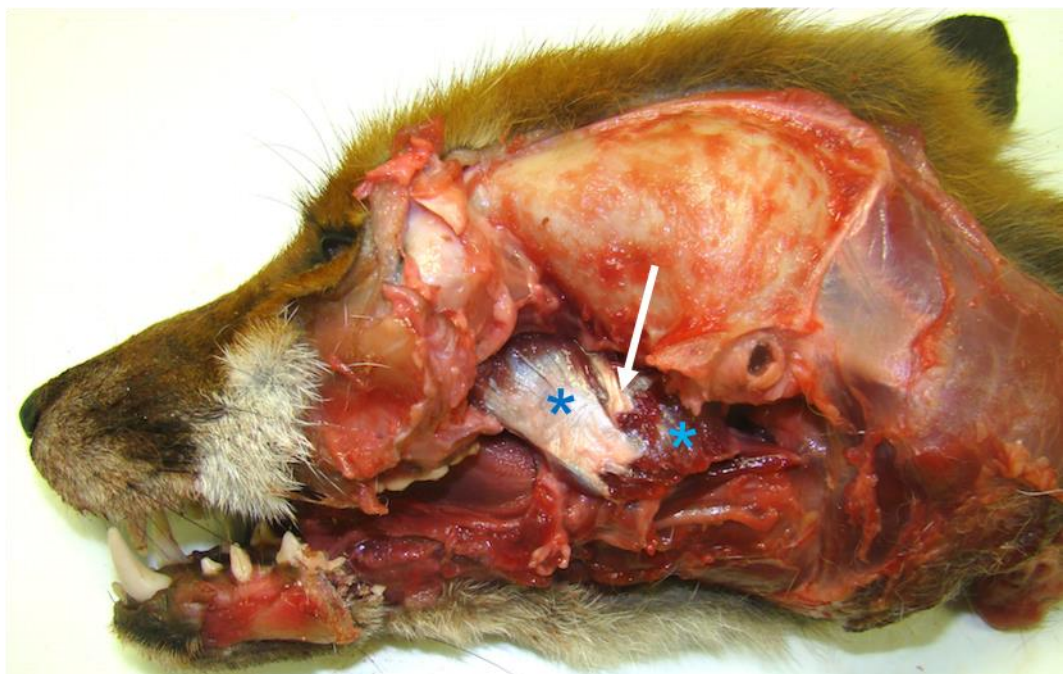


Figure 2.28. *Vulpes vulpes*. The pterygoids consist of two muscles, the large medial (blue asterisks) and much smaller lateral pterygoids (white arrow).



Figure 2.29 *Ex situ* pterygoid muscles. *Vulpes vulpes*. The lateral pterygoid (LP) is much smaller than the medial pterygoid (MP), contributing approximately 3% to the total pterygoid mass.

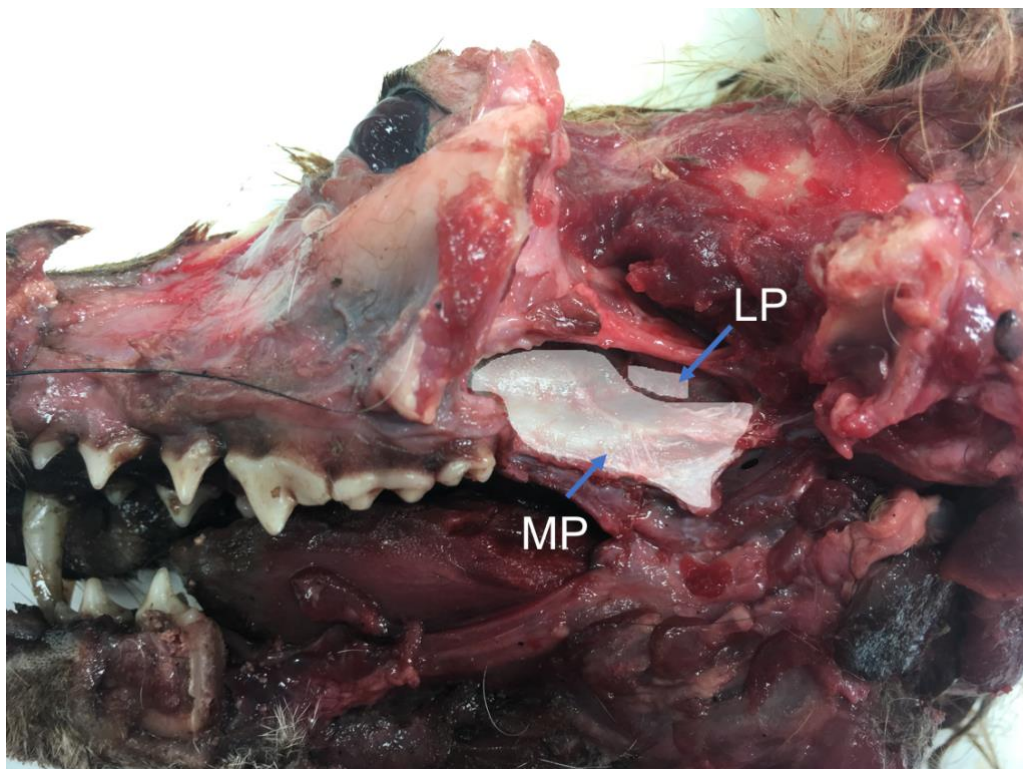


Figure 2.30 *Vulpes vulpes*, mandible and zygomatic arch removed, and sphenoid plate cleaned and digitally highlighted to show the origin of medial (MP) and lateral (LP) pterygoid muscles.

**Table 2.5 Mean muscle subdivisions and contribution to individual muscle masses, mean individual muscle masses and their contribution to total jaw adductor mass.**

Species and number of individuals	Suprazygomatic temporalis (g)	Suprazygomatic temporalis as a percentage of temporalis	Superficial temporalis (g)	Superficial temporalis as a percentage of temporalis	Deep temporalis (g)	Deep temporalis as a percentage of temporalis	Superficial masseter (g)	Superficial masseter as a percentage of masseter	Deep masseter (g)	Deep masseter as a percentage of masseter	Zygomatocmandibularis (g)	Zygomatocmandibularis as a percentage of masseter	Pterygoids (g)	Temporalis as a % of total muscle mass	Masseter as a % of total muscle mass	Pterygoids as a percentage of total muscle mass
<i>Alopex lagopus</i> (1)	2.2	4.9	18.9	43.1	22.8	52.0	8.1	54.3	2.5	16.4	4.4	29.3	4.5	69.3	23.6	7.1
<i>Canis lupus</i> (3)	10.6	6.0	73.4	40.9	95.5	53.1	34.1	40.2	26.4	31.2	24.0	28.7	25.7	62.0	29.1	8.9
<i>Canis mesomelas</i> (1)	3.7	7.9	18.5	39.7	24.4	52.4	10.0	49.3	4.3	21.2	6.0	29.5	6.7	63.3	27.6	9.1
<i>Chrysocyon brachyurus</i> (1)	9.5	8.9	48.2	45.5	48.4	45.6	26.0	42.2	8.6	13.9	27.1	44.0	12.2	59	34.4	6.8
<i>Cuon alpinus</i> (1)	5.9	7.3	48.5	59.5	27.2	33.2	15.61	38.3	14.7	36.4	10.3	25.3	10.4	61.5	30.6	7.8
<i>Lycaon pictus</i> (3)	12.2	8.3	76.7	51.9	58.8	39.8	41.7	46.2	28.5	31.5	20.1	22.3	19.5	57.4	35.1	7.6
<i>Nyctereutes procyonoides</i> (1)	1.8	9.2	8.1	41.8	9.5	49.0	4.5	42.9	3.5	33.1	2.6	24.1	3.1	58.6	32.0	9.4
<i>Otocyon megalotis</i> (1)	0.8	6.7	6.1	44.3	6.6	49.0	3.7	56.8	1.5	21.5	1.4	21.5	2.3	64.2	29.1	6.7
<i>Speothos venaticus</i> (1)	2.3	5.4	22.1	51.7	18.3	42.9	11.5	46.7	3.0	12.2	10.1	41.1	5.1	58.9	34.0	7.0
<i>Vulpes corsac</i> (4)	0.5	3.5	6.01	41.7	7.9	54.8	3.3	51.0	1.7	25.3	1.6	23.8	2.2	62.3	28.2	9.5
<i>Vulpes vulpes</i> (1)	2.8	6.0	21.8	45.7	23.1	48.3	9.4	49.2	3.3	17.4	6.4	33.3	5.8	65.8	26.3	7.9
<i>Vulpes zerda</i> (1)	0.2	4.1	2.8	51.6	2.4	44.3	1.3	54.3	0.7	29.1	0.4	16.7	0.9	62.3	27.2	10.5

## **2.5 Discussion.**

Many previous studies have taken a broad approach and compared canids in relation to other families within Carnivora or even other orders, with a view to identifying interfamilial or inter-order differences (Christiansen and Adolfssen, 2005; Wroe *et al.*, 2005; Wroe *et al.*, 2007). The challenge of this thesis was to capture interspecific differences between closely related species to identify adaptations in form and function that are reflected by dietary or behavioural correlates. Despite the limited sample size, a broad range of canid morphologies and habits is represented within this dataset. The diversity of scale covers two orders of magnitude in the Canidae, which is reflected in the dataset used in this thesis. Interspecific differences are greater than intraspecific ones (Table 2.5). Both CT and MR imaging modalities were used to capture the internal and topographical morphology of at least one individual animal from each species. Imaging datasets were used in subsequent chapters to identify and test interspecific differences.

The canid jaw adductor muscles adhere to the mammalian plan that comprises the temporalis, masseter and pterygoids. To reflect their carnivorous diet, where a wide gape and strong jaw adduction is required, the temporalis muscles dominate, making up the largest constituent of the total jaw adductor mass, with a mean of 62% (Table 2.5). The masseter has a mean of 30% contribution and the pterygoid has a mean of 9% contribution. This is broadly in line with findings from other authors regarding the make-up of the jaw adductor muscles within the carnivorans (Table 2.6). In carnivorans the temporalis makes up between 49.7% and 73.3%, the masseter between 18% and 40.5% and the pterygoids between 5% and 12.5%. This is in contrast to herbivorous mammals where the masseter muscles dominate jaw closure and make up to 54% of the jaw adductor mass in the horse or up to 80 % in some rodents (Turnbull, 1970; Cox *et al.*, 2012). The pterygoids make up to 30.9% contribution to total jaw adductor mass in the herbivorous species, much greater than

seen in the carnivorans (Table 2.6). This is attributable to the pterygoids, in concert with the contralateral masseter, performing translational movements of the mandible, an action not seen in canid jaw movements. It was notable in all species that the divisions between the individual muscles, as well as between their subdivisions was often indistinct, and absolute separation was impossible as many fascicles crossed between bellies. This observation has also been noted in other carnivorans by previous authors (Davis, 1955, 1964; Turnbull, 1970; Hartstone-Rose *et al.*, 2012). In their work on felid masticatory muscles Hartstone-Rose *et al.* (2012) speculated that the reduced functional compartmentalisation of the jaw adductors in carnivores has led to lesser degree of morphological separateness in the jaw adductor muscles.

**Table 2.6 Comparative mammalian jaw adductor muscle percentage contributions to total jaw adductor muscle mass as reported by previous authors.**

Author	Family	Species	% contribution to total jaw adductor mass		
			Masseter	Temporalis	Pterygoids
Turnbull (1970)	Equidae	<i>Equus caballus</i>	54.5	14.5	30.9
	Felidae	<i>Felis catus</i>	35.2	54.3	10.5
	Erinaceidae	<i>Echinosorex gymnura</i>	26.9	61.2	11.8
	Didelphidae	<i>Didelphis virginiana</i>	34.2	57	8.9
	Cervidae	<i>Odocoileus virginianus</i>	46.1	29.3	24.6
	Bovidae	<i>Ovis aries</i>	52.6	23.5	23.9
	Sciuridae	<i>Sciurus niger</i>	61	19.4	19.6
	Muridae	<i>Rattus norvegicus</i>	54.1	32.6	13.2
	Hystricidae	<i>Hystrix cristata</i>	71.8	16.6	11.5
Davis (1955, 1964)	Ursidae	<i>Tremarctos ornatus</i>	26.8	64	8.4
	Ursidae	<i>Ursus americanus*</i>	28	65.1	6.7
	Canidae	<i>Canis lupus familiaris</i>	26.6	64.4	8.9
	Felidae	<i>Panthera onca</i>	28.2	64.1	7.6
	Ursidae	<i>Ailuropoda melanoleuca</i>	36.6	59.7	3.6
	Procyonidae	<i>Procyon lotor</i>	23	69.2	7.6
	Ursidae	<i>Ursus maritimus</i>	21.1	73.3	5.5
Hartstone-Rose <i>et al.</i> (2012)	Felidae	<i>Caracal caracal</i>	31	59.3	9
	Felidae	<i>Leptailurus serval</i>	18	69	12.5
	Felidae	<i>Leopardus pardalis</i>	32	62.4	5.3
	Felidae	<i>Lynx rufus</i>	40.5	49.7	10
	Felidae	<i>Neofelis nebulosa</i>	39	56	5
	Felidae	<i>Panthera onca</i>	33	59.5	7
	Felidae	<i>Panthera pardus</i>	30	62	8
	Felidae	<i>Panthera uncia</i>	31	61	9
	Felidae	<i>Panthera tigris</i>	35	59	7

\*Dissected by Stark (1935), reported in Davis (1955).